# Loss-Of HSPB8 leads to prolonged stress granules disassembly via impaired CASA-complex ultimately causing FUS-aggregation.

Inauguraldissertation

zur Erlangung des akademischen Grades

Doktor der Medizinwissenschaften (Doctor rerum humanarum)

der Universitätsmedizin Rostock

vorgelegt von

Kanza Saleem

Indian

Rostock, 18.09.2023

Gutachter

1. Gutachter: Prof. Dr. Dr. Andreas Hermann

2. Gutachter: Prof. Dr. med. Susanne Petri

3. Gutachter: Prof. Dr. Dr. Markus Kipp

Date of Submission: 18.09.2023

Date of Defense: 05.03.2024

# Table of Content

## Abbreviations

| | |
|---|---|
| Aβ | amyloid β-peptides |
| ACD | α-crystallin domain |
| AD | alzheimer disease |
| ALS | amyotrophic lateral sclerosis |
| APLP | autophagosome-lysosome pathway |
| AR | androgen receptor |
| ARpolyQ | AR protein |
| BAG3 | bcl-2-associated athanogene 3 |
| BDNF | brain-derived neurotrophic factor |
| C9orf72 | chromosome 9 open reading frame 72 |
| cAMP | cyclic adenosine monophosphate |
| CASA | chaperone-assisted selective autophagy |
| CCT | chaperonin-containing TCP-1 |
| CMT | charcot–Marie–Tooth |
| CMT2L | charcot-Marie-Tooth disease type 2L |
| cvHsp | cardiovascular Hsp |
| CTD | c-terminal domain |
| CT51 | cancer/testis antigen 51 |
| DEPs | disassembly Engaged Proteins |
| dHMN | distal hereditary motor neuropathy |
| DMEM | dulbecco's modified eagle medium |
| DPRs | dipeptide repeat proteins |
| DRG | dorsal root ganglia |
| DMSO | dimethyl sulfoxide |
| DTT | dithiothreitol |
| EDTA | ethylene diamine tetra-acetic acid EGFP |
| EGFP | enhanced green fluorescent protein |
| fALS | familial amyotrophic lateral sclerosis |
| FBS | fetal bovine serum |
| FTD | frontotemporal degeneration |
| FUS | fused in sarcoma |
| GDNF | glial cell-derived neurotrophic factor |
| HBP | human brain pericytes |
| HCHWA-D | hereditary cerebral hemorrhage with amyloidosi of the Dutch type |
| HSC70 | consecutive form of heat shock protein 70 |
| HSP70 | heat shock protein 70 |
| HSP90 | heat shock protein 90 |
| HSPB6 | human small heat shock protein Hsp20 |
| HSPB8 | heat shock protein beta-8 |
| HSV-2 | herpes simplex virus type 2 |

| | |
|---|---|
| ICP10 | large subunit (R1) of HSV-2 ribonucleotide reductase |
| IDR | intrinsically disordered region |
| iPSC | induced pluripotent stem cells |
| LLPS | liquid-liquid phase separation |
| LRR | leucine-rich repeat |
| MAP2 | microtubule associated protein 2 |
| MN | motor neurons |
| MNDs | motor neuron diseases |
| mRNP | messenger ribonucleoprotein |
| MSA | multiple system atrophy |
| MTOC | microtubule organization center |
| NPC | neuronal progenitor cells |
| OPTN-1 | optineurin |
| PBS | phosphate buffered saline |
| PCR | polymerase chain reaction |
| PD | parkinson's disease |
| PK | protein kinase |
| PLO | poly-L-ornithine |
| PN | proteostasis network |
| PNS | peripheral nervous system |
| PQC | protein quality control |
| PTMs | post-translational modifications |
| RBP | RNA-binding proteins |
| RPM | rotations per minutes |
| sALS | sporadic amyotrophic lateral sclerosis |
| SBMA | spinal and bulbar muscular atrophy |
| SDS | sodium dodecyl sulfate |
| SG | stress granule |
| sHSP | small heat shock protein |
| SOD1 | superoxide dismutase-1 |
| TBK1 | TANK binding kinase 1 |
| TDP-43 | TAR DNA-binding protein 43 |
| TIAR | T-cell-restricted intracellular antigen 1-related protein |
| TLR4 | Toll-like receptor 4 |
| UBQLN-2 | ubiquilin |
| UPS | ubiquitin-proteasome system |
| VAPB | vesicle associated membrane protein B |
| VCP | valosin-containing protein |

# ZUSAMMENFASSUNG

HSPB8 spielt eine einzigartige Rolle in der zellulären Reaktion auf Stress und fungiert als Vermittler bei der Präsentation fehlgefalteter Substrate an HSP70 zur anschließenden Verarbeitung. Es wurde eine starke Korrelation zwischen der Menge an HSPB8 und fehlgefalteten Proteinen innerhalb von SGs dokumentiert (Ganassi et al., 2016). Das endgültige Schicksal fehlgefalteter Proteine hängt von der durch HSPB8 erleichterten Rekrutierung von BAG3 ab (Carra et al., 2008). Die Bindung von BAG3 und SQSTM1 führt zur Rekrutierung von HSPB8, BAG3 und HSP70 zu Substraten, die für spezifische Autophagie vorgesehen sind und allgemein als CASA bezeichnet werden (Crippa et al., 2010a; Gamerdinger et al., 2011). Der Verschmelzungsschritt zwischen Autophagosomen und Lysosomen ist ein kritischer Schritt in diesem Prozess, und Studien deuten darauf hin, dass HSPB8 für diesen Prozess benötigt wird (Crippa et al., 2010; XC Li et al., 2017; Rusmini et al., 2017).

Einerseits verursachen Mutation im HSPB8-Gen selbst Erkrankungen, typischerweise eine Neuropathie des Charcot-Marie-Tooth (CMT) Typ 2L, wie von Nakhro et al. (2013) und Tang et al. (2005) berichtet. Zusätzlich werden diese Mutationen auch mit einer distalen erblichen motorischen Neuropathie (dHMN) Typ 2A in Verbindung gebracht, wie von Al-Tahan et al. (2019), Ghaoui et al. (2016) und Irobi et al. (2004) dargelegt. Andererseits haben mehrere Studien Hinweise darauf geliefert, dass HSPB8 an der Beseitigung von Proteinaggregaten beteiligt ist, die mit ALS-assoziierten Proteinen verbunden sind. Insbesondere die Arbeiten von Crippa et al. (2010b, 2016), Carra et al. (2013) und Rusmini et al. (2013, 2015) haben konsequent die Beteiligung von HSPB8 an der Entfernung dieser pathologischen Aggregate gezeigt. Interessanterweise zeigte die mRNA-Analyse von ALS-Autopsien eine erhöhte HSPB8-Expression in Rückenmarksproben im Vergleich zu altersangepassten gesunden Kontrollen (Anagnostou et al., 2010).

Studien legen nahe, dass Mutationen im HSPB8-Gen die Proteostase, die SG-Biologie und die Autophagie behindern, drei entscheidende Pathways der Proteindegradation und somit Proteinhomöostase, welche insb. als entscheidend für lange Motoneuronen im peripheren Nervensystem angesehen werden (Varlet et al., 2017).

Wir haben daher untersucht, ob der Funktionsverlust von HSPB8 die aus humanen induzierten pluripotenten Stammzellen (iPSC) abgeleiteten Motoneuronen beeinflusst. Pathophysiologisch vermuten wir, dass HSPB8-KO die Dynamik von SGs beeinflusst und dass dieser Effekt mit Veränderungen in der Proteostase und erhöhtem Zelluntergang in Verbindung steht. Ein weiteres Ziel dieser Forschung war es, die an CASA beteiligten Proteine und ihre Regulation im Falle von HSPB8-Verlust zu untersuchen und ob diese die Aggregation eines Schlüsselproteins, beeinflussen, das bei ALS aggregiert, nämlich Fused in Sarcoma (FUS), , da jede Dysfunktion in diesem Prozess zu neurodegenerativen Störungen führen kann

Unsere Ergebnisse legen nahe, dass HSPB8 eine entscheidende Rolle bei der Regulation der Dynamik von SG und dem Zellsüberleben spielt. Die Studie unterstreicht auch die komplexe Regulierung von SGs und die Beteiligung mehrerer Chaperone an diesem Prozess. Insgesamt deuten die Ergebnisse dieser Studie darauf hin, dass der CASA-Komplex, bestehend aus HSPB8, BAG3, HSP70 und CHIP, möglicherweise nicht der alleinige Mechanismus für die Auflösung von Stressgranula ist. Es ist offensichtlich, dass die Dysregulation durch eine übermäßige Ansammlung fehlgefalteter Proteine auch die upstream-Komponenten des CASA-Komplexes beeinflusst. Darüber hinaus hebt die Studie die kompensatorischen Bemühungen des molekularen HSP90-Wegs zur Aufrechterhaltung der Protein-Homöostase hervor; es kann jedoch den Verlust von HSPB8 nicht vollständig ausgleichen. Zusätzlich zur selektiven Autophagie, die durch CASA repräsentiert wird, zeigt auch das proteasomale System eine erhöhte Expression in Abwesenheit von HSPB8, was die Komplexität der Mechanismen zur Qualitätskontrolle von Proteinen weiter unterstreicht. Die Ergebnisse dieser Studie deuten darauf hin, dass das Fehlen von HSPB8 zu verringerten Mengen von p62 führt, was einerseits auf einen potenziellen Mangel an ordnungsgemäßer Proteinubiquitinierung hinweist und andererseits die normale Bildung von Autophagosomen und Autolysosomen behindert. Das Fehlen signifikanter Veränderungen in den K48-Polyubiquitinierungsniveaus, die in HSPB8-knockout-Neuronen beobachtet wurden, passt zu den Ergebnissen der verringerten p62-Niveaus. Die Ergebnisse legen nahe, dass HSPB8 eine Rolle bei der Beseitigung von FUS-Aggregaten spielen kann, jedoch nicht bei der Regulation der FUS-Proteinexpression und des ordnungsgemäßen Kern-Zytoplasma-Transports.

Zusammenfassend präsentiert meine Dissertation neuartige Erkenntnisse über den Regulationsmechanismus von HSPB8 in menschlichen Motoneuronen. Dies kulminiert in einer Reihe von Regulationsereignissen, die CASA und verschiedene für die Aufrechterhaltung der Integrität von

Proteinabbau-Systemen, einschließlich des Autophagie-Lysosom-Wegs, wichtige Komponenten betreffen. Diese Störung führt letztendlich zur Unfähigkeit, Proteine polyubiquitinieren zu können, was zur Aggregation von fehlgefalteten Proteinen und schließlich zu einer Verringerung der Zelllebensfähigkeit führt.

# 1   INTRODUCTION

## 1.1   Small heat shock proteins

Small heat shock proteins (sHSPs) are a type of molecular chaperones that do not have an ATPase domain. They are small proteins, typically between 12 and 43 kDa, with a core α-crystallin domain (ACD) surrounded by variable N-terminal and C-terminal domains (De Jong et al., 1998; Franck et al., 2004; Haslbeck et al., 2005; Mchaourab et al., 2009; Treweek et al., 2015; Zhu & Reiser, 2018). There are 10 known α-crystallin domain-containing sHSPs (small heat shock proteins) in mammals, known as HSPB1 (HSP27), HSPB2 (myotonic dystrophy kinase binding protein, MKBP), HSPB3 (HSP17), HSPB4 (αA-crystallin), HSPB5 (αB-crystallin), HSPB6 (HSP20), HSPB7 (cardiovascular HSP, cvHSP), HSPB8 (HSP22), HSPB9 (cancer/testis antigen 51, CT51) and HSPB10 (outer dense fibre protein 1, ODFP1) (Kappé et al., 2003; Kampinga et al., 2009). In general, sHSPs bind to proteins that have not yet fully folded by interacting with hydrophobic residues exposed on the protein's surface, to stabilize it and prevent further misfolding or aggregation (Sharma et al., 1997; Van Montfort et al., 2001; Haslbeck et al., 2005; Jaya et al., 2009). Therefore, sHSPs act at an early stage in the process of handling misfolded proteins, often before ATP-dependent chaperone complexes attempt to refold them (Mchaourab et al., 2009; Bakthisaran et al., 2015; Haslbeck & Vierling, 2015).

## 1.2   Heat shock protein beta-8 (HspB8)

### 1.2.1   Background and Classification

A new human gene, called H11, was first discovered in human melanoma cells. It was found to be similar to the large subunit (R1) of herpes simplex virus type 2 (HSV-2) ribonucleotide reductase (also known as ICP10) (Smith et al., 2000). Research using FISH and M-FISH showed that H11 is a member of a stress-related gene family and is located on chromosome 12 in the q24.1-12q24.31 region (Yu et al., 2001). In the same year, an independent study by Charpentier et al. identified five new genes (E2IG1-5) that are activated by estrogen. E2IG1, the most highly induced transcript, was identified as a potential small heat shock protein (sHSP) and had 54% similarity to HSPB5 (Charpentier et al.,2000).In 2001, Benndorf et al. found a 22 kDa protein that had an α-crystallin domain (ACD) in its sequence and was closely related to other members of the sHSP family, particularly HSPB1. As a result, it was

named HSP22 (Benndorf et al., 2001). Later it was found that the sequence of these three genes was identical. Therefore, it was named HSPB8, being the eighth known human sHSP.

## 1.2.2 Structure Overview

HSPB8, also known as sHSP22, H11, E2IG1, or CRYAC, is unique among HSPBs as it primarily exists as monomers and homodimers, although it can also form heterodimers with other HSPBs (Arrigo, 2013; Kumar CHOWDARY et al., 2004; Shatov et al., 2020). HSPB8 is made up of 196 amino acids and has a molecular mass of 21.6 kDa. Its ACD is located near the C-terminal domain (CTD), between amino acids 86 and 176. The short CTD interacts with hydrophobic regions of the substrate during chaperone activity to prevent aggregation. Unlike other members of the HSPB family (HSPB1, HSPB2, HSPB4, and HSPB5), HSPB8 does not have the conserved I/V-X-I/V motif that allows for oligomeric assembly (Mogk et al., 2018; Saji et al., 2008). This motif interacts with the neighbouring ACD in a pocket between strands β4 and β8, serving as a link between the dimers. Instead, HSPB8 binds to two I/V-X-I/V domains, known as IPV domains, in the Bcl-2-associated athanogene 3 (BAG3) protein via a hydrophobic pocket (Fuchs et al., 2010). This interaction explains why HSPB8 preferentially binds to BAG3 rather than forming large oligomers. In this binding, two HSPB8 molecules and one BAG3 molecule combine to create a functional chaperone complex (Cristofani et al., 2021). HSPB8 has multiple potential phosphorylation sites, however, only phosphorylation at Ser-14, Ser-24, Ser-27, Ser-57, Thr-63, Thr-87, and Tyr-118 has been reported and are shown in figure 1.1 (Benndorf et al., 2001; Rikova et al., 2007). Phosphorylation of Ser-24, Ser-27, and Thr-87 was found to lead to an increase in HSPB8 dimerization and a decrease in its degradation. However, phosphorylation of Ser-24 and Ser-27 reduces HSPB8 chaperone activity, while phosphorylation of Thr-87 enhances HSPB8 chaperone activity (Shemetov & Gusev, 2011).
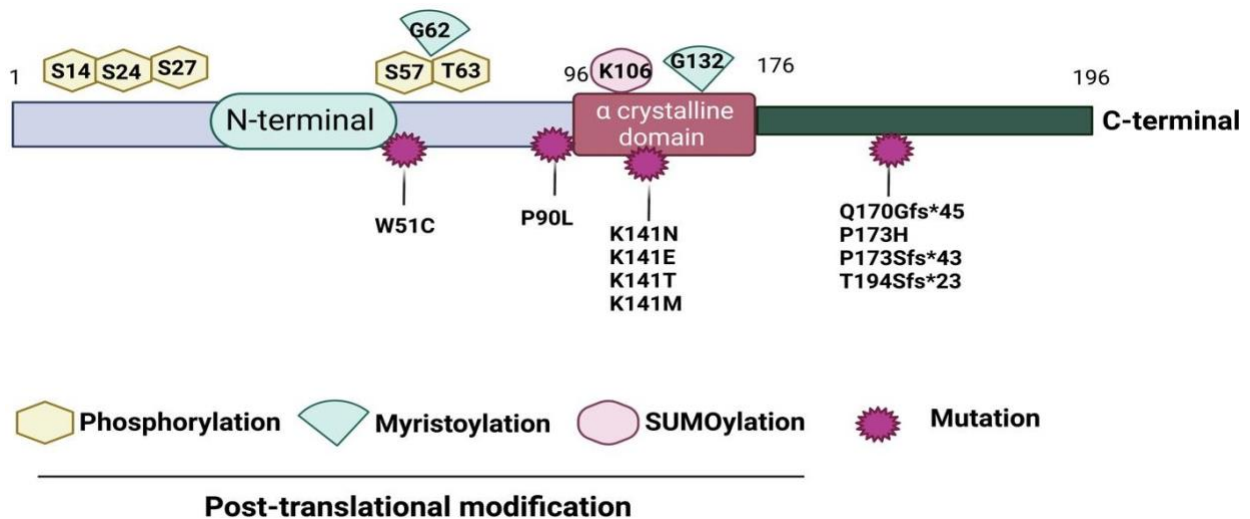
*Figure 1.1:* **HSPB8 schematic structure, post-translational modifications, and mutations**.

Post-translational modification residues are reported: phosphorylation sites are indicated in yellow, predicted myristoylation sites in orange, and a SUMOylation site in light blue. Red stars indicate HSPB8 mutations reported in the literature - W51C: reported in one melanoma line; K141N, K141E, K141T, and K141M: Charcot–Marie–Tooth type 2L, myopathy, and distal hereditary motor neuropathy (dHMN) ; Q170Gfs*45, P173H, P173Sfs*43, T194Sfs*23: dHMN and myopathy. The figure was generated using Illustrator and adapted from R. Cristofani et al., 2021.

### 1.2.3  Location and expression of HSPB8 in the brain

HSPB8 is found in many different types of tissues and is highly expressed in human skeletal and smooth muscle, heart, and brain (Cristofani et al., 2021). The expression of HSPB8 was observed to increase in muscle, stomach, liver, lung, and kidney during development, while its level remained relatively constant in the heart (Verschuure et al., 2003). Interestingly, a temporary drop of HSPB8 is observed directly after birth in the cerebellum and cortex, followed by an increase again back to foetal levels or even higher. Such temporal regulation of expression may mediate stress resistance in order to protect these brain regions against stress before and during delivery. However, this effect is not seen in hippocampus and striatum (Verschuure et al., 2003). HSPB8 interacts and is found in the same location as various other proteins, indicating its potential involvement in multiple signalling pathways. The variation in HSPB8 expression levels in different brain regions may be related to variations in stress-buffering mechanisms. HSPB8 is primarily expressed in the neurogenic niche of the hippocampus and has a diffuse expression throughout the brain. In rats, HSPB8 expression is relatively

low in the hippocampus during embryonic and postnatal stages, but increases significantly in adulthood. This suggests that the need for this stress protein increases in the brain as it matures (Kirbach & Golenhofen, 2011). Recent studies have shown that HSPB8 is highly expressed during neurogenesis in the adult hippocampus in vivo and during the differentiation of adult neural precursor cells in vitro.

## 1.3 Structural plasticity of HSPB8

Small heat shock proteins, found in all kingdoms, have a characteristic ACD composed of six or eight beta-strands arranged in two sheets (De Jong et al., 1998). This domain is located at both the N-terminal and C-terminal ends. To date, only x-ray crystallographic structures of sHSPs from bacteria and plants have been obtained (Hilario et al., 2011). The flexible structure of these small heat shock proteins appears to play a crucial role in their ability for client protein binding and chaperone function (Benesch et al., 2010; Leroux et al., 1997; Mchaourab et al., 2009; Peschek et al., n.d.; Stengel et al., 2010). The structure of animal sHSPs is difficult to determine due to their high mobility, varying sizes, and different oligomeric states. Predictions of the secondary structure of HSPB8 suggest that it is composed of mostly beta-strands and has an unordered, randomly coiled structure (Kim et al., 2006). The data from far-UV CD suggests that HSPB8 has a mainly disordered structure, which is further supported by its increased vulnerability to proteolysis and its ability to resist thermal denaturation (Kasakov et al., 2007). Therefore, it is thought that heat shock protein B8 falls under the category of intrinsically disordered proteins (Kazakov et al., 2009). HSPB8 stands out from other mammalian sHSPs due to its lack of a defined tertiary structure. One possible reason for this is the absence of the β2 strand, a feature commonly found in many other sHSPs (Kasakov et al., 2007), which contributes to HSPB8's intrinsic disorder. The lack of the β2 strand in HSPB8 prevents the formation of the beta-strand, which leads to destabilization of the entire ACD. Additionally, since the β2 strand is known to play a crucial role in intersubunit interactions, its absence may disrupt the formation of stable dimers of HSPB8 (Stamler et al., 2005). With its inability to form stable dimers, it is unlikely that HSPB8 plays a rolein the formation of high molecular mass oligomers. According to size-exclusion chromatography, HSPB8 primarily exists as an equilibrium mixture of monomers and dimers in vitro (Kumar CHOWDARY et al., 2004). However, native gel electrophoresis by Kim et al. showed the presence of large molecular mass oligomers of HSPB8 which can be broken down into smaller oligomers. It is suggested that at low concentrations, HSPB8 exists in the form of a mixture of monomers and dimers, while at high

concentrations, it has the ability to form large molecular weight oligomers, as seen from the high protein concentration inside the electrophoretic band (Kim et al., 2004, 2006).

## 1.4   The protein-protein interactions of HSPB8

The presence of heterooligomeric complexes of HSPB8 with other sHSPs was confirmed through yeast two-hybrid analysis, in addition to its interaction with itself (Fontaine et al., 2005; Sun et al., 2004). Recently, HSPB8 was discovered to possess a unique structural organization. In contrast to other sHSPs (such as HSPB1, HSPB5, and HSPB6) that form mixed large complexes, HSPB8 does not form stable complexes with either HSPB1 or HSPB5 (Datskevich et al., 2012). Carra et al were the first to report that HSPB8 interacts strongly and forms tight complexes with BAG3 in mammalian cells. This interaction is mediated by the hydrophobic groove formed by the β4 and β8 strands in HSPB8 and the two IPV motifs in BAG3. It has been proposed that BAG3 serves as an obligate partner for HSPB8, directly impacting its stability (Shemetov & Gusev, 2011). In this context, HSPB8 can be considered as an "atypical" member of the sHSP family. This may help to explain the different mechanisms of intracellular action of various sHSPs. For instance, HSPB1, HSPB5, and HSPB6 primarily function as reservoirs for misfolded or unfolded proteins until they are processed by ATP-dependent chaperones (Bakthisaran et al., 2015). In contrast, HSPB8 is primarily associated with selective autophagic removal of damaged or misfolded proteins. The fate and function of proteins may be dictated by HSPB8 (Pereira et al., 2017).

## 1.5   Stress-induced HSPB8 expression

HSPB8 has two potential binding sites for heat shock factors located 1,000 base pairs upstream from its translation start site (Kumar CHOWDARY et al., 2004). Heat shock treatment in MCF-7 cell line revealed a significant upregulation of HSPB8 expression (as reported in Chowdary et al., 2004) and in cultured neurons. However, HSPB8 expression was not induced by heat in HeLa cells. This suggests that the ability of HSPB8 to be induced by heat is dependent on the severity of the stress and is specific to certain cell types. In addition to heat stress, a wide range of other stressors can lead to a significant increase in HSPB8 expression. Studies have shown that ischemia/reperfusion (I/R) injury or chronic pressure-overload left ventricular hypertrophy can lead to increased HSPB8 expression in the heart (Depre et al., 2002). In cultured hippocampal neurons, while not induced by heat stress, the levels of HSPB8 mRNA and protein were found to be increased in response to sublethal sodium arsenite,

oxidative and hyperosmotic stress (Bartelt-Kirbach & Golenhofen, 2014). An Insult of oxygen-glucose deprivation/reoxygenation (OGD/R) leads to an Increase In HSPB8 In mouse neuroblastoma N2a cells. Additionally, a study in a rat model of stroke found that HSPB8 is significantly upregulated in the area surrounding the infarcted cerebral cortex (Bartelt-Kirbach et al., 2017). Literature indicates that HSPB8 may play a crucial role in the neuronal response to stress, specifically I/R injury, and may provide neuroprotection. Research has also shown that HSPB8 expression is greatly elevated in motor neurons that survived in the spinal cord and affected muscles of transgenic G93A-SOD1 mice (Crippa et al., 2010b). Additionally, studies have found that HSPB8 expression is also elevated in the spinal cord of patients with Amyotrophic Lateral Sclerosis (ALS) (Anagnostou et al., 2010). Studies have also observed a strong increase in HSPB8 expression in skeletal muscle, another affected area, during the progression of ALS and spinal and bulbar muscular atrophy (SBMA) in mice (Carra et al., 2013; Rusmini et al., 2013, 2015).

## 1.6 HSPB8-associated diseases

### 1.6.1 Mutation of HSPB8-associated neuropathy

The majority of mutations in the HSPB8 gene have been identified in individuals diagnosed with Charcot–Marie–Tooth (CMT) type 2L (Nakhro et al., 2013; Tang et al., 2005) neuropathy, and distal hereditary motor neuropathy (dHMN) type 2A (Al-Tahan et al., 2019; Ghaoui et al., 2016; Irobi et al., 2004). These neuropathies are clinically and genetically characterized disorders, characterized by a gradual degeneration of neurons in the peripheral nervous system (PNS) (Irobi et al., 2006). Recently, a novel causative mutation in the HSPB8 gene, specifically the substitution of adenine with cytosine at position 422 (422A>C) resulting in the Lys141Thr (K141T) mutation, was identified through exome sequencing in a Korean individual with sporadic CMT2 (Nakhro et al., 2013). Recent studies have revealed that HSPB8 mutations have an impact on muscle tissue in addition to the previously known involvement in peripheral motor neuropathy. This is supported by the functional data of HSPB8 as a crucial component in maintaining the stability of proteins and cellular homeostasis within muscle tissue. Despite the ubiquitous distribution of HSPB8, mutations such as HSPB8K141N and HSPB8K141E have been found to specifically result in degeneration of motor neuron neurites, with minimal impact on sensory neurons and no effect on cortical neurons or glial cells. These findings provide insight into the predominant motor neuron phenotype observed in distal hereditary motor neuropathy and

Charcot-Marie-Tooth disease type 2L (Irobi et al., 2012). The K141E and K141N mutated forms of HSPB8, which are associated with disease, were found to exhibit a "loss of function" in certain studies. The chaperone-like activity of HSPB8 was significantly diminished in the presence of these mutations (Carra et al., 2005). The pathological development of peripheral neuropathies is postulated to be at least partly mediated by the decreased chaperone activity of the disease-associated K141E and K141N mutated forms of HSPB8.

## 1.6.2  HSPB8-associated myopathy

Lately, two families with genetic mutations in the HSPB8 gene have been identified, resulting in a dual presentation of peripheral motor neuropathy and a rimmed vacuolar myofibrillar myopathy (Ghaoui et al., 2016). It is hypothesized that HSPB8´s role is crucial for preserving the structural stability of muscle cells, and a malfunction in CASA leads to the development of muscular dystrophy and cardiomyopathy (Ulbricht et al., 2015). The research conducted by Bouhy et al. has uncovered a pivotal pathomechanism Implicated In the development of distal myopathy In a mouse model. Specifically, their findings establish a direct link between the accumulation of mutant Hspb8K141N and the impaired degradation of Hspb8-positive aggregates through the Hspb8/Bag3-mediated autophagy pathway. This compelling evidence highlights the crucial role played by these dysregulated processes in driving the pathogenesis of distal myopathy.

## 1.6.3  HSPB8-associated other neurodegenerative diseases

The aggregation of misfolded proteins in the form of protein aggregates is a defining characteristic of numerous neurodegenerative disorders (Soto, 2003). Amyotrophic lateral sclerosis (ALS) is a neurodegenerative disorder with a primarily sporadic form (sALS), accounting for 85% of cases, and a familial form (fALS), accounting for 15% of cases. The clinical presentation of sALS and fALS is indistinguishable. Familial forms of ALS have been linked to specific genetic mutations, including those affecting superoxide dismutase-1 (SOD1), TAR DNA-binding protein 43 (TDP-43), fused-in-sarcoma/translocated-in-liposarcoma (FUS/TLS), sequestosome-1 (SQSTM1/p62), optineurin (OPTN-1), ubiquilin (UBQLN-2), valosin-containing protein (VCP), and TANK binding kinase 1 (TBK1), among others (Taylor et al., 2016). Many of these gene products are involved in autophagy-related pathways, key players in the protein quality control (PQC) system, or have been observed to mislocalize and aggregate, resulting in proteotoxicity (Robberecht & Philips, 2013; Taylor et al., 2016). Multiple

research studies have demonstrated that the accumulation of misfolded proteins in conditions such as fALS, sALS, and SBMA disrupts the normal degradation pathways. This can lead to an overburdeningof the ubiquitin-proteasome system (UPS) or blockages caused by the presence of polyQ expansions (Ciechanover & Kwon, 2015; Rusmini et al., 2016), the clearance of misfolded protein aggregates through the autophagic pathway could be hindered, resulting in a disruption of autophagic flux (Rusmini et al., 2013). A review article by Rusmini et al. in 2016 proposed that the protein HSPB8 plays a vital role in maintaining the functionality and survival of motoneurons. In their study, Crippa et al. (2010b) observed a significant increase in the levels of HSPB8 protein in the anterior horn motoneurons of transgenic (tg) ALS SOD1-G93A mice that were at the end-stages of disease, in comparison to wild-type mice. This upregulation was found to be associated with the presence of diffuse and non-aggregated mutant SOD. It is well established that enhancing the clearance of misfolded proteins can inhibit the formation and accumulation of protein aggregates, thereby reducing their toxicity and slowing the progression of associated neurodegenerative disorders (Takalo et al., 2013). In in vitro studies using cultured motoneurons, it has been observed that HSPB8 expression is significantly upregulated in response to proteasome dysfunction (Crippa et al., 2010 a,b). Furthermore, analysis of mRNA levels in autopsy samples of spinal cord from patients with ALS revealed that HSPB8 expression is elevated compared to that in spinal cord samples from age-matched healthy controls (Anagnostou et al., 2010).

As previously discussed, HSPB8, has the ability to recognize and interact with a wide range of misfolded protein conformations, thus preventing their aggregation and promoting their clearance via autophagy. This includes proteins such as alpha-synuclein, which is associated with neurodegenerative disorders such as Parkinson's disease (PD), multiple system atrophy (MSA), and dementia with Lewy bodies (Bruinsma et al., 2011); Zn-superoxide dismutase1 (SOD1), which is linked to ALS (Crippa et al., 2010b); and various truncated forms of TDP-43, which are associated with both ALS and FTD (Crippa et al., 2016), as well as five different RAN, translated DPRs from the C9Orf72 gene, which is linked to ALS and FTD (Cristofani et al., 2017). Therefore, HSPB8 plays a critical role in the progression of various neurodegenerative diseases.

## 1.7 Mechanisms of assembly and disassembly of stress granules

### 1.7.1 Characteristics of stress granules

With the progression of research, it has become evident that, in addition to membrane-enclosed organelles, the cell also harbours membrane less compartments. In 1899, American biologist Edmund Wilson reported the initial observation of this phenomenon in the literature, documenting the presence of small, dense spheres within the cytoplasm of starfish eggs that displayed distinct characteristics from their surrounding environment and were capable of fusion (Wilson et al 1899). Recently, various membrane less organelles, including the nucleolus, nuclear speckles, germ granules, stress granules (SG), and processing bodies (P-bodies), have been identified in eukaryotic cells (Gomes & Shorter, 2019). Despite the extensive knowledge of the properties and functions of these structures, the mechanisms by which they are formed and the impacts of their distinct architectures on cellular function remain to be fully understood.

Stress granules (SG) are cytoplasmic, membrane less entities that emerge in response to stress and comprise messenger ribonucleoprotein (mRNP) stalled in translation, multiple RNA-binding proteins (RBP), and additional proteins (Nover et al., 1989). Along with nucleolus, and P-bodies, SG are grouped under the classification of RNP granules, characterized by high concentrations of RNA and proteins as shown in Figure 1.2. However, unlike the other aforementioned RNP granules that persist in the cell under normal physiological conditions, SG only forms in response to stress and exists only temporarily (Spector, 2006). Exposure to environmental or internal stress can severely disrupt cellular homeostasis and, if not properly addressed, can ultimately result in cellular death. In an effort to defend itself, the cell activates a variety of conserved stress response pathways, which among other effects, leads to a decrease in global translation and an upregulation of a stress-specific proteome. Formation of SG is a component of the complex stress response mechanism aimed at mitigating damage caused by stress through regulation of translation, protection of untranslated mRNA, reduction of energy expenditure, modulation of signalling pathways, and maintenance of protein and RNA homeostasis (Arimoto et al., 2008; Buchan & Parker, 2009; N. Kedersha et al., 2013; Ross Buchan, 2014). Stress granules are spherical structures of varying diameters, ranging from 100 nm to multiple micrometers, dependent on the cell type and stress conditions (Mahboubi et al., 2013; Mahboubi & Stochaj, 2017). They are composed of two distinct phases: a stable, less mobile inner core and a highly dynamic outer shell with liquid-like properties (Jain et al., 2016). The assembly of SG is a complex and regulated process,

typically triggered by inhibition of protein translation. The phosphorylation of the eukaryotic translation initiation factor eIF2α is the classical pathway for initiation of translation suppression and SG formation (N. Kedersha et al., 2002). However, alternative pathways, not involving eIF2α, may also contribute, depending on the type of stress (Thedieck et al., 2013). Translation inhibition results in the disassembly of polysomes, releasing free mRNA that is subsequently sequestered into stress granules (Hofmann et al., 2021).
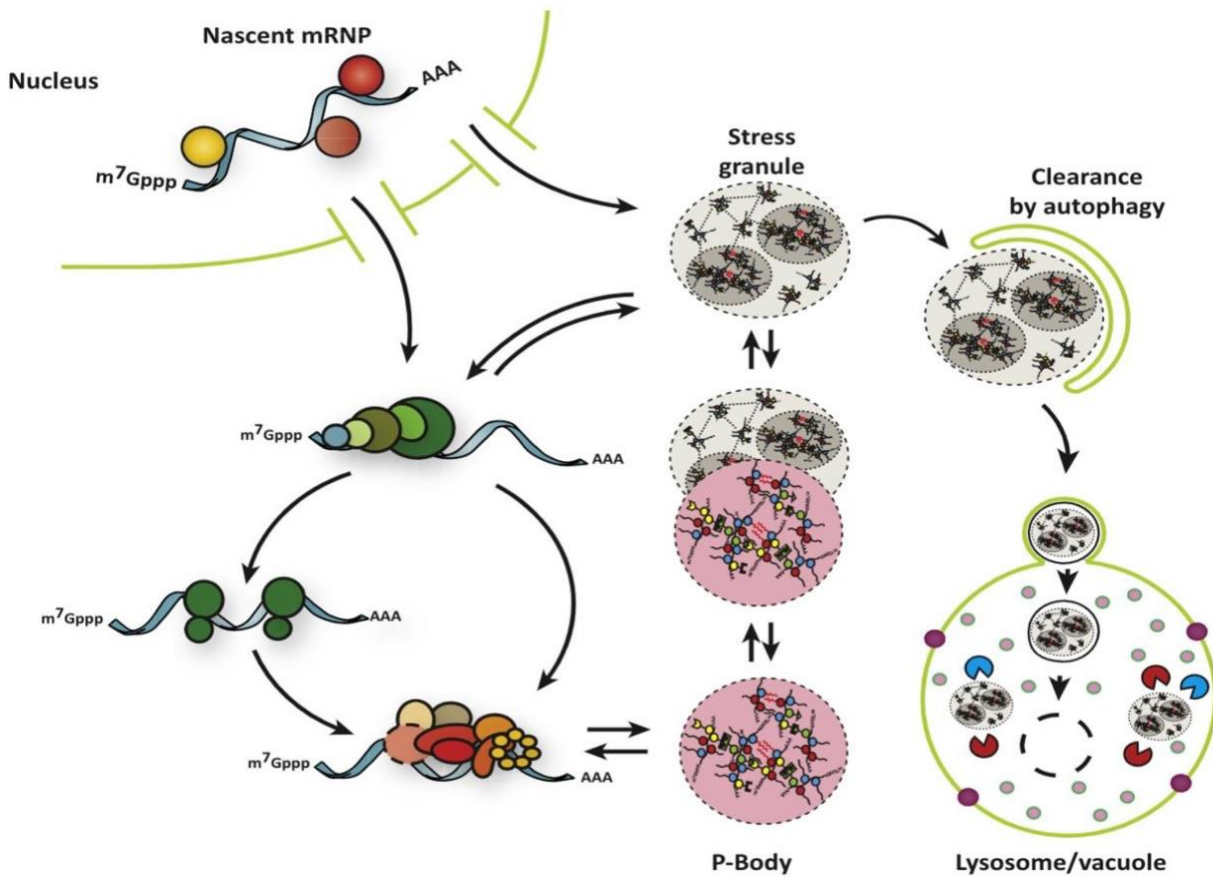


*Figure 1.2:* **Stress Granules Are Dynamic and Have Multiple Fates**.

Stress granules form from untranslating messenger ribonucleoproteins (mRNPs). They can interact with P bodies, exchange components with the cytoplasm, and undergo autophagy. Figure reprinted from DSW Protter et al., 2018.

### 1.7.2 Assembly of stress granules

The assembly of SGs involves a two-step process, with the first step being the inhibition of translation initiation and the subsequent breakdown of polysomes. The second step, which follows the translational inhibition and polysome disassembly, results in the formation of noticeable cytoplasmic foci and is regulated by various proteins referred to as SG nucleators (Anderson & Kedersha, 2006). These nucleators can induce SG formation even in the absence of stress when overexpressed (Anderson & Kedersha, 2009; N. L. Kedersha et al., 1999; Ohn et al., 2008; Tourrière et al., 2003; Buchan & Parker, 2009; Erickson & Lykke-Andersen, 2011). The initiation of stress granule assembly is facilitated by the clustering of SG nucleating proteins in the cytoplasm. The primary nucleators are RNA-binding proteins RBP that contain leucine-rich repeat (LRR) domains and intrinsically disordered regions (IDR), which promote liquid-liquid phase separation (LLPS) through electrostatic interactions (Lin et al., 2015). Some of the well-studied nucleating proteins include G3BP1, G3BP2, TIA1, TIAR, and FMRP (Reineke & Neilson, 2019). A diagrammatic illustration of the composition of the SG has been shown in Figure 1.3. The assembly of SG is said to initiate with the formation of a stable core, which is then followed by the assembly of the shell (Jain et al., 2016) (Niewidok et al., 2018). The formation of mature, biphasic SG occurs when persistent stress and repression of translation result in the reversible recruitment of non-translating mRNPs and additional RNA-binding proteins to the initial SG foci (Panas et al., 2016). In addition to an increasing number of proteins associated with SGs, SGs also contain mRNAs that have ceased translation and predominantly encode housekeeping proteins. However, a specific subset of transcripts, such as the Heat shock protein 70 (HSP70), are not present in SGs and are selectively translated during stress conditions (Paul Anderson, Nancy Kedersha 2002). The assembly and disassembly of stress granules are influenced by various protein chaperones. Evidence from studies in yeast and mammalian cells has shown that inhibition of the Hsp70 function leads to an increase in stress granule formation and/or a delay in disassembly. Additionally, both Hsp70 and Hsp40 proteins can be localized within stress granules in yeast and mammalian cell autophagy (Cherkasov et al., 2013; Mazroui et al., 2007; Walters et al., 2015).

Several studies have demonstrated a correlation between the capacity of cells to form stress granules (SGs) and their viability during stress conditions (Arimoto et al., 2008; Eisinger-Mathason et al., 2008; Lavut & Raveh, 2012; Zou et al., 2011, 2012). However, the precise composition of stress granules and the mechanism of their assembly remain highly redundant and context-dependent (Aulas et al., 2017). This implies that granules can assemble in a unique manner in response to specific cellular

conditions and stress granules may serve different functions for various types of stress (Protter etal., 2018).
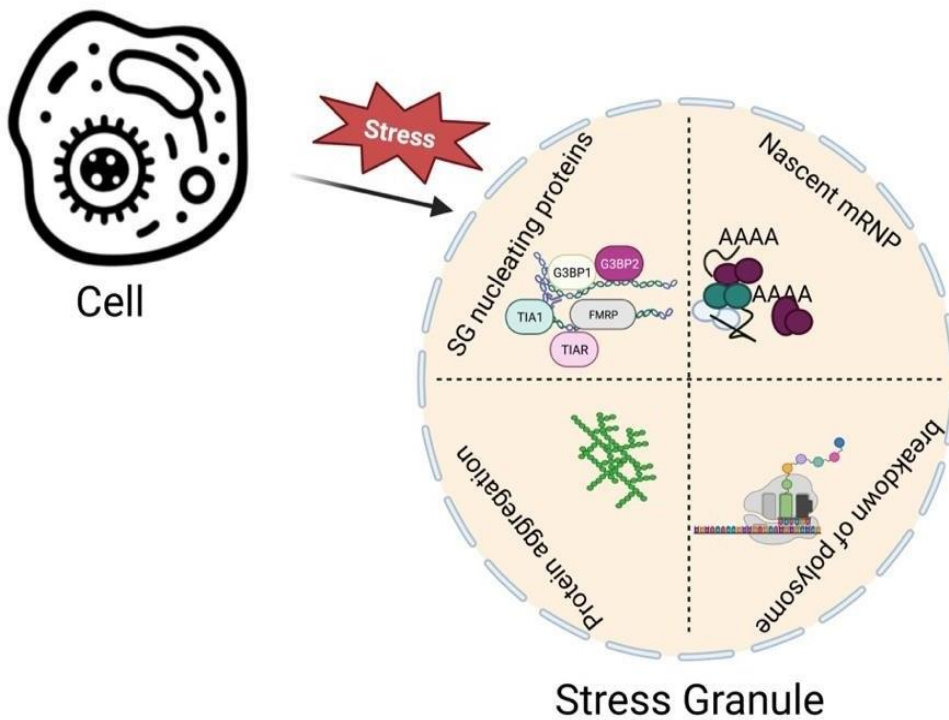


*Figure 1.3:* **Schematic representation of Stress granules composition during the time of stress.** Image created from BioRender**.**

## 1.7.3  Disassembly of stress granules

The proper disassembly of SG after stress removal is a crucial aspect of restoring normal cellular metabolism (Mahboubi & Stochaj, 2017). The initial stage of SG disassembly involves the dispersal of the less stable outer shell, enabling the release of soluble RNA-binding proteins into the cytoplasm or nucleus and facilitating the liberation of messenger ribonucleoprotein to the cytoplasm (more details can be seen in Fig. 1.4), thereby enabling the resumption of translation (Wheeler et al., 2016; Mahboubi & Stochaj, 2017). According to a study by Wheeler et al. (2016), the stability of SG cores is maintained through either ATP-dependent disaggregation by proteins such as VCP and heat shock protein 70 (Hsp70), or removal via autophagy. Additionally, mutations in VCP have been shown to result in the accumulation of abnormal SG structures (Seguin et al., 2014).
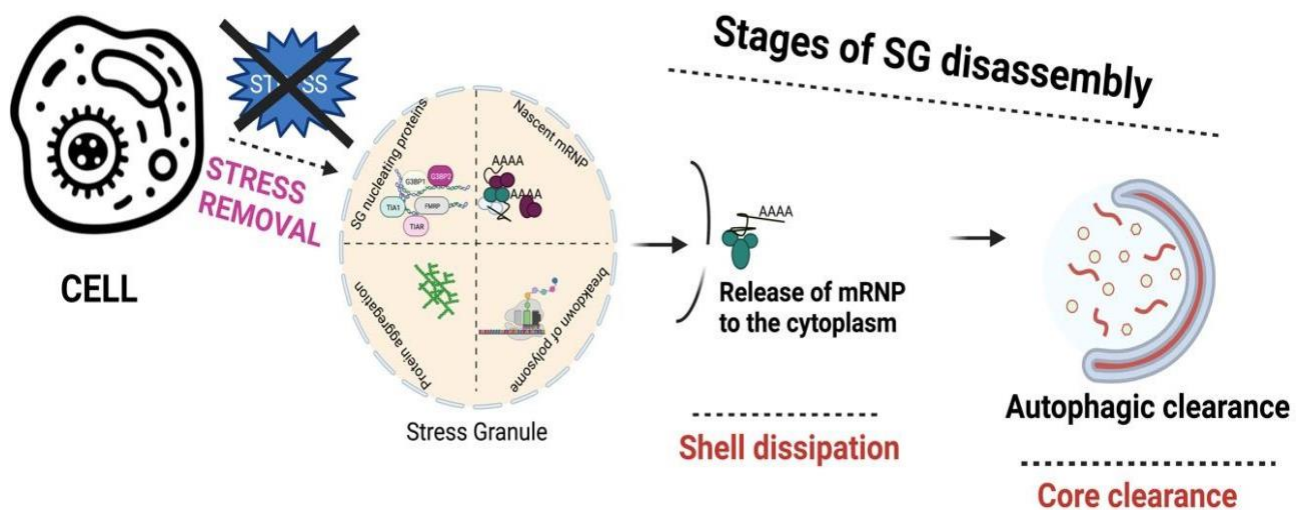
*Figure 1.4:* **Schematic representation of Stress granules disassembly after the removal of stress.**

Disassembly is likely to occur through shell dissipation by exchange of weakly associated granule (shell) mRNPs into a recovering translational mRNP pool. More stable core assemblies may then be disassembled by ATP-requiring remodeling complexes or autophagy. Image created using BioRender and adapted from Wheeler et al., 2016.

## 1.8   Crucial role of HSPB8 in Stress granules

Small heat shock proteins act as holdases, which are chaperones that bind misfolded proteins and deliver the bound substrate to HSP70 for proper refolding or degradation (Lee & Vierling, 2000). Ganassi et al. observed that the recruitment of HSPB8 by DriP-containing stress granules increases as the activity of HSP70 is inhibited by VER. This supports the hypothesis that HSPB8 functions as a mediator in presenting misfolded substrates to HSP70 for subsequent processing. The presence of HSPB8 within stress granules has been suggested to function as an ATP-independent holdase, neutralizing both misfolded proteins (such as Ubc9TS) and DriPs. There is a strong correlation between the amount of HSPB8 and misfolded proteins within SGs, providing evidence for HSPB8's role as a chaperone "holder" (Ganassi et al., 2016). The rapid kinetics of HSPB8 recruitment, in combination with its intrinsic disordered protein nature, suggests a unique role for HSPB8 in the cellular response to stress (Sudnitsyna et al., 2012), proposed that dissociated HSPB8 exhibits a high affinity for phase-separated stress granules and may be increasingly retained within SGs in the presence of misfolded proteins. An emerging concept in the field is that many proteins that localize to membrane-less liquid-like compartments contain extended regions of intrinsic disorder (Brangwynne et al., 2015; Gilks et al., 2004, n.d.; A. Patel et al., 2015). Once within SGs, HSPB8 mediates the recruitment of BAG3 to facilitate

substrate transfer and processing by the BAG3-HSP70 complex (Ganassi et al., 2016). While HSPB8 binds misfolded proteins to prevent their aggregation, it does not possess the ability to refold the substrate or direct it towards degradation (Carra et al., 2005). The ultimate disposition of the misfolded proteins is contingent upon HSPB8-mediated recruitment of BAG3 (Carra et al., 2008). The interaction between BAG3 and SQSTM1 results in the association of HSPB8, BAG3, and HSP70 with substrates targeted for autophagy (Crippa et al., 2010a; Gamerdinger et al., 2011). It is significant to note that the BAG3-mediated targeting of chaperone-based aggresomes is distinct from previously described mechanisms, as the transfer of misfolded proteins to the aggresome occurs in the absence of substrate ubiquitination (Gamerdinger et al., 2011). Ganassi et al. propose that HSPB8 is recruited to SGs to keep DriPs (and other misfolding-prone proteins) in a ready state for transfer to BAG3-HSP70. The control of DriPs within SGs by HSPB8 and the timely sorting of DriPs into perinuclear aggregates by BAG3-HSPB8 is essential to preserve the composition and dynamics of SGs (granulostasis). In line with this proposal, even a mild depletion of BAG3-HSPB8 leads to the conversion of SGs into an aberrant and Rnase-resistant state.

## 1.9   Cellular protein quality control and HSPB8

### 1.9.1   The chaperone functionality of HSPB8

sHSPs are ATP-independent molecular chaperones that play important roles in cellular proteostasis. Usually acting as holdases, sHSPs bind to misfolded proteins preventing their non-specific interaction and, ultimately, irreversible aggregation (Haslbeck et al., 2005). In vitro experimentation revealed that HSPB8 demonstrated chaperone-like properties by inhibiting the aggregation of insulin induced by DTT (dithiothreitol) and thermal aggregation of citrate synthase. Upon exposure to elevated temperatures, HSPB8 underwent conformational alterations, leading to an increase in surface hydrophobicity. This change was linked to the temperature-dependent chaperonic property of HSPB8 (Bukach et al., 2004). In a study using cardiomyocytes, the expression of recombinant HSPB8 proteins was increased and it was found that HSPB8 acted as a chaperone to directly disrupt the formation of amyloid oligomers by the HSPB5 R120G protein (Sanbe et al., 2007). In transgenic mice overexpressing the HSPB5 R120G mutation (R120G TG), the administration of geranylgeranylacetone, a pharmacological inductor of HSPB8, was observed to result in a reduction of amyloid aggregate formation and an improvement in cardiac function, as well as increased survival of the mice (Sanbe et al., 2009). The chaperone activity

of HSPB8 was evaluated using Htt43Q, a polyglutamine protein, as a model system (Carra et al., 2005). Additionally, clinical evidence indicates that HSPB8 directly interacts with amyloid β-peptides (Aβ) in the pathological lesions present in the brains of Alzheimer´s disease (AD) patients and in those with hereditary cerebral haemorrhage with amyloidosis of the Dutch type (HCHWA-D). In isolated human brain pericytes (HBP), the overexpression of HSPB8 was found to alter Aβ aggregation and Aβ-mediated cytotoxicity in a dose-dependent manner, suggesting a potential role for HSPB8 in regulating the formation of classic senile plaques (Wilhelmus et al., 2006).

### 1.9.2   HSPB8-mediated proteolytic degradation via CASA

The hypothesis proposes that HSPB8 enables the proteasome-mediated degradation of particular proteins that impede cardiac hypertrophy under physiological conditions. The primary mechanisms for intracellular degradation are widely recognized to be the ubiquitin-proteasome system (UPS) and autophagy (Cichanover, 2005). In situations where the UPS is overwhelmed or compromised, cellular machinery can activate autophagy as a means to ensure proper clearance of substrates. The effectiveness of this process is contingent upon an operational retrograde transport mechanism, facilitated by dynein and select chaperones, including the HSPB8-BAG3 complex (Cristofani et al., 2017). As previously discussed, HSPB8 combines with BAG3, which then attracts HSP70 and CHIP's C-terminus to form a chaperone complex. This complex engages with the autophagy adapter SQSTM1/p62 (Gamerdinger et al., 2011) which recognizes substrates with specificity and directly binds to the autophagosomal marker protein LC3, directing ubiquitinated substrates to autophagosomes for degradation through autophagy. The term used to describe this process is chaperone-assisted selective autophagy (CASA) (Arndt et al., 2010).

The CASA pathway, initially characterized as a mechanism of autophagy triggered by tension, has been found to detect the mechanical unfolding of large cytoskeleton components and facilitate their removal and degradation during muscle contraction (Arndt et al., 2010). In cells experiencing mechanical strain, the important target of CASA is the cytoskeletal protein filamin (FLN), also recognized as an actin-crosslinking protein. A mechanosensitive region of FLN can be bound by the BAG3/HSP70/HSPB8 complex in a collaborative way, promoting the removal of damaged proteins through a selective autophagy pathway (Ulbricht et al., 2013).On the other hand, Fuchs et al., 2015 reported the HSPB8/BAG3 complex as a crucial regulator of mitotic actin-based structures remodelling, spindle orientation, and proper chromosome segregation. Interestingly, these functions were found

to operate independently from the HSP70/HSC70 chaperone system (Fuchs et al., 2015). Despite further work is needed to in-depth characterize the exact role of HSPB8 in different aspects of filament biology. , it is hypothesized that this role is crucial for preserving the structural stability of muscle cells, and a malfunction in CASA leads to the development of muscular dystrophy and cardiomyopathy (Ulbricht et al., 2015). The CASA machinery plays a crucial role in preparing mammalian cells to rapidly adjust to biological processes that require frequent actin assembly and disassembly. The most significant alterations in cytoskeletal organization and dynamics occur in eukaryotic cells during mitosis. In diseases characterized by misfolded proteins that have a tendency to aggregate, such as motor neuron diseases (MNDs), a process called aggrephagy can be used to deliver these misfolded proteins to the microtubule organization centre (MTOC) for assembly into aggresomes (Bennett et al., 2005; Johnston et al., 2002; Neil F. Bence 2001). It involves the recognition of misfolded proteins by a complex of the HSPB8 and its partner BAG3 (Cristofani et al., 2017, 2021). Once formed, the HSPB8/BAG3 complex associates with HSPAs/HSP70s that are bound to the carboxyl terminus of HSC70-interacting protein (CHIP or STUB1), which is a U-box-containing E3 ubiquitin-protein ligase that tags misfolded proteins with a polyubiquitin chain for recognition by autophagy receptors such as SQSTM1/p62 for CASA as shown in Figure 1.5. CASA complex is then transported to the MTOC along microtubules by the dynein machinery that is bound to BAG3 (Cristofani et al., 2017, 2021). Next, the autophagy receptors allow for LC3-II-mediated insertion into autophagosomes. The importance of CASA specifically in neuromuscular cell homeostasis is emphasized by the fact that mutations in most of its members lead to neuronal or muscular disorders (Tedesco et al., 2022). CASA has also been shown to participate in removing protein aggregates linked to neurodegenerative disorders, such as FTD and ALS. In familial ALS models of motor neurons, the multi-heteromeric complex HSPB8/BAG3/HSP70/CHIP was found to interact with mutant SOD1 and activate selective autophagy to eliminate misfolded proteins (Crippa et al., 2010b). As the mere act of overexpressing HSPB8 appeared to be enough to reestablish proteostasis, HSPB8 was regarded as a critical factor in the process (Crippa et al., 2010b). HSPB8's pro-degradative function extends beyond SOD1, as the same mechanism was observed to occur with misfolded and aggregate-prone TDP-43 species (Crippa et al., 2010a). Recent findings have revealed that the HSPB8-BAG3 activity exhibits some similarities with the CASA process. This activity appears to operate independently from the HSP70/HSC70 chaperone system, which suggests a unique mode of action. Moreover, this discovery supports the concept that not all sHSPs' cellular functions require specific interactions with the HSP70 system. HSPB8 has been found to efficiently mediate the degradation of the polyglutamine protein Htt43Q by interacting with

BAG3, whereas HSPB1 or HSPB5 did not demonstrate the same efficiency (Carra et al., 2008). The proposed paradigm suggests that HSP70 is dispensable in this process, with HSPB8 fulfilling the role of substrate recognition capacity, and BAG3 facilitating the interaction between the substrate-loaded complex and the p62 ubiquitin adaptor. Furthermore, HSPB8 and BAG3 have been shown to induce phosphorylation of the translation initiation factor 2 (eIF2 alpha) in a HSP70-independent manner, leading to the inhibition of protein synthesis and the stimulation of autophagy as shown in Figure 1.5. These findings indicate that HSPB8 is situated at the intersection of protein synthesis and protein degradation pathways (Carra, 2009). It has been observed that the BAG3 domain interacts with HSP70, while the PXXP domain of BAG3 binds to other client proteins. This suggests that HSPB8 may be responsible for recognizing misfolded proteins and, in conjunction with BAG3 and a PXXP-interacting partner, activate the macroautophagy machinery (further details can be seen in. Fig. 1.5). There is a possibility that BAG3 could link chaperone-bound substrates to macroautophagy by associating with other chaperones. Thus, the function of the HSPB8-BAG3 complex in client handling may diverge depending on client specificity and the presence of stress conditions (F. Li et al., 2018).
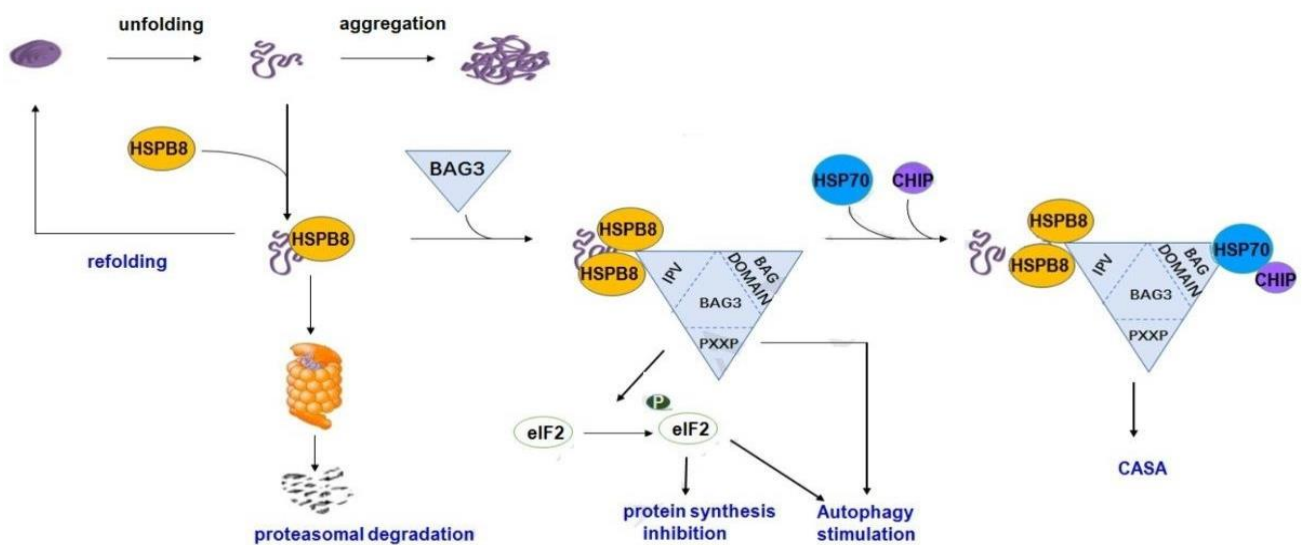


*Figure 1.5:* **Participation of HSPB8 in protein quality control.**

HSPB8 is only indicated to assist misfolded or unfolded proteins to regain or acquire the normal folding. In most conditions, HSPB8 facilitate the degradation of terminally misfolded proteins in collaboration with proteolytic machinery including proteasome or autophagy. Through interaction with BAG3, HSPB8 predominantly targets misfolded promotes autophagic removal of misfolded proteins. Adapted from Fazhao Li et al., 2018.

Ganassi et al., 2016 reported that immediately following stress, HSPB8 dissociates from the BAG3-HSP70 subcomplex and is recruited into SGs (Figure 1.6). These results suggest that the HSPB8-BAG3-HSP70 complex undergoes partial dissociation during proteotoxic stress and that HSPB8 has both BAG3-independent and -dependent roles. Inhibition of proteasomal degradation resulted in a significant increase in HSPB8 levels, even in cells depleted of BAG3, providing further support for the idea that HSPB8 has a BAG3-independent function. Under these conditions, upregulation of HSPB8 may promote the nucleation of ubiquitinated microaggregates, upstream of BAG3 (Guilbert et al., 2018). Additionally, HSPB8 was found to play a role in regulating the molecular assembly of p62, which in turn promotes p62 recruitment to the BAG3 machinery, thereby facilitating the sequestration of misfolded proteins (Guilbert et al., 2018). In recent studies, it has been shown that HSPB8 is capable of recognizing and aiding in the autophagy-mediated clearance of dipeptide repeat proteins (DPRs) derived from the C9ORF72 transcript that contains an expanded G4C2 stretch. This transcript has been identified as the genetic cause of ALS and FTD (Cristofani et al, 2017b). The observed results indicate that in addition to classical misfolded proteins, HSPB8 is involved in mitigating a wide range of abnormal peptides in cells that have the potential to form aggregates. BAG3 facilitates the degradation of (poly)-ubiquitinated and misfolded proteins through autophagy (Yew et al., 2005).
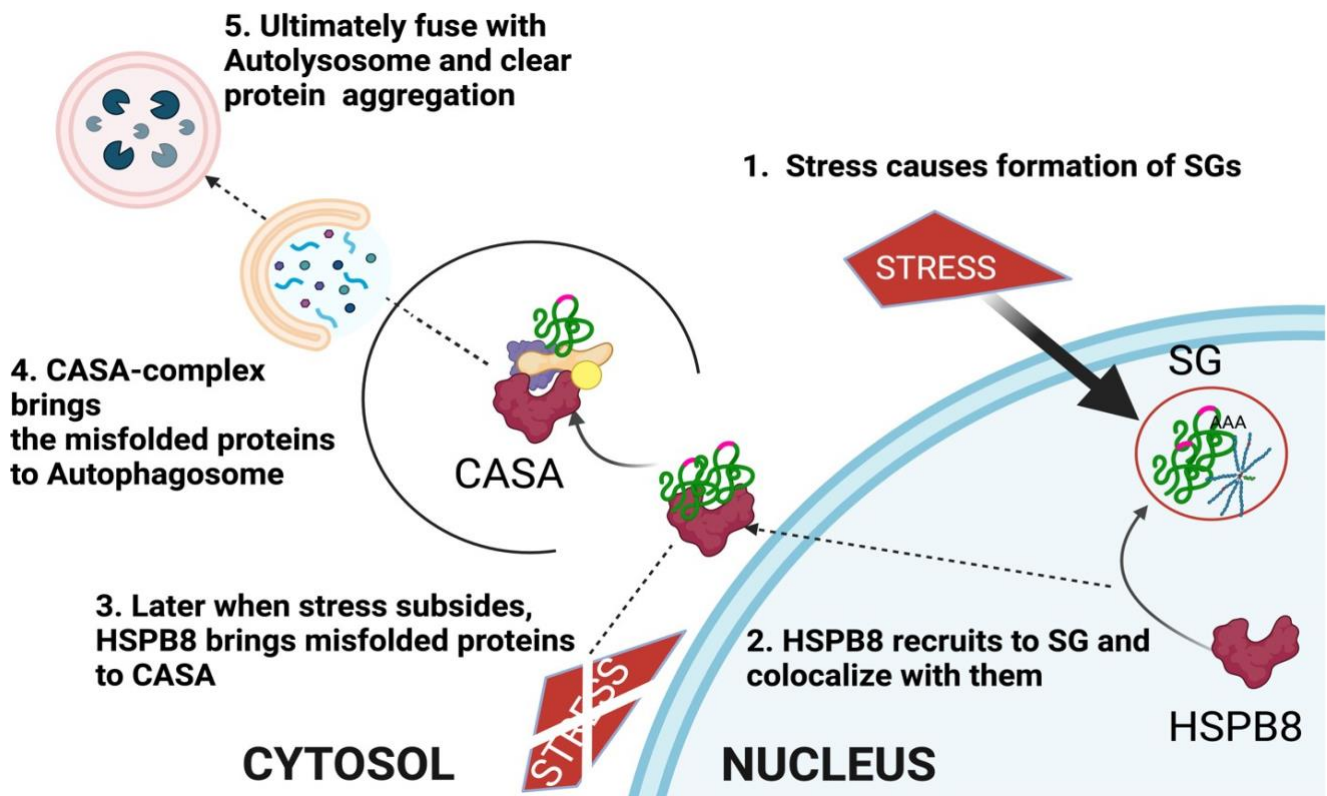
*Figure 1.6:* **Role of HSPB8 in misfolded protein clearance.**

Immediately after stress HSPB8-dissociate from the CASA-complex and recruits to the SG. At the time of stress it colocalize to the SGs and when the stress is over, it brings all the non-native protein to the CASA either for proper folding or for degradation. Later CASA-complex brings all the misfolded protein to autophagosome and further these protein get degraded by fusing to lysosome. Figure has been generated using BioRender.

## 1.10 Role of HSPB8 in UPS and CASA

In recent years, the intricate relationship between proteasome saturation, HSPB8 expression, and protein quality control has garnered significant attention. When the proteasome becomes overwhelmed by misfolded proteins, an intriguing phenomenon occurs: the upregulation of HSPB8 expression. HSPB8, working in conjunction with its partners BAG3 and HSC70, plays a crucial role in guiding misfolded proteins towards autophagy, facilitating their degradation. However, there are instances where the transportation of cargo by dynein and the formation of autophagosomes encounter obstacles, leading to the activation of unknown factors that trigger de novo transcription of BAG1. Consequently, BAG1 associates with HSP70/CHIP, redirecting misfolded proteins towards the ubiquitin-proteasome system (UPS) for degradation (Rusmini et al., 2017) (see Figure 1.7). The sciatic nerve of mice homozygous for the K141E and K141N knock-in mutations exhibited HSPB8-positive aggregates, which were associated with decreased markers of autophagy effectiveness (Bouhy et al., 2018). Recent findings suggest that HSPB8K141N may disrupt the turnover of autophagosomes by hindering their co-localization and subsequent fusion with lysosomes, rather than affecting autophagosomes co-localized with protein aggregates (Kwok et al., 2011) (X. C. Li et al., 2017). Trehalose is a disaccharide that has been shown to regulate autophagy by inducing lysosomal enlargement and membrane permeabilization. This process occurs through the induction of the protein HSPB8, which plays a key role in mediating the effects of trehalose on lysosomal function. Overall, the induction of lysosomal enlargement and membrane permeabilization by trehalose, through the induction of HSPB8, represents a novel mechanism by which autophagy can be regulated. This process may have important implications for the treatment of various diseases, including neurodegenerative disorders and cancer, which are associated with defects in lysosomal function and autophagy  (Rusmini et al., 2019).
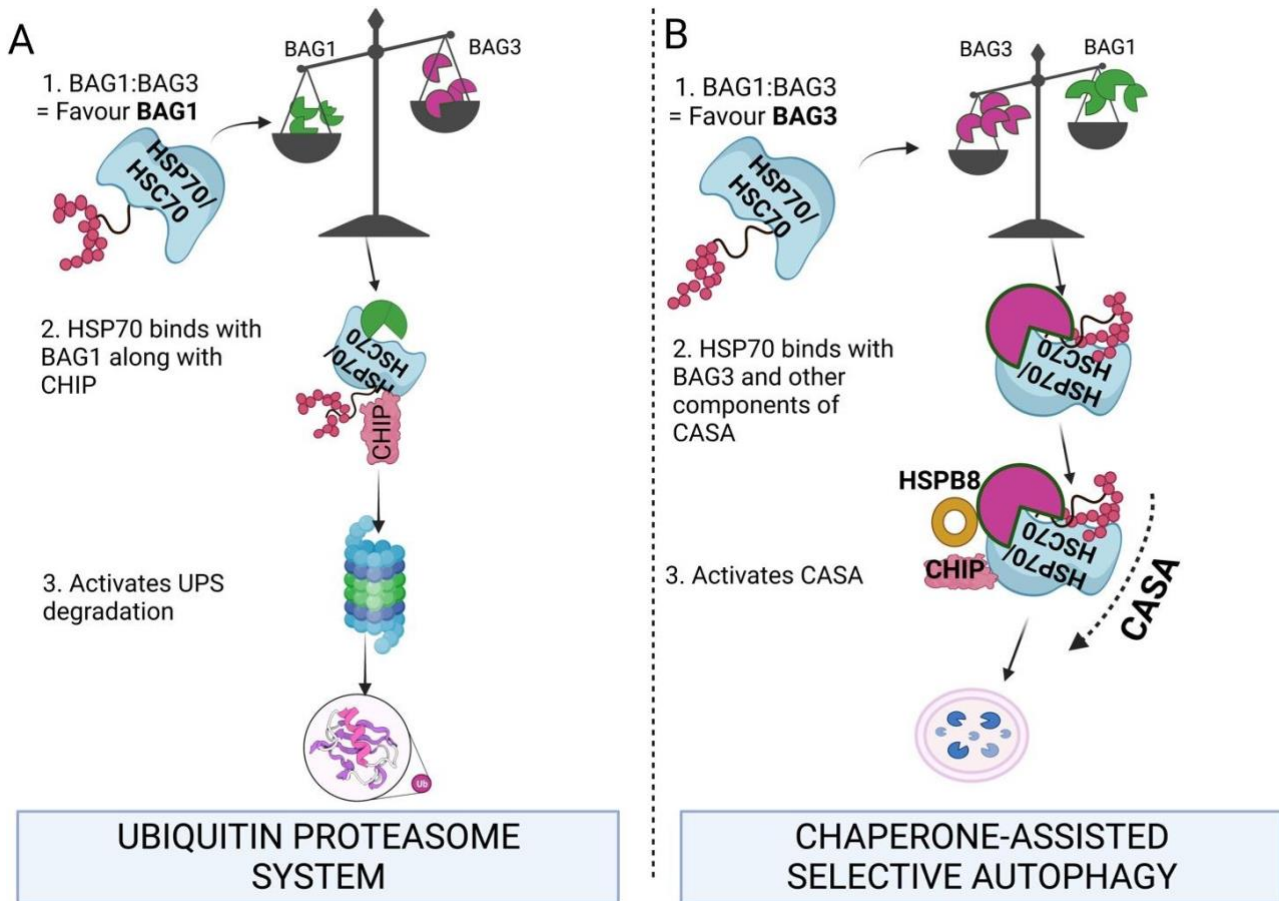
*Figure 1.7:* **BAG proteins regulated transition from proteasomal degradation to autophagosomal degradation.**

A) When BAG1 level is elevated (1) Ratio of BAG1 is higher than BAG3 (2) HSP70 bound non-native protein delivered to BAG1 and bind with CHIP and other proteins for further degradation (3) These degraded or non-native proteins get cleared by UPS pathway. B) When BAG3 level is elevated (1) When BAG3 is higher the clearance system shifts to CASA (2) HSP70 brings non-native proteins to the BAG3 and later on other components of CASA also participate (3) These misfolded protein further delivered to CASA for further processing which to be next rerouted to autophagosomes for degradation. Image has been generated by using BioRender.

## 2 OBJECTIVE OF THIS STUDY

HSPB8 has a unique role in the cellular response to stress and functions as a mediator in presenting misfolded substrates to HSP70 for subsequent processing. A strong correlation between the amount of HSPB8 and misfolded proteins within SGs has been documented (Ganassi et al., 2016). The final fate of misfolded proteins depends on the recruitment facilitated by HSPB8 of BAG3 (Carra et al., 2008). The binding of BAG3 and SQSTM1 leads to the recruitment of HSPB8, BAG3, and HSP70 to substrates designated for specific autophagy, which are commonly referred to as CASA (Crippa et al., 2010a; Gamerdinger et al., 2011). The fusion step between autophagosomes and lysosomes is a critical step in this pathway, and studies suggest that HSPB8 is required for this process (Crippa et al., 2010; XC Li et al., 2017; Rusmini et al., 2017). On the one hand, multiple studies have demonstrated that HSPB8 is implicated in the clearance of protein aggregates resulting from genes associated with ALS (Crippa et al., 2010b; Crippa et al., 2016; Carra et al., 2013; Rusmini et al., 2013, 2015).

The predominant mutations in the HSPB8 gene have been found in individuals diagnosed with Charcot-Marie-Tooth (CMT) type 2L neuropathy, as reported by Nakhro et al. (2013) and Tang et al. (2005). Additionally, these mutations are also associated with distal hereditary motor neuropathy (dHMN) type 2A, as indicated by studies conducted by Al-Tahan et al. (2019), Ghaoui et al. (2016), and Irobi et al. (2004). Several studies have provided compelling evidence implicating HSPB8 in the clearance of protein aggregates linked to ALS-associated genes. Notably, the works of Crippa et al. (2010b, 2016), Carra et al. (2013), and Rusmini et al. (2013, 2015) have consistently demonstrated HSPB8's involvement in the removal of these aggregates.

Studies propose that such genetic mutations in the HSPB8 gene impede proteostasis, SG response and autophagy, highlighting these pathways as crucial for long motor neurons situated in the peripheral nervous system (Varlet et al., 2017). Interestingly, ALS autopsy mRNA analysis showed elevated HSPB8 expression in spinal cord samples compared to age-matched healthy controls (Anagnostou et al., 2010).

We thus wanted to address the function of HSPB8 in human motor neurons. For this, we investigated whether and how HSPB8 loss of function affect human induced pluripotent stem cells (iPSC)-derived motor neurons. Pathophysiologically, we speculate that HSPB8 KO affects the dynamics of SGs and that this effect is associated with alterations in proteostasis and heightened cellular demise. Furthermore, another objective of this research was to examine the proteins involved in CASA, and their regulation in case of HSPB8 loss and whether these affect the aggregation of one key aggregating protein in ALS, namely Fused in sarcoma (FUS), as any dysfunction in this process may lead to neurodegenerative disorders.

# 3 MATERIALS AND METHODS

## 3.1 Materials

### 3.1.1 Instruments

*Table 3.1*: **Instrument**

| Name | Company |
|---|---|
| Analytical Balance — CP225D-0CE | Satorius AG, Germany |
| Axiovert 200M with Apotome | Carl Zeiss, Germany |
| Balance SBA 52 | Scaltec Instruments GmbH, Germany |
| CASY Cell Counter and Analyzer TT+ | Innovatis Technologies Inc., USA |
| Centrifuge | Labnet international,USA |
| Centrifuge 5403 | Eppendorf, Germanz |
| Centrifuge Biofuge Pico | Thermo Fisher Scientific, USA |
| Centrifuge Biofuge Primo | Thermo Fisher Scientific, USA |
| Centrifuge Hermle Z 283 K | Hermle Labortechnik GmbH, Germany |
| Cooling box with rotor | Privileg, Germany |
| Electrophoresis Cell Criterion | Bio-Rad Laboratories, USA |
| Gel documentation Dunkelhaube D4 | Biostep GmbH, Germany |
| Gel electrophoresis system E865 | Consort, Belgium |
| Gel electrophoresis system PSU EPS600 | Pfizer, New York, USA |
| Imager LAS3000 | Fujifilm, Tokyo, Japan |
| Incubating orbital shaker 3500l | VWR International, USA |
| Incubator Heracell 150 | Thermo Fisher Scientific, USA |
| Incubator Heracell 150i | Thermo Fisher Scientific, USA |
| Laminar flow hood Clean Wizard V 100 | Kojair Tech Oy, Vilppula, Finland |
| Laminar flow hood Herasafe HS | Thermo Fisher Scientific, USA |
| Laser Scanning Confocal Microscope LSM780 | Carl Zeiss, Germany |
| Laser Scanning Confocal Microscope LSM  900 with Airyscan 2 | Carl Zeiss, Germany |
| Light Cycler Nano | Roche, Switzerland |
| Light Cycler 480II | Roche, Switzerland |

| | |
|---|---|
| Manual pipettes | Eppendorf, Germany |
| Microplate reader Sunrise | Tecan Group, Switzerland |
| Microplate reader Spark | Tecan Group, Switzerland |
| Multichannel pipette | Brand GmbH & Co. KG, Germany |
| Odyssey 9120 Fluorescent Imager<br>Odyssey XF Imager | LI-COR Biosciences, USA<br>LI-COR Biosciences, USA |
| Pipette 35lpha35p35bl, PIPETBOY | Integra Biosciences, Switzerland |
| Pipette set | Eppendorf, Germany |
| PCR cycler – Mastercycler gradient | Eppendorf, Germany |
| PowerPac Universal Power Supply | Bio-Rad Laboratories, USA |
| Real time PCR cycler MX3000P | Agilent, USA |
| RotaMax 150 Shaker | Heidolph, Germany |
| Shaking incubator 3032 | GFL, Germany |
| Spark Multimode Microplate Reader | Tecan Group, Switzerland |
| Stereo preparation microscope<br>Stemi DV4SteREO CL 1500 ECO | Carl Zeiss, Germany |
| Thermo shaker PST-60HL-4 Lab4You | Dewert Labortechnik, Germany |
| Thermomixer – Thermomixer 5436 | Eppendorf, Germany |
| Thermomixer – Thermomixer Comfort | Eppendorf, Germany |
| Trans-Blot Turbo Transfer System | Bio-Rad Laboratories, USA |
| Transiluminator – BioView UST 30M-8R | Biostep GmbH, Germany |
| Water bath | Memmert GmbH & Co. KG, Germany |
| Water bath — Julambo SW22 | JULAMBO Labortechnik GmbH, Germany |

### 3.1.2 Chemicals and reagents

Table 3.2: **Chemicals and reagents**

| Name | Company |
|---|---|
| 4-15% Criterion TGX Precast midiproteins gels | Bio-Rad Laboratories, USA |
| Acetic Acid | Sigma-Aldrich, USA |
| Agarose | Biozym Biotech Trading GmbH, Germany |
| Ampicillin | Carl Roth GmbH & Co. KG, Germany |

| Bromophenol Blue | Sigma-Aldrich, USA |
|---|---|
| BSA Fraction V | Thermo Fisher Scientific, USA |
| CASY Clean Buffer | Roche, Switzerland |
| CASY Ton Buffer | Roche, Switzerland |
| Complete Protease Inhibitor Cocktail Tablets | Sigma-Aldrich, USA |
| DAPI Fluoromount G | SouthernBiotech, USA |
| Dithiothreitol | Sigma-Aldrich, USA |
| DMSO | Sigma-Aldrich, USA |
| Doxycyclin Hyclate | Sigma-Aldrich, USA |
| dNTP Mix, 10 µM each | Thermo Fisher Scientific, USA |
| D-Sorbitol | Sigma-Aldrich, USA |
| EDTA | Thermo Fischer Scientific, USA |
| Ethanol | VWR International GmbH, Germany |
| Etoposide | Sigma-Aldrich, USA |
| Fluoromount | SouthernBiotech, USA |
| HEPES Buffer | Thermo Fischer Scientific, USA |
| Hydrogen peroxide 30% (w/w) in H2O | Sigma-Aldrich, USA |
| Isopropanol | VWR International GmbH, Germany |
| Laminin | Sigma-Aldrich, USA |
| Matrigel Matrix | Corning Inc., USA |
| NaCl | Merck Group, Germany |
| Paraformaldehyde 4% solution | Seipt, Klinikapotheke UKD, Germany |
| PCR Grade Water | Biotechrabbit, Germany |
| Phosphate Buffered Saline, pH 7.4 | Thermo Fischer Scientific, USA |
| PhosSTOP Phosphatase Inhibitor Tablets | Sigma-Aldrich, USA |
| Pierce™ Protein-Free (PBS) Blocking Buffer | Thermo Fisher Scientific, USA |
| Ponceau S-Lösung | Sigma-Aldrich, USA |
| Poly-L-Ornithine | Sigma-Aldrich, USA |
| Precision Plus Protein Dual Xtra Prestained Protein Standard | Bio-Rad Laboratories, USA |
| RIPA Lysis and Extraction Buffer | Thermo Fischer Scientific, USA |
| Revert™ 700 Total Protein Stain Kits for Western Blot Normalization | Thermo Fisher Scientific, USA |
| Skim milk powder | Sigma-Aldrich, USA |
| Sodium Arsenite | Sigma-Aldrich, USA |
| Sodium Bicarbonate | Thermo Fischer Scientific, USA |
| Sodium Dodecyl Sulphate | Carl Roth GmbH & Co. KG, Germany |

| | |
|---|---|
| Sterile Rnase-free water | Thermo Fisher Scientific, USA |
| Tris-HCL | Carl Roth GmbH & Co. KG, Germany |
| TritonX-100 | Thermo Fisher Scientific, USA |
| Tween 20 | Serva Elektrophoresis GmbH,GERMANY |

## 3.1.3 Commercially available kits

Table 3.3: **Commercially available kits**

| Name | Company |
|---|---|
| ECL Prime Western Blotting Detection Reagent | GE Healthcare, USA |
| Expand High Fidelity PCR System | Sigma-Aldrich, Germany |
| miRNeasy Mini Kit | Qiagen, Germany |
| FastStart Universal SYBR Green Master Mix (ROX) | Roche, Switzerland |
| High-Capacity cDNA Reverse Transcription Kit | Thermo Fischer Scientific, USA |
| Pierce BCA Protein Assay Kit | Thermo Fischer Scientific, USA |
| PrestoBlue Viability Assay | Thermo Fischer Scientific, USA |
| Premo Autophagy Assays with Sensor Tandem Sensor RFP-GFP-LC3B | Thermo Fischer Scientific, USA |
| QIAquick Gel Extraction Kit | Qiagen, Germany |
| QuantiTect Reverse Transcription Kit | Qiagen, Germany |
| QuantiTect Syber Green PCR Kit | Qiagen, Germany |
| Quick-RNA Miniprep Kit | Zymo Research, USA |
| Trans-Blot Turbo Midi Nitrocellulose Transfer Packs | Bio-Rad Laboratories, USA |
| ZR Plasmid Miniprep Kit | Zymo Research, USA |

### 3.1.4 Cell culture media and supplements

*Table 3.4:* **Cell culture media and supplements**

| Name | Company |
|---|---|
| Accutase | Sigma-Aldrich, USA |
| B27 Supplement, w/o vitamin A | Thermo Fischer Scientific, USA |
| β-Mercaptoethanol | Thermo Fischer Scientific, USA |
| DMEM High Glucose Medium | Thermo Fischer Scientific, USA |
| DMEM/F12 Medium | Thermo Fischer Scientific, USA |
| Fetal Bovine Serum | Sigma-Aldrich, USA |
| GlutaMAX Supplement | Thermo Fischer Scientific, USA |
| MEM Non-Essential Amino Acid Solution | Thermo Fischer Scientific, USA |
| N2 Supplement | Thermo Fischer Scientific, USA |
| Neurobasal Medium | Thermo Fischer Scientific, USA |
| Penicillin and Streptomycin | Thermo Fischer Scientific, USA |
| Penicillin-Streptomycin-Glutamine | Thermo Fischer Scientific, USA |
| Trypsin | Thermo Fischer Scientific, USA |

### 3.1.5 Growth factors and small molecules

*Table 3.5***: Growth factors and small molecules**

| Name | Company |
|---|---|
| Activin A | Peprotech, USA |
| Ascorbic Acid | Sigma-Aldrich, USA |
| BDNF | Promega, USA |
| Chiron 99021 | Cayman Chemical, USA |
| DBcAMP | Sigma-Aldrich, USA |
| GDNF | Sigma-Aldrich, USA |
| Retinoic Acid | Sigma-Aldrich, USA |
| TGFβ-3 | Promega, USA |

### 3.1.6 Cell lines

All the cell lines used in this study were previously generated and characterized in the Hermann laboratory or in the laboratories of the collaborators or were purchased from a commercially available source. The detailed information is presented in the Table 3.6. All the cell lines were routinely tested for mycoplasma contamination.

*Table 3.6*: **Cell lines**

| Cell line | Description (Sex/age at biopsy/genotype) | Characterized in |
|---|---|---|
| KOLF-WT | M/55-59Y/healthy Control | Wellcome Trust Sanger Institute; Hinxton; United Kingdom |
| KOLF-HSPB8KO | M/55-59Y/genetically modified Via CRISPR/CAS9 | Wellcome Trust Sanger Institute; Hinxton; United Kingdom |
| iPSC SL FUS-P525L EGFP | F/58/genetically modified FUS-P52L-EGFP | (Naumann et al., 2018) |
| iPSC SL FUS-WT-EGFP | F/58/isogenically modified to FUS-WT-EGFP | |
| iPSC LL FUS-P525L-EGFP | M/n.a./ genetically modified FUS-P525L-EGFP | (Wheeler et al., 2019) |
| iPSC LL FUS-WT-EGFP | M/n.a./ isogenically modified to FUS-WT-EGFP | |
| iPSC CTR1 | F/48/healthy control | (Japtok et al., 2015 ; Naumann et al., 2018) |
| iPSC CTR2 | M/60/healthy control | (Japtok et al., 2015 ; Naumann et al., 2018) |
| iPSC CTR3 | F/45/healthy control | |
| iPSC CTR4 | F/50/healthy control | |
| iPSC FUS-R521C | F/58/p. R521C | (Japtok et al., 2015 ; Naumann et al., 2018) |
| HSPB8-myc Flip | Doxycycline/tetracycline dependent overexpression cassette of HSPB8 | Kind gift by Professor Dr. S Carra (University of Modena and Reggio Emilia, Italy) |

## 3.1.7 Antibodies

Table 3.7: **Primary antibodies**

| Name | Host | Dilution | Company | Reference No. |
|---|---|---|---|---|
| BAG1 | rabbit | 1:1000 | abcam | ab32109 |
| BAG3 | rabbit | 1:1000 | abcam | ab47124 |
| FUS | rabbit | 1:2000 | Sigma- Aldrich | HPA008784 |
| G3BP1 | rabbit | 1:500 | abcam | ab181150 |
| HSPB8 | rabbit | 1:1000 | abcam | ab151552 |
| HSPB8 | rabbit | 1:1000 | Sigma-Aldrich | HPA015876 |
| HSPB8 | rabbit | 1:1000 | Sigma-Aldrich | SAB2101100 |
| HSPB8 | rabbit | 1:1000 | Invitrogen | PA5-76780 |
| HSPB8 | rabbit | 1:1000 | Cell signalling | 3059 |
| HSP40 | rabbit | 1:1000 | Enzo | ADI-SPA-400-D |
| HSP70/HSP72 (C92F3A-5) | mouse | 1:1000 | Enzo | ADI-SPA-810 |
| HSP73(1B5) | rat | 1:1000 | Enzo | ADI-SPA-815-D |
| HSP90 | rabbit | 1:1000 | Cell Signaling Technoloy | 4874S |
| HSP90 | rabbit | 1:200 | abcam | ab13492 |
| LAMP2 | Mouse | 1:50 | abcam | ab25631 |
| LC3B(E5Q2K) | Mouse | 1:1000 | Cell signaling | 83506S |
| MAP2 | chicken | 1:2000 | abcam | ab5392 |
| Anti-P62/SQSTM1 | rabbit | 1:1000 | Sigma-Aldrich | P0067 |
| TIAR | mouse | 1:500 | BD Biosciences | 610352 |
| β-Actin | mouse | 1:10.000 | Sigma-Aldrich | A5441 |

Table 3.8: **Secondary antibodies**

| Name | Host | Dilution | Company | Reference No. |
|---|---|---|---|---|
| Goat anti-Chicken IgG (H+L) | Alexa Fluor 647 | 1:500 | Invitrogen | A21449 |
| Goat anti-Mouse IgG | Alexa Fluor 488 | 1:500 | Invitrogen | A11029 |

| | | | | |
|---|---|---|---|---|
| (H+L) | | | | |
| Goat anti-Mouse IgG (H+L) | Alexa Fluor 568 | 1:500 | Invitrogen | A11031 |
| Goat anti-Rabbit IgG (H+L) | Alexa Fluor 488 | 1:500 | Invitrogen | A11034 |
| Goat anti-Rabbit IgG (H+L) | Alexa Fluor 568 | 1:500 | Invitrogen | A11036 |
| Goat anti-Rat IgG (H+L) | Alexa Fluor 488 | 1:500 | Invitrogen | A11006 |
| Goat anti-Mouse IgG | DyLight 680 | 1:10 000 | Rockland Immunochemicals | 610-144-121 |
| Goat anti-Mouse IgG | DyLight 800 | 1:10 000 | Rockland Immunochemicals | 610-145-003 |
| Goat anti-Rabbit IgG | DyLight 800 | 1:10 000 | Rockland Immunochemicals | 611-145-122 |
| Goat anti-Rabbit IgG | DyLight 680 | 1:10 000 | Rockland Immunochemicals | 611-144-002 |
| Goat anti-Rat IgG | DyLight 680 | 1:10 000 | Rockland Immunochemicals | 612-144-002 |
| Goat anti-Rat IgG | DyLight 800 | 1:10 000 | Rockland Immunochemicals | 612-145-002 |

### 3.1.8 Primers

Table 3.9: *Primers*

| Name | Forward Primer | Reverse Primer |
|---|---|---|
| GAPDH | CGGAGTCAACGGATTTGGTCGTAT | ATTGATGACAAGCTTCCCGTTC |
| HSPB8-201 | CCCTGGAAAGTGTGTGTGAATG | GCAGGAAGCTGGATTTTCTTTG |
| HSPB8-202 | AAGCCAGAGGAGTTGATGGTG | CAGTAACGATTTTGTCTGCCTGT |
| HSPB8-204 | CCAGGCACCCTAAGGTCGG | CTCTGCAGGAAGCCAGACACC |
| HSPB8-206 | GAAGAGAAACAGCAAGAAGGTGG | ACCTCTGCAGGAAGCCTCAC |
| HSPB8-207 | GAAGAGAAACAGCAAGAAGGTGG | ACGATTTTGTTGGATTTTCTTTGTGAA |
| HSPB8-210 | GAAGAGAAACAGCAAGAAGGTGG | TCACCTGCTGCCTGTTTACTT |
| HSPB8 gDNA | TGGTACAACACATGGAAGATTTGG | GCACCGAGCAGATGAGATGA |

## 3.1.9 Consumables

*Table 3.10* **: Consumables**

| Name | Company |
|---|---|
| Cell Culture Flasks 25ml, 75ml | Corning, USA |
| Cell Culture Plates (4-, 6-, 12-, 24-well) | Sarstedt, Germany; Thermo Fischer Scientific, USA; TPP Techno Plastic Products AG, Switzerland; Corning, USA |
| Cell Scraper | Carl Roth, Germany |
| Conical Bottom Centrifuge Tubes 15ml, 50ml | Greiner Bio-One, Austria |
| Costar® Stripette® 2-50ml | Corning, USA |
| Falcon® Round-Bottom Tubes with Cell Strainer Cap | STEMCELL Technologies, Canada |
| Glass Cover Slips | Thermo Fischer Scientific, USA |
| MicroAmp™ Reaction Tube, 0.2ml | Thermo Fischer Scientific, USA |
| Minisart® Syringe Filters 0.45µm, 0.2µm | Sartorius, Germany |
| Nalgene® Freezing Container | Sigma Aldrich, Germany |
| PVDF Syringe Filters, 0.45µm, 0.2µm | Sigma-Aldrich, USA |
| Superfrost® Microscope Slides | Thermo Fischer Scientific, USA |
| µ-Slide 8 Well Glass Bottom | Ibidi, Germany |

## 3.1.10 Software

*Table 3.11* **: Software**

| Software | Function | Source |
|---|---|---|
| Adobe Illustrator CC 2017 21.0 | Graphics design | Adobe Systems, USA |
| CellProfiler 2.2.0 | Image analysis | Open source (Carpenter et al., 2006) |
| Enrichr | Analysis and visualization of gene lists | Open source (Chen et al.,2013 ; Kuleshov et al., 2016) |
| FiJi ImageJ 2.2.0 | Image and video analysis | Open source (Schindelin et al., 2009) |
| GeneMANIA | Gene network prediction | Open source https://genemania.org/ |
| GraphPad Prism 8 | Statistical analysis | GraphPad Software Inc.,USA |

| Image Studio Lite 5.2 | Western Blot quantification | LI-COR Bioesciences, USA |
|---|---|---|
| KNIME 3.7.2 | Data handling | KNIME AG, Switzerland |
| LightCycler Nano | qPCR data analysis | Roche, Switzerland |
| Zen 2011 | Protein-protein interaction network analysis | Open source (von Mering et al., 2003) |

## 3.2 METHODS

### 3.2.1 Filter retardation assay

The cells cultured in a 6-well plate were washed once with PBS followed by removing PBS and adding 200ul cold activated RIPA Buffer supplemented with cOmplete Protease Inhibitor Cocktail Tablets and PhosSTOP Phosphatase Inhibitor Tablets (Table 3.2). Cells were scraped off of the surface of the dish using a scraper and incubated on ice with RIPA buffer on the shaker for 20 minutes. The cell suspension was then centrifuged at 13,000 x g for 15 minutes at 4°C. The supernatant containing protein was transferred to a fresh tube. 15ug of samples has been diluted in RIPA to make the final Volume to 120ul. Meanwhile the acetate cellulose membrane were incubated in 20% methanol and whatmann paper has been soaked in RIPA. Incubating the membrane in methanol until it turn gray followed by discarding methanol and adding RIPA for 30 seconds. When the membrane was ready, loading was done followed by vaccum suction of the samples. After all the samples has been completely soaked to the membrane. Membrane has been obtained by disassembling the device. Membrane has been washed with 20% methanol, followed by a quick wash with TBS-T buffer. Membrane has been checked with Ponceau Staining or Total Protein staining (Table 3.2). After the total protein staining, membrane was incubated in the blocking buffer (5% skim milk powder in TBS-T buffer: 20 mM Tris, 137 mM NaCl, 0.1% Tween 20, pH 7.5) for 1 hour at the room temperature with mild shaking. The appropriate primary antibody dilution was prepared in 3% skim milk in TBS-T buffer and after the blocking step the membrane was incubated with this solution for 1hour with mild shaking. The membrane was washed 3 times for 5 minutes with TBS-T buffer followed by incubation for 1 hour at the room temperature with mild shaking in the darkness in an appropriate secondary antibody diluted in 3% skim milk in TBS-T. Next, the membrane was washed 3 times for 5 minutes with TBS-T buffer and 1 time for 5 minutes with TBS buffer without Tween 20. Depending on the used secondary antibodies and on the detection system, the membrane was either let to dry and then immunofluorescence was detected using

Odyssey XF Imager (Table 3.1). The immunofluorescence images were analyzed and quantified using Image Studio Lite software.

### 3.2.2 Immunofluorescence Stainings

For immunofluorescence staining, the cells were seeded on PLO/laminin coated µ-Slide 8-well chamber slides (see section 3.2.5.2) at the density of 50,000 cells per cm$^2$. The cells were washed once with PBS and fixed with ice-cold 4% paraformaldehyde solution pH 7.4 for 10 minutes at the room temperature. After washing the cells 3 times with PBS, the cell membrane was permabilized by incubating the cells for 10 minutes at the room temperature with 0.2% (v/v) TritonX-100 in PBS. Next, blocking of unspecific biding sites was performed by incubating the cells for 1 hour at the room temperature with Pierce™ Protein-Free Blocking Buffer (Table 3.2). An appropriate dilution of primary antibodies was prepared in the blocking buffer and the cells were incubated with this solution at 4°C overnight. On the following day, the cells were washed 3 times for 5 minutes with PBS. Next, the secondary antibodies were diluted in the blocking buffer and added to the cells. The cells were then incubated for 1 hour at the room temperature in the darkness. The cells were washed 3 times for 5 minutes with PBS and stained were mounted with DAPI Fluoromount G later they were stored at 4°C for future usage.

### 3.2.3 Protein isolation and Western Blot

### 3.2.3.1 Protein isolation

In order to harvest the total protein fraction, the cells cultured in a 6-well plate were washed once with PBS followed by removing PBS and adding 90-200ul cold activated RIPA Buffer supplemented with cOmplete Protease Inhibitor Cocktail Tablets and PhosSTOP Phosphatase Inhibitor Tablets (Table 3.2). Cells were scraped off of the surface of the dish using a scraper and incubated on ice with RIPA buffer on the shaker for 20 minutes. The cell suspension was then centrifuged at 13,000 x g for 15 minutes at 4°C. The supernatant containing protein was transferred to a fresh tube and stored at -80°C. Alternatively cells were collected in pellet by centrifugation and frozen at -80°C later these pellets were suspended in 90-200ul activated RIPA buffer followed by the incubation on ice with shaking for 40-60 minutes. The samples were then centrifuged at 13,000 x g for 15 minutes at 4°C. The supernatant was collected and stored at -80°C.

### 3.2.3.2 Protein concentration measurement

To measure protein concentration in the prepared samples, Pierce BCA Protein Assay Kit (Table 3.3) was used according to the manufacturer instructions. First, samples for standard curve were prepared by diluting 2 mg/ml BSA stock solution with water to the range of concentrations between 0 and 10 µg/ml. Next, the protein samples were diluted 5 times using water. After that, 10 µl of protein samples and samples for standard curve were pipetted in triplicate into 96-well plate and then 200 µl of BCA reagent was added to each well. A blank sample was prepared by mixing 10 µl of RIPA buffer and 200 µl BCA reagent. The plate was then incubated for 30 minutes in the darkness ant 37°C and shaking at 300 RPM. Colorimetric measurement was performed using microplate reader at the wavelength 570 nm. The protein concentration was calculated using a standard curve method.

### 3.2.3.3 Western blot

To prepare Western blot samples, the volume of protein sample containing 20 µg of total protein was mixed with 6 µl of 5X SDS loading buffer (0.25% bromophenol blue, 0.5M dithiothreitol, 50% glycerol, 10% SDS and 0.25 M Tris-HCl pH 6.8) and filled up with water to the final volume of 30 µl. 4-15% Polyacrylamid Criterion Precast Midi Gel (Table 3.2) was placed in a Criterion Electrophoresis Cell (Table 3.1) and the cell was filled with SDS running buffer (25 mM Tris, 0.2 M Glycine, 0.01% SDS). The samples and the Protein Plus Marker (Table 3.2) were pipetted on the gel and the electrophoresis was performed first at 100 V for 10 minutes and then at 200 V for 45 minutes. The gel was then removed from the cast and a transfer stack was assembled using the Trans-Blot Turbo Midi Nitrocellulose Transfer Packs (Table 3.3) according to the manufacturer instructions. The stack was placed in the Trans-Blot Turbo Transfer System (Table 3.1) and the transfer was performed for 7 minutes at 25 V and 1.3 A. After the transfer is completed membrane was dried for 1 hour to allow protein binding tightly to the membrane, preventing potential signal loss. After this the membrane was incubated in the blocking buffer (5% skim milk powder in TBS-T buffer: 20 mM Tris, 137 mM NaCl, 0.1% Tween 20, pH 7.5) for 1 hour at the room temperature with mild shaking. The appropriate primary antibody dilution was prepared in 3% skim milk in TBS-T buffer and after the blocking step the membrane was incubated with this solution overnight at 4°C with mild shaking. On the following day, the membrane was washed 3 times for 5 minutes with TBS-T buffer. Then the membrane was incubated for 1 hour at the room temperature with mild shaking in the darkness with an appropriate secondary antibody dilution prepared in 3% skim milk in TBS-T. Next, the membrane was washed 3 times for 5 minutes with TBS-T buffer and 1 time for 5 minutes with TBS buffer without Tween 20. Depending on the used

secondary antibodies and on the detection system, the membrane was either let to dry and then immunofluorescence was detected using Odyssey 9120 Fluorescent Imager (Table 3.1). The immunofluorescence images were analyzed and quantified using Image Studio Lite software

### 3.2.4 qRNA isolation, reverse transcription and quantitative polymerase chain reaction

#### 3.2.4.1 RNA isolation and reverse transcription

If not described otherwise, RNA isolation was performed using Quick-RNA Miniprep Kit (Table 3.3) according to the manufacturer instructions. RNA concentration was measured using Qubit fluorometer or a microplate reader with NanoQuant plate. For reverse transcription High Capacity cDNA Synthesis Kit (Table 3.3) was used. The reaction was prepared by mixing 1 µg of RNA with 2 µl of 10X RT Buffer, 0.8 µl of 25X dNTP Mix (100 mM), 2 µl of 10X Random Primers and 1 µl of Reverse Transcriptase. The mix was then filled up to the final reaction volume of 20 µl with Rnase free PCR Grade Water and the reaction was performed with the thermal profile described in the table 3.12.

*Table 3.12*: **Thermal Profile of the Reverse Transcription Reaction**

| Temperature | Time |
|-------------|-------------|
| 25°C | 10 minutes |
| 37°C | 120 minutes |
| 85°C | 5 minutes |
| 4°C | hold |

#### 3.2.4.2 Quantitative polymerase chain reaction

For quantitative polymerase chain reaction (qPCR) FastStart SYBR Green Kit (Table 3.3) was used. The master mix was prepared by mixing 25 µl of FastStart SYBR Green Master,1.5 µl of 10 µM Primer Forward (final concentration 300 nM), 1.5 µl of 10 µM Primer Reverse (final concentration 300 nM) and 17 µl of PCR Grade Water. Next, 5 µl of cDNA synthesized as described in the section 2.2.3.1 was pipetted into MicroAmp™ Reaction Tube and 45 µl of an appropriate master mix was added. The reaction was performed using LightCycler Nano or Light Cycler 480II (Table 3.1) with the thermal profile described in the table 3.13.

*Table 3.13:* **Thermal Profile of qPCR Reaction**

| Step | | Temperature | Time |
|---|---|---|---|
| Initial Denaturation | | 95°C | 10 minutes |
| | Denaturation | 95°C | 20 seconds |
| 40x | AnnealingElongation | varying | 20 seconds |
| | | 72°C | 20 seconds |
| Pre-Melt Hold | | 95°C (4°C/sec) | 10 seconds |
| Initial Melting | | 65°C (4°C/sec) | 1 minute |
| Final Melting | | 95°C (0.1°C/sec) | 1 second |

## 3.2.5 Cell culture

All the cell lines were cultured in the cell culture incubator at 37°C, with a stable level of 5% $CO_2$ and 21% $O_2$. The cell culture work was performed under sterile conditions at the laminar flow hood. All the media and solutions applied to the cells were pre-warmed to 37°C. These conditions were used unless indicated otherwise.

## 3.2.5.1 Cell culture media

All the basic media and supplements were handled and stored according to the manufacturer instructions. Growth factors and small molecules were aliquoted and stored at — 20°C and freshly added to each batch of medium.

*Table 3.14*: **Cell culture media formulation**

| Name | Formulation |
| --- | --- |
| N2B27 Basic Medium | 48.75 % (v/v) DMEM/F12 48.75% (v/v) + Neruobasal medium 1% (v/v) +Penicillin Streptomycin-Glutamine + 1% (v/v) B27 Supplement, w/o vitamin A 0.5% (v/v) + N2 Supplement |
| NPC Expansion Medium | N2B27 basic medium + 3 µM CHIR99021 + 150 µM Ascorbic Acid + 0.5 µM Purmorphamine |
| NPC Patterning Medium | N2B27 basic medium + 1 ng/ml BDNF + 1 ng/ml GDNF + 200 µM Ascorbic Acid + 0.5 µM Purmorphamine + 1 µM Retinoic Acid |
| Maturation Medium for Spinal Motor Neurons | N2B27 basic medium + 2 ng/ml BDNF + 2 ng/ml GDNF + 200 µM Ascorbic Acid + 100 µM DBcAMP + 1 ng/ml TGFβ-3 |
| Freezing Medium for NPC | 90% (v/v) N2B27 basic medium 10% (v/v) DMSO |
| HeLa Cells Medium | 89% (v/v) DMEM High Glucose Medium 10% (v/v) Fetal Bovine Serum +1% Penicillin and Streptomycin |

### 3.2.5.2 Cell culture dish coatings

Coating of the cell culture dishes was performed for enhanced cell attachment and growth in monolayer. The following volumes of the respective coating solutions were used: for 6-well plates 1 ml/well, for 24-well plates 500 µl/well and for µ- slide 8 well 200 µl/well.

### 3.2.5.2.1 Matrigel® coating

Matrigel® was thawed overnight at 4°C, pre-diluted with DMEM/F12 medium to the protein concentration of 2 mg/ml, aliquoted and stored at -20°C. For coating, Matrigel® was further diluted to the final concentration of 100 µg/ml in DMEM/F12 medium and this solution was added to the dish. The dish was then incubated for either 1 hour at 37° C or overnight at 4°C. Prior the use, Matrigel®

solution was removed and appropriate cell culture medium was added immediately to avoid drying of the coated dish.

In the first step, the dishes were pre-coated with poly-L-ornithine (PLO). For this purpose, 15% (v/v) PLO solution in PBS was added to the dishes, which were then incubated overnight at 37°C in the shaking incubator. Next, the plates were washed 3 times with PBS and were allowed to dry at the room temperature. This was followed by and overnight incubation with 1% (V/V) Laminin solution in PBS at 37°C in the shaking incubator. The dishes were then washed 2 times with PBS and the appropriate medium was added immediately to prevent drying.

## 3.2.6 Cell counting

Cell count using CASY cell counter was performed according to the manufacturer instructions. Briefly, cell suspension at the appropriate dilution was prepared in 10 ml of CASY Tone Buffer and 3 measurements were taken using CASY resulting in the readout of cell number/ml as well as cell viability.

## 3.2.7 Expansion and differentiation of neuronal progenitor cells

### 3.2.7.1 Expansion

Neuronal progenitor cells (NPC) of ventral-posterior characteristic were generated from iPSC using small-molecule approach and characterized previously in the Hermann laboratory according to protocol published by Reinhardt et al., 2013. For the maintenance, NPC were expanded on Matrigel®-coated 6-well plates in the NPC Expansion Medium. The medium was changed every 2-3 days until the culture reached 80-90% of confluence and then the cells were passaged. To passage the culture, the cells were washed once with PBS and then incubated with accutase solution (0.5 ml/well of a 6-well plate) for 5 minutes in 37°C. Next, 1 ml/well of N2B27 Basic Medium was added and the cell suspension was gently pipetted up and down to assure complete detachment of the cells. The cell suspension was then collected and centrifuged at 1200 rotations per minutes (RPM) for 5 minutes. The supernatant was discarded and the cell pellet was re-suspended in an appropriate volume of N2B27 Basic Medium. The cells were plated at 1:10 ratio on the freshly prepared Matrigel®-coated plates (see section 3.2.5.2.1) in the NPC expansion medium.

### 3.2.7.2 Differentiation to spinal motor neurons

To induce the differentiation of NPC into spinal motor neurons (MN), NPC were passaged as described in the section 3.2.7.1 and seeded on the Matrigel®-coated dish in the NPC Patterning Medium (day 0 of differentiation). The cells were maintained in the NPC Patterning Medium for 6 following days, with medium change every 2-3 days. On day 6, the medium was changed to the Maturation Medium for Motor Neurons with an addition of 5 ng/ml Activin A. On day 7 of the differentiation, the cells were split as described previously and plated on PLO/Laminin coated dishes (see section 3.2.5.2.2 ) at the density of 60,000 – 75,000 cells per cm$^2$ in the Maturation Medium for Motor Neurons. MN were cultivated until at least day 28 of differentiation in the Maturation Medium for Motor Neurons and the medium was changed every other day.

### 3.2.8 Cultivation of HeLa cells

HeLa cells were maintained in appropriate media described in the section 3.2.5.1 with the medium changed every 2-3 days, until the culture reached 80-90% confluence and then the cells were split. To do that, the cells were washed once with PBS and 0.5 ml of 0.25% trypsin per 1 well of a 6-well plate was added. Next, the cells were incubated for 5 minutes at 37°C and after that, the respective culture medium with 10% FBS was added to the cells. After gentle pipetting up and down, the cells were transferred to a 15 ml falcon tube and centrifuged at 1200 RPM for 5 minutes. The supernatant was discarded and the pellet was re-suspended in the appropriate volume of fresh medium. The cells were seeded on the new dish at the ratio 1:10.

### 3.2.9 Freezing and thawing of the cells

For the long-term storage of all cell lines, the cryo-stocks of the cells were prepared. In order to freeze the cells, the culture was detached from the dish with a suitable method for each cell type and after the centrifugation at 1200 RPM for 5 minutes, followed by resuspension in an appropriate freezing medium (see Table 3.14) . Routinely, one confluent well of a 6-well plate was used to prepare 1 cryo-stock in the volume of 1 ml. These cryo-vials were then placed in the Nalgene® Freezing Container filled with isopropanol to enable slow cooling at the rate of -1°C/minute and stored at -80°C for 24 hours. After that, the cryo-stocks were transferred to the liquid nitrogen tank for long term storage.

To revive the cells after freezing, the cryo-stock was thawed up in a water bath at 37°C and the cell suspension was diluted with 5 ml of appropriate culture medium. The cells were then centrifuged at

1200 RPM for 5 minutes followed by resuspending of the cell pellet in the culture medium and later plated onto a fresh dish.

### 3.2.10 Analysis of the cell cultures

### 3.2.10.1 Stress granules formation

The cells were seeded at the format suitable either for the immunofluorescence stainings (see section 3.2.2) or for running western blot (see section 3.2.3.3). The Hela cells were treated with 200 µM sodium arsenite and spinal motor neurons were treated with 500 µM sodium arsenite for 1 hour . After the treatement, the cells were fixed for immunofluorescence staining or samplers were isolated for the western blot.

### 3.2.10.2 Analysis of stress granules and co-localization with FUS granules

To analyze stress granules number and their co-localization with FUS, immunofluorescence staining of the cells was performed as described in the section 3.2.2 with anti-TIAR antibody or G3BP1 antibody to label stress granules and anti-MAP2 antibody was used to label neurons. Fluorescence microscopy imaging was performed using Laser Scanning Confocal Microscope LSM. At least 10 images of randomly chosen fields of view were acquired for each treatment and each independent experiment. The images were taken as z-stacks of 6 sections with a z-step of 1 µm to allow for co-localization analysis. If not stated otherwise, 63x oil immersion objective was used. The maximum intensity projection was performed for each image with FiJi ImageJ software and the automated quantification was performed with CellProfiler software. CellProfiler workflow for quantification and co-localization of FUS granules with stress granules was designed as follows:

1. Identify nuclei using DAPI positive staining

2. Identify MAP2 region using MAP2 staining

3. Include nuclei into the MAP2 region

4. Identify stress granules using TIAR staining OR G3BP1 staining

5. Identify FUS granules

6.  Relate the detected objects (FUS granules or stress granules) to MAP2 area including nuclei

7. Include nuclei into the MAP2 region

 8. Identify stress granules using TIAR staining OR G3BP1 staining

9. Include nuclei into the MAP2 region

10. Identify stress granules using TIAR staining OR G3BP1 staining

11. Identify FUS granules

12. Relate the detected objects (FUS granules or stress granules) to MAP2 area including nuclei

13. Measure size, shape, number and intensity of the detected objects

14. Shrink detected stress granules to a point

15. Shrink detected FUS granules *to a point*

16. Expand detected objects by 1 pixel

17. Relate FUS granules to stress granules to detect co-localization

18. Export the results to a spreadsheet

The results were further filtered and processed using KNIME software. The obtained number of, stress granules per MAP2 area as well as the co-localization with FUS results were processed with GraphPad Prism 7 software for statistical analysis and preparing a graphical representation of the results. Representative line scans and related fluorescence intensity profiles were generated using FiJi ImageJ.

### 3.2.10.3 Kinects of Stress granules disassembly assay

To analyze the dynamics of stress granules disassembly, the time course experiments has been done on the NPCs or on the spinal motor neurons, the NPCs cells were stressed with 500 µM sodium arsenite for 1 hour followed by the time-course recovery experiments. After 1 hour of treatment arsenite has been removed, twice washed with PBS, followed by adding fresh medium. The cells were fixed for the immunofluorescence staining after 30 minutes, 60 minutes and 180 minutes post-treatment. In the case of spinal motor neurons, neurons were treated with 500 µM sodium arsenite for 1 hour, after treatment cells were washed twice with PBS and a regular maturation medium was added. Post-treatment recovery time course has been performed, cells were fixed after 2hr recoveries up to 8hour full recovery. The fixed cells were then stained with DAPI Fluoromount G, to label the nuclei and the fluorescence images were acquired using LSM 900 confocal microscope (Zeiss) as 10 confocal z-stacks with 0.5 µm z-step using 63x objective with oil immersion. The images were then processed to generate a maximum intensity projection using Fiji ImageJ software and the stress granules number per cell was automatically quantified using CellProfiler 2.2.0.

### 3.2.10.4 Cell viability analysis

The cell viability was analyzed using PrestoBlue Viability Assay (ThermoFisher Scientific). Briefly, the cells were incubated with the PrestoBlue reagent diluted 1:10 in the medium without phenol red (N2B27 Basic Medium prepared with DMEM/F12 minus phenol red (Thermo Fischer Scientific, USA) and Neurobasal minus phenol red (Thermo Fischer Scientific, USA)) for 1 hour. After this time, the medium was collected and transferred into the microplate. The fluorescence was measured at 590 nm with a microplate reader and the viability was calculated in reference to the non-treated cells. The results were normalized to the non-treated control

### 3.2.10.5 Autophagosomes and autolysosomes Formation

The cells were seeded at the format suitable for the live cell imaging on PLO/laminin coated µ-Slide 8-well chamber slides (see section 3.2.5.2) at the density of 50,000 cells per cm$^2$. Add 2ul reagent Premo Autophagy Assays with Sensor Tandem Sensor RFP-GFP-LC3B as mentioned in Table 3.3. per 10,000 cells in media. Incubate the cells for 16hours at 37C. Later image the cell with Live cell imaging. RFP and GFP signal represent the autophagosomes, when GFP signal is quenched and only RFP remains they are called autolysosomes.

### 3.2.10.6 Quantification of Autophagosomes and autolysosomes

To quantify the number of autophagosomes and autolysosomes LSM microscope has been used. At least 7-8 pictures has been of randomly chosen fields of view were acquired for each independent experiment. If not stated otherwise, 63x oil immersion objective was used. Later counting was performed for each image with FiJi ImageJ software using the cell counter plugin. Manually the dots which were positive for GFP and RFP were calculated as Autophagosomes and dots which are only positive for RFP were count as Autolysosomes

### 3.2.10.7 Quantification of lysosomes

To analyze number of lysosomes, immunofluorescence staining of the cells was performed as described in the section 3.2.2 with LAMP2 antibody to label lysosomes and anti-MAP2 antibody was used to label neurons. Fluorescence microscopy imaging was performed using Laser Scanning Confocal Microscope LSM. At least 10 images of randomly chosen fields of view were acquired for each treatment and each independent experiment. The images were taken as z-stacks of 6 sections with a z-step of 1 µm. If not stated otherwise, 63x oil immersion objective was used. The maximum intensity projection was performed for each image with FiJi ImageJ software and the automated quantification

was performed with CellProfiler software. CellProfiler workflow for quantification was designed as follows:

1. Identify nuclei using DAPI positive staining

2. Identify MAP2 region using MAP2 staining

3. Include nuclei into the MAP2 region

4. Identify lysosomes using LAMP2 staining

5.  Relate the detected objects (LAMP2 or lysosomes) to MAP2 area including nuclei

6. Measure size, shape, number and intensity of the detected objects

7. Export the results to a spreadsheet
The results were further filtered and processed using KNIME software. The obtained number of lysosomes per MAP2 area were processed with GraphPad Prism 7 software for statistical analysis and preparing a graphical representation of the results. Representative line scans and related fluorescence intensity profiles were generated using FiJi ImageJ.

## 3.2.11 Statistics

For the statistical analysis, GraphPad Prism 7 software was used. For all the quantitative analysis, three or more independent experiments (sample size n ≥ 3) were performed. Detailed information about the sample size for each quantification are provided in the respective figure legend. The graphs represent either pooled data as a mean value or individual values (dot plot) with mean value. If not stated otherwise, the error bars represent standard error of the mean (SEM). Routinely, two-tailed unpaired Student's t-test was used to compare two groups with one independent variable. Welch's correction was used for the groups with unequal variances. For the experimental setup with more than two groups and/or more than two variables, One-way ANOVA or Two-way ANOVA was used. The suitable post-hoc test was chosen for each analysis based on the data set. Information about the statistical test and post- hoc test for each analysis is provided in the description of the respective figure. The results with p-value ≤ 0.05 were considered statistically significant. The following annotation was used to report p-value range: *p ≤ 0.05, **p ≤ 0.01, ***p ≤ 0.001, ****p ≤ 0.0.

# 4 Results

## 4.1 Characterization of cell lines and generating spinal motor neurons

### 4.1.1 Overview of the cell model and HSPB8 protein expression

Generation of the iPSC cell line was done by the lab of Prof. Hyun Kate Lee using CRISPR/Cas9 knocking out of the exon2 for HSPB8 (overview in Figure 4.1 A). To generate motor neurons, iPSCs were previously differentiated in Hermann's laboratory to NPCs of ventral-posterior characteristics using a small molecule-based approach based on the protocol published by (Reinhardt et al., 2013). NPCs were further differentiated into motor neurons using the protocol described in section 3.2.7.2 (overview in Figure 4.1C). To validate the removal of exon2 from HSPB8 gene, sanger sequencing has been done. For the sequencing the gDNA was isolated from the smNPCS by the ZR plasmid mini prep. Kit mentioned in the Table 3.3. After isolating the gDNA samples along with primers (see table 3.9) were sent for analysis. HSPB8(KO) did not show the sequence for exon 2, which was seen in the control (overview in Figure 4.1 A). Further validation of this truncation has been done with the PCR. There were no traces of exon2 in the HSPB8(KO) (Figure 41B). For most of the experiments, the cells were analyzed after 21 days of maturation. To label the motor neurons, immunofluorescence staining was performed as described in section 3.2.2 using MAP2 (not shown here).
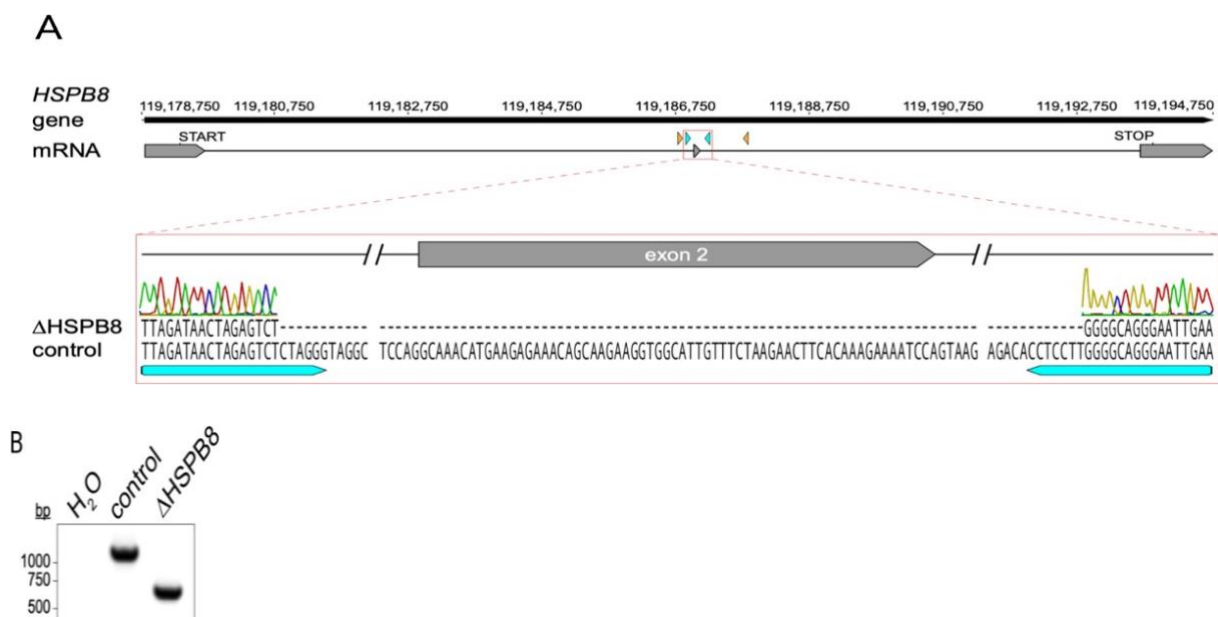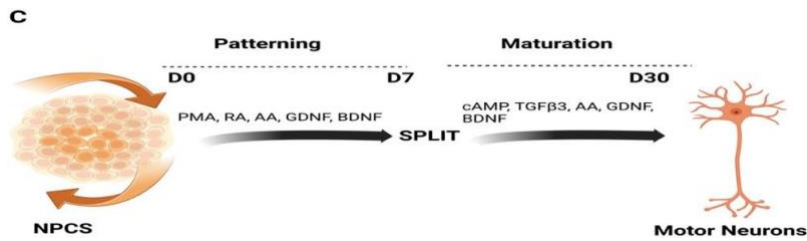
*Figure 4.1:* **Overview of cell lines and generation of spinal motor neurons**

(A) Workflow of cell line generation via CRISPR/CAS9 HSPB8-KO and validation with sequencing showing the removal of exon2 from HSPB8 gene done by Stephanie Spannl and the lab of Prof. Hyun Kate Lee. (B) PCR showing the truncated band for the HSPB8 validating that exon2 has been successful removed done by Stephanie Spannl and the lab of Prof. Hyun Kate Lee. (C) A schematic representation of motor neuron differentiation protocol.

To further validate the knock-out conditions western blot was run using five different HSPB8 antibodies. For the antibody establishment, we used the following cell lines: HSPB8-myc Flip HeLa cell line carrying a doxy/tetracycline dependent overexpression cassette of HspB8 which was tagged with the myc protein and wiltype and HSPB8 knockout iPSC-derived NPCs and neurons for more details please refer to Table 3.6. HeLa cells were treated with doxycycline for 12 hours to overexpress the HSPB8 which served as positive control, non-treated HeLa cells as negative controls, respectively. Out of the five HSPB8 antibodies tested, only two worked on the western blot. Results from the other three antibodies entitled cell signalling 3059, sigma SAB2101100 and abcam ab151552 which did not detected HSPB8 are not shown. Sigma HPA015876 antibody worked specifically and only on the samples of Hela cells which were overexpressing HSPB8 (Figure 4.2 A).

Invitrogen PA5-76780 HSPB8 antibody worked in all the samples (Figure 4.2 B) and showed clear reduction if not loss of HSPB8 in case of HSPB8 excision of exon2. (Figure 4.2 B,C)
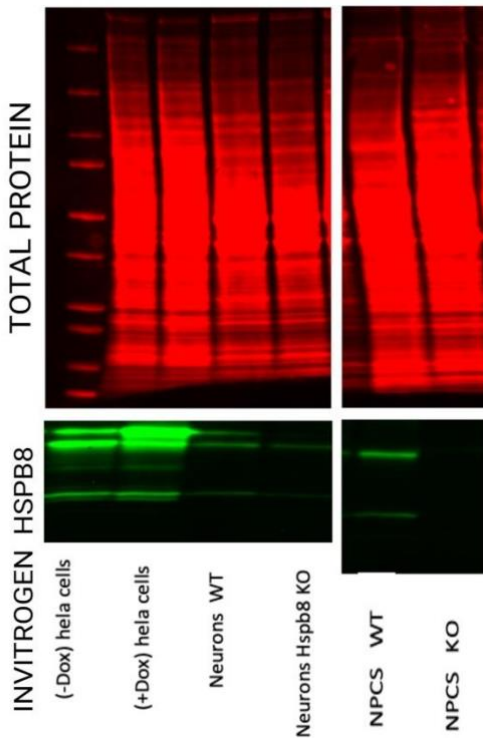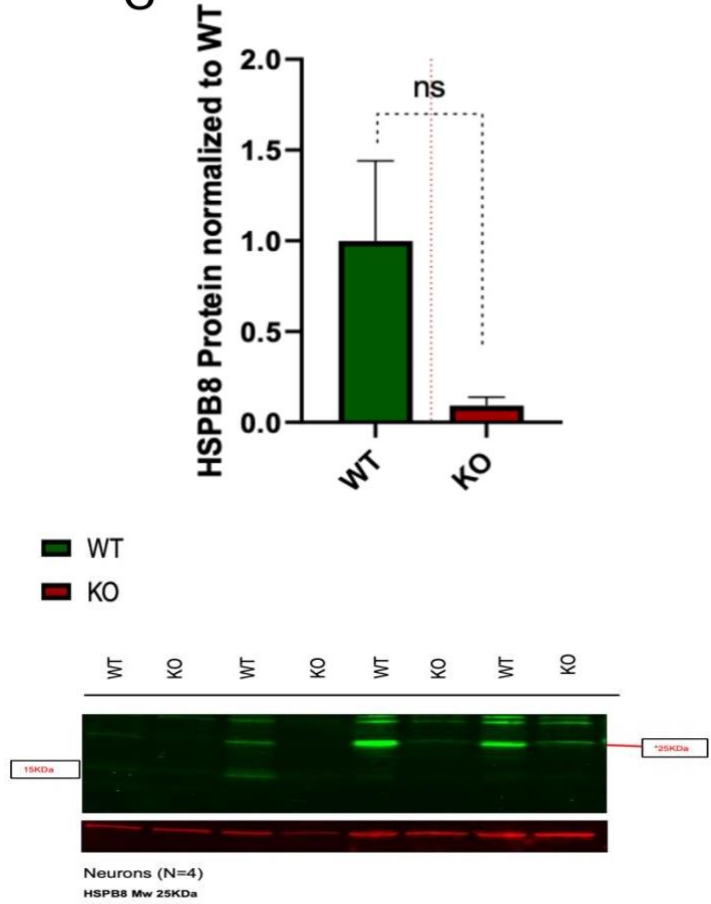
**A**

expression of Sigma HPA015876 (HSPB8)

Total Protein

Green: B-actin
Red: HSPb8

HSpb8 signal

250
150
100
50
37
25
20

(-Dox) hela
(+Dox) hela
Neurons WT
Neurons HSPB8 KO
Neurons WT
Neurons HSPB8 KO

(-Dox) hela cells
(+Dox) hela cells
Neurons WT
Neurons Hspb8 KO
Neurons WT
Neurons Hspb8 KO

**B**

TOTAL PROTEIN

INVITROGEN HSPB8

(-Dox) hela cells
(+Dox) hela cells
Neurons WT
Neurons Hspb8 KO
NPCS WT
NPCS KO

**C**

HSPB8 Protein normalized to WT

ns

2.0
1.5
1.0
0.5
0.0

WT    KO

WT
KO

WT  KO  WT  KO  WT  KO  WT  KO

15KDa                              *25KDa

Neurons (N=4)
HSPB8 Mw 25KDa

57

*Figure 4.2:* **Western blot results for HSPB8 antibodies**

(A) Western blot images represent the expression of Sigma HPA015876. Total protein staining (top) and HSPB8 antibody staining (bottom) only expressed in overexpressed Hela cells, β-actin represents the loading control (B) Representative images of the fluorescence Western blot expressing Invitrogen HSPB8 antibody PA5-76780 in all the samples, nevertheless, HSPB8(KO) samples expressed positive signal (C) The graph represents the level of HSPB8 normalized to β-actin. Followed by right side representative fluorescence western blot images detecting HSPB8 Invitrogen antibody. The graph represents the level of HSPB8 normalized to β-actin. In the HSPB8(KO) lower level of HSPB8 has been observed. Data are presented as mean ± SEM. N = 3 biological replicates. Statistical analysis with unpaired two-tailed student's t-test. For the samples with unequal variances, Welch's correction was applied.

## 4.2 Detection of HSPB8 antigen in control and arsenite-treated conditions via immunofluorescence

### 4.2.1 Testing polyclonal antibodies in different cell types

We next evaluated the five HSPB8 antibodies in immunofluorescence staining of the three different cell-types, namely Hela, NPCs and spinal motor neurons. Out of these five antibodies, three gave a detectable signal. Surprisingly, first tested antibody Invitrogen PA5-76780 resulted in the detection of false positive signal in the HSPB8(KO)-derived neural progenitor cells (Figure 4.3 A). To ensure there was no experimental error, a similar experiment was performed on the spinal motor neurons and the same results were recapitulated (Figure 4.3 B). To verify that these results were not antibody specific, another sigma Sigma HPA015876 were tested only on the neural progenitor cell (NPC). The results aligned with the previous antibody, which was detecting a non-specific signal (Figure 4.3 C). To investigate whether this was not exclusion bias, titration of the antibodies were conducted for both the antibodies, including the positive control overexpressed HSPB8 Hela cells (results are not attached here). Nevertheless, no observed differences were found between WT and KO in the expression of HSPB8. To explore the non-specificity, the functional aspect of HSPB8 with these antibodies was tested. Ganassi et al., 2016, reported that HSPB8 was recruited to the stress granules under stress conditions. To analyze the influence of HSPB8 on SG, the cells were treated with sodium arsenite (500 µM for 1 hour, oxidative stress). This treatments was shown previously to induce SG formation (N. L. Kedersha et al., 1999). After arsenite was applied, the cells were fixed and immunofluorescence staining with TIAR as a SG marker was performed. For this experiment all the settings including antibody dilution (1:500), independent on the cell type and microscope exposure time, were kept constant to exclude any experimental/technical

influence. Interestingly, out of these two antibodies only Sigma HPA015876 HSPB8 antibody co-localized with the TIAR in the WT and KO-derived neurons (Figure 4.3 D). However, other antibody from Invitrogen did not show any SG colocalization under arsenite stress (results not showed here)..
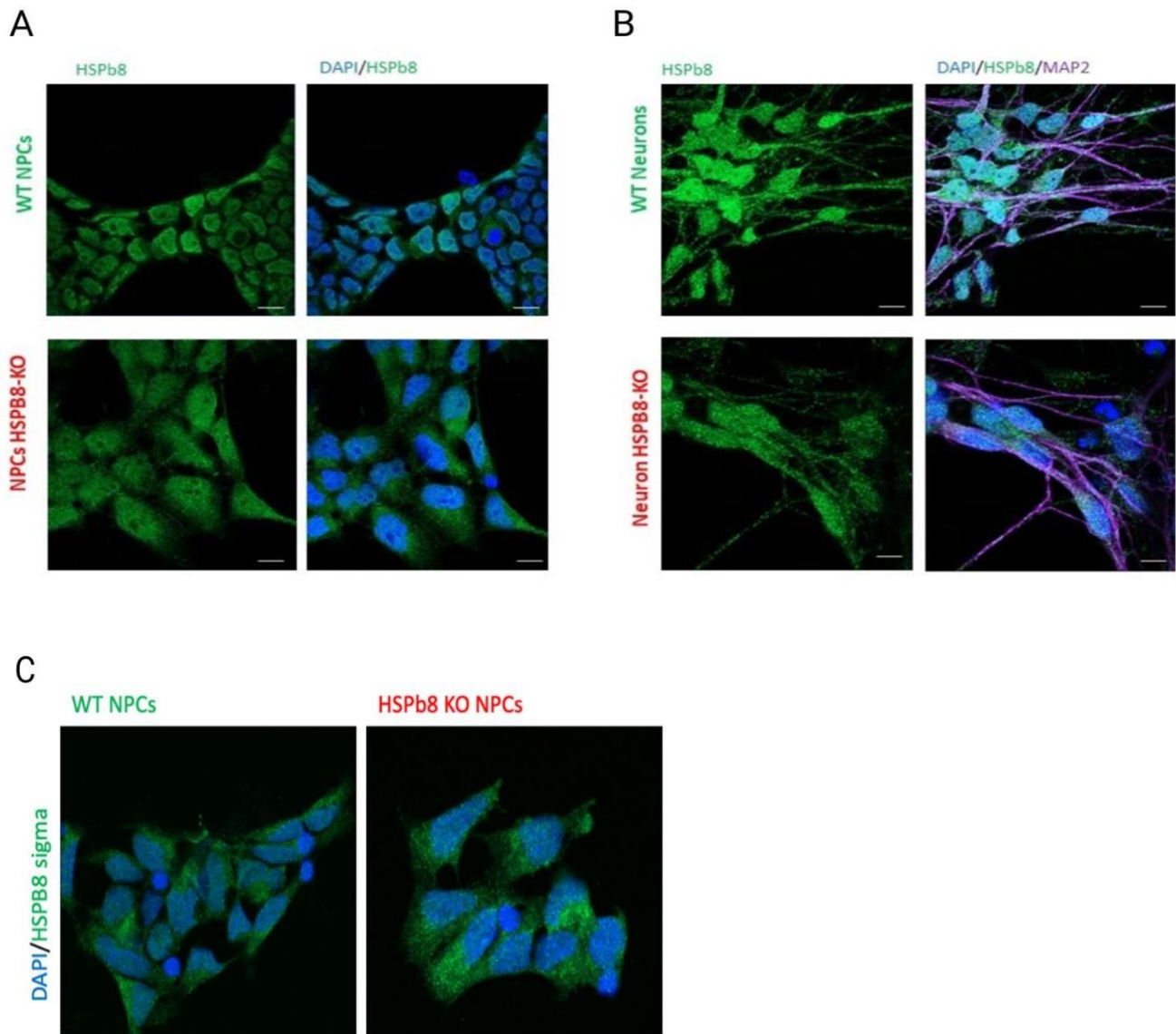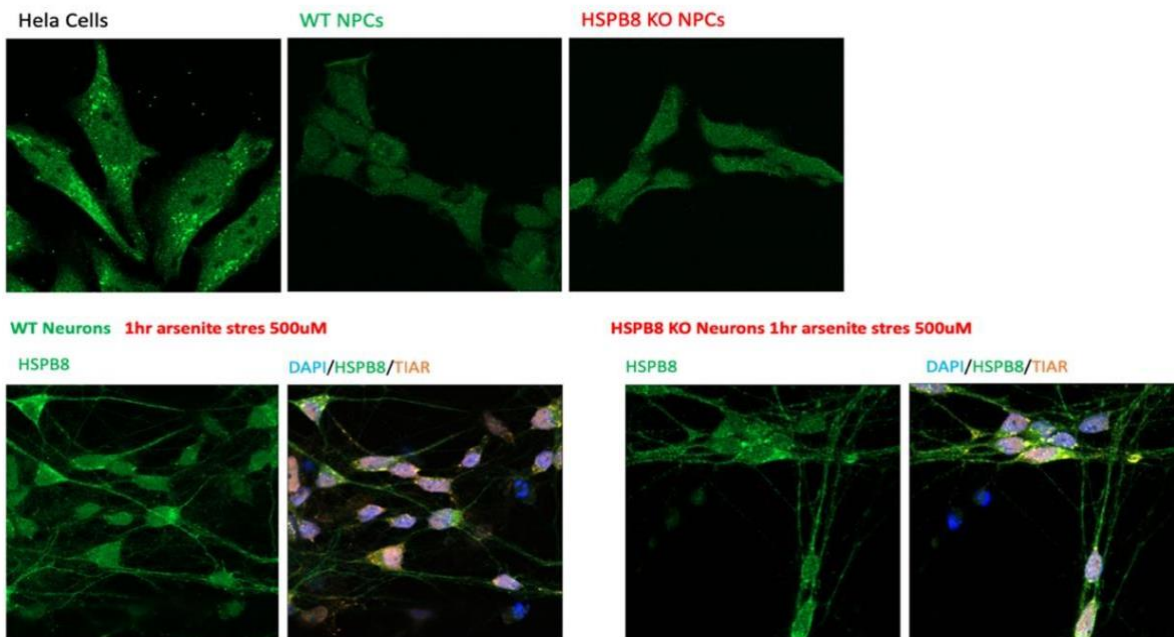
*Figure 4.3:* **HSPB8 antibodies expression via Immunofluorescence in different Cell types**

(A) Representative image of immunofluorescence staining for NPCs (left panel) with Invitrogen antibody PA5-76780 (B) Representative image of immunofluorescence staining for Neurons (right panel) with Invitrogen antibody (C) Representative images of immunofluorescence staining of NPCs expressing HSPB8 Sigma antibody HPA015876 (D) Immunofluorescence staining of different cell-types expressing Sigma HSPB8 antibody. WT neurons (bottom left) and HSPB8-KO (bottom right) with arsenite treatment .The images represent the co-localization using HSPB8 in green and orange (TIAR) channel. Scale bar 10 μm.

### 4.2.2   *Probing HSPB8(KO) validated monoclonal HSPB8 abcam 151552 antibody*

After conducting tests for HSPB8 antibodies in the above section and having observed positive expression in HSPB8(KO), concerns were raised about their specificity. Both the antibodies mentioned in the above section were polyclonal and had not been commercially validated under knock-out conditions, making it likely that they were binding to non-specific regions. To ensure the accuracy of the results, the search for a monoclonal antibody was initiated. In 2021, Abcam finally created and validated a monoclonal antibody ab151552 that was usable in knock-out conditions. The new antibody's efficacy was tested in our cell line by conducting immunofluorescence, as shown in Figure 4.4. The results showed that the monoclonal antibody yielded similar results to the polyclonal antibodies. Specifically, the monoclonal antibody was co-localizing with the TIA-1 marker for SGs in Figure 4.4B. The immunofluorescence was conducted when neurons were stressed with arsenite both in WT and

HSPB8(KO). Thus, we found no commercially available antibody working properly in IFF. We thus decided not to use these antibodies in IFF/ICC applications, which unfortunately put our plan aside to analyse HSPB8 expression, subcellular localization studies (e.g. SG), in neurons from other established ALS models.
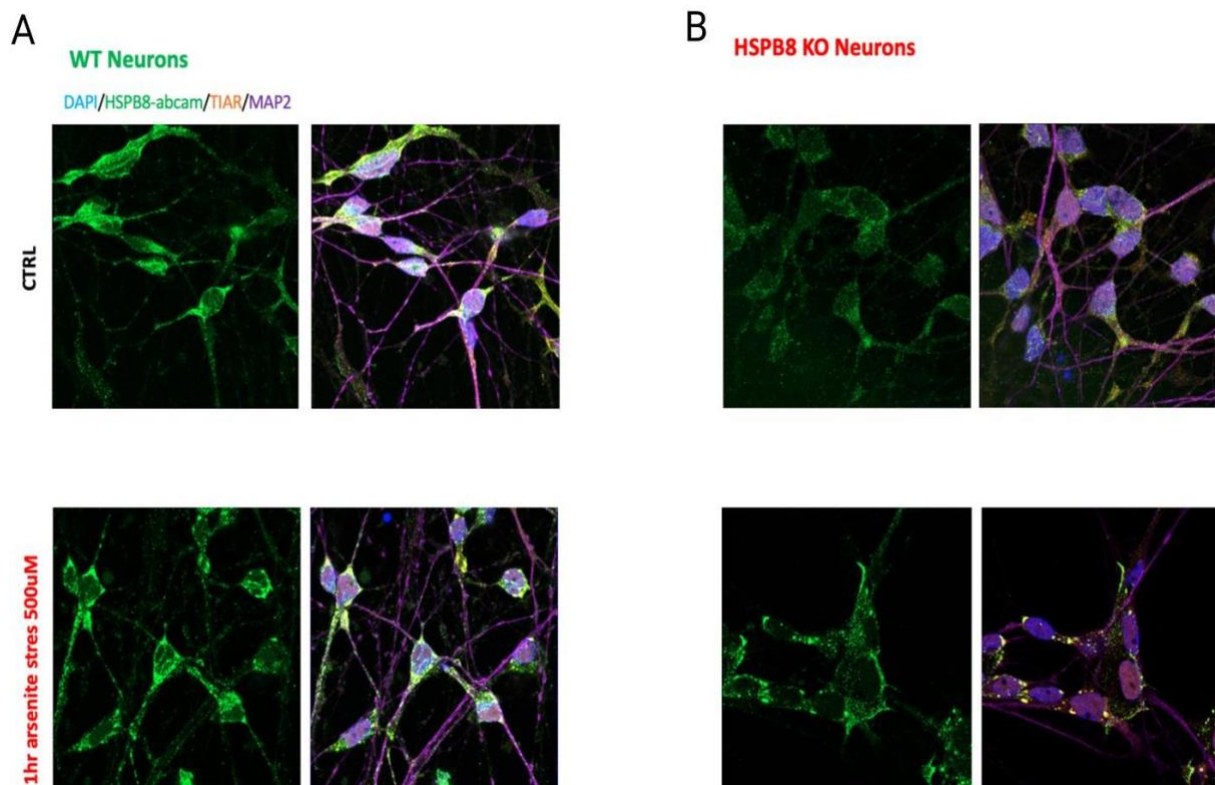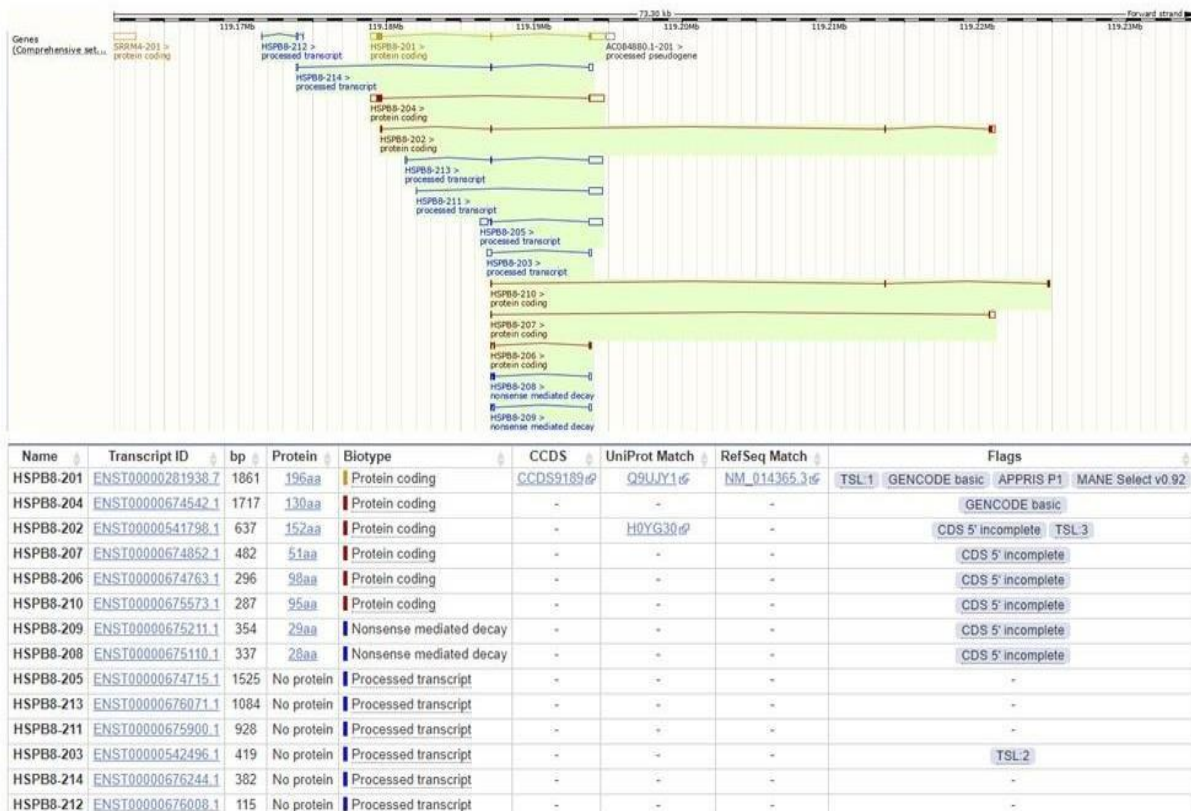


.

*Figure 4.4:* **Expression of abcam antibody, HSPB8 knock-out validated**

(A) Representative picture depict the expression of HSPB8 antibody in the WT neurons, upper lane represents the Ctrl cell lower lane shows the neurons which are stressed with aresnite, white arrow shows that HSPB8 recruits to the SGs. (B) Representative image of Immunofluorescence for HSPB8(KO) upper lane represents the false positive expression of HSPB8 antibody in Control HSPB8(KO), lower lane shows the non-specific recruitment of HSPB8 antibody to the SGs. The images represent the co-localization using HSPB8 in green and orange (TIAR) channel. Scale bar 10 μm.

## 4.3 Analyzing other HSPB8 isoforms through qPCR

Due to an absence of commercially proper HSPB8 working antibody and these false positive results from all the immunofluorescence stainings using the above mentioned antibodies. The intriguing question to follow was could it be possible that cutting out exon 2 only affected the classical HSPB8 isoform but might result in the activation of other potential isoforms, which are detected by the HSPB8 antibodies. Fig. 4.5 A depicted all the transcripts for HSPB8, specifically only protein coding transcripts had been chosen for the analysis. For this investigation total RNA had been isolated form the NPCs samples, followed by qPCR. Results were evident there was no trace of any other isoform in the KO (Figure 4.5 B). For few isoforms particularly 204, 206 and 210. Both in the WT and KO qPCR curve was not suitable for the analysis.



| Name | Transcript ID | bp | Protein | Biotype | CCDS | UniProt Match | RefSeq Match | Flags |
|------|--------------|-----|---------|---------|------|--------------|-------------|-------|
| HSPB8-201 | ENST00000281938.7 | 1861 | 196aa | Protein coding | CCDS9189 | Q9UJY1 | NM_014365.3 | TSL:1  GENCODE basic  APPRIS P1  MANE Select v0.92 |
| HSPB8-204 | ENST00000674542.1 | 1717 | 130aa | Protein coding | - | - | - | GENCODE basic |
| HSPB8-202 | ENST00000541798.1 | 637 | 152aa | Protein coding | - | H0YG30 | - | CDS 5' incomplete  TSL:3 |
| HSPB8-207 | ENST00000674852.1 | 482 | 51aa | Protein coding | - | - | - | CDS 5' incomplete |
| HSPB8-206 | ENST00000674763.1 | 296 | 98aa | Protein coding | - | - | - | CDS 5' incomplete |
| HSPB8-210 | ENST00000675573.1 | 287 | 95aa | Protein coding | - | - | - | CDS 5' incomplete |
| HSPB8-209 | ENST00000675211.1 | 354 | 29aa | Nonsense mediated decay | - | - | - | CDS 5' incomplete |
| HSPB8-208 | ENST00000675110.1 | 337 | 28aa | Nonsense mediated decay | - | - | - | CDS 5' incomplete |
| HSPB8-205 | ENST00000674715.1 | 1525 | No protein | Processed transcript | - | - | - | - |
| HSPB8-213 | ENST00000676071.1 | 1084 | No protein | Processed transcript | - | - | - | - |
| HSPB8-211 | ENST00000675900.1 | 928 | No protein | Processed transcript | - | - | - | - |
| HSPB8-203 | ENST00000542496.1 | 419 | No protein | Processed transcript | - | - | - | TSL:2 |
| HSPB8-214 | ENST00000676244.1 | 382 | No protein | Processed transcript | - | - | - | - |
| HSPB8-212 | ENST00000676008.1 | 115 | No protein | Processed transcript | - | - | - | - |

B



*Figure 4.5:* **Expression of HSPB8 isoforms in NPCS on a transcript level**

(A) Image depict all the HSPB8 isoforms which are available on the ensemble website (B) Representative image of qPCR graph for HSPB8 for NPCs. The graph represents the relative HSPB8 isoform mRNA, mean ± SD for n =2 biological replicates.

## 4.4 Loss-of-functional HSPB8 leads to FUS aggregation

### 4.4.1 Investigating FUS expression and aggregation

Mounting evidences had reported that expression pattern/level of HSPB8 chaperone had been associated in the clearance of aggregated ALS-associated proteins (Anagnostou et al., 2010; Crippa et al., 2010 a,b Crippa et al., 2016; Cristofani et al., 2017). Fascinatingly enough there was no reported data on HSPB8(KO) and its association with FUS ALS. To address this specific query, the focus was to check the protein-expression of FUS in the spinal motor neurons in WT and KO using Western Blot. There was no noticeable difference in FUS protein expression between WT and KO, as shown in Fig. 4.6 A. To reverse engineer the same question but with HSPB8 expression in FUS-ALS cell line-derived neurons, protein samples had been isolated from the neurons. This was followed by the western blot to check the expression of Invitrogen antibody PA5-76780 (working ab. On the WB) may be seen in Fig. 4.2 C. In all the ALS-related cell line-derived neurons the expression of HSPB8 antibody was not homogenous, due to this variability in expression, results interpretation were not performed (Figure 4.6 B). Returning back to the main query of FUS aggregation in the HSPB8(KO), in general no change had been observed in the FUS protein expression. Next step was to detect FUS-aggegated proteins. To investigate the FUS-aggregates precisely, sensitive technique filter retention assay had been used. Proteins from the motor neurons had been isolated followed by filter retardation assay. The level of FUS protein retained in the filter (putatively the aggregated form of FUS) was evaluated. Remarkably, the levels of FUS aggregates were increased in HSPB8(KO) Fig. 4.6 C,D.
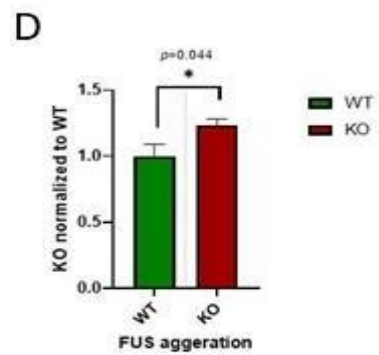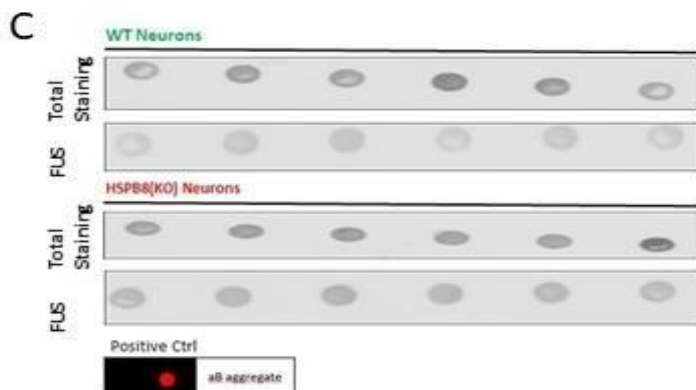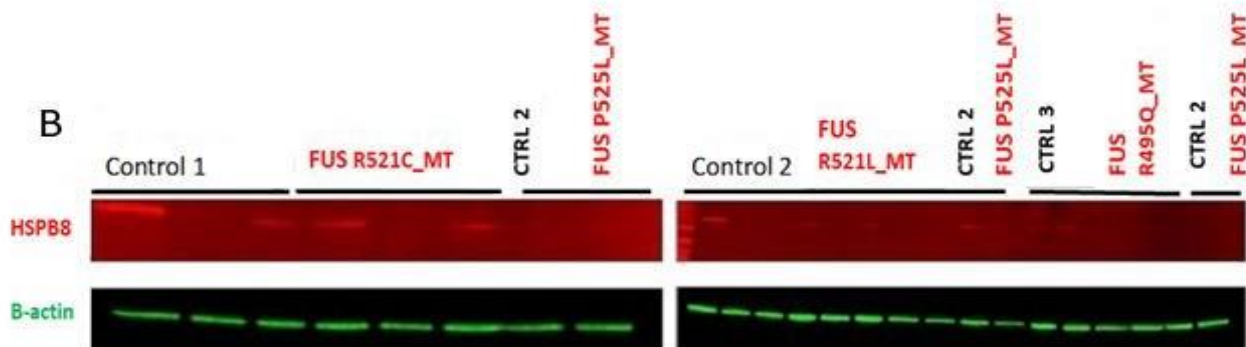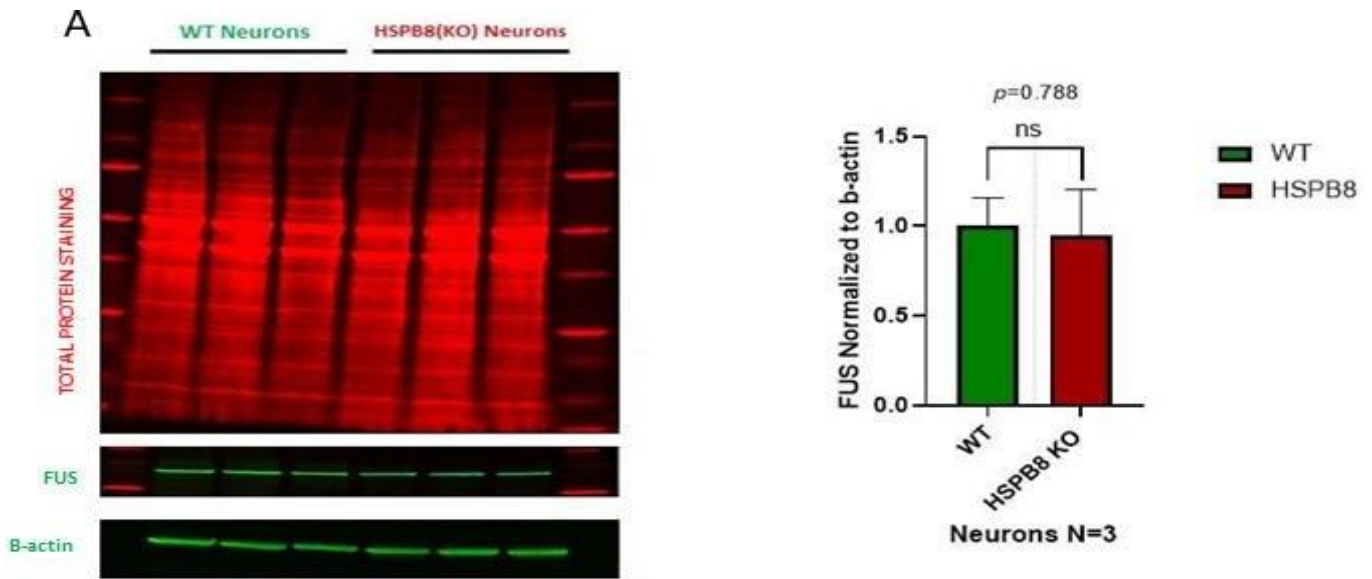
*Figure 4.6*: **FUS expression and aggregation**

(A) Picture shows fluorescent Western Blot detecting FUS protein in spinal motor neurons. The graph represents the level of FUS protein normalized to β-actin. Data are presented as mean ± SEM. N = 3 biological replicates. Statistical analysis with unpaired two-tailed student's t-test. (B) Image shows fluorescent Western Blot detecting HSPB8 protein in ALS-cell line derived spinal motor neurons (C) Representative picture of the filter trap assay for FUS aggregates. Total protein aggregates for WT and KO (each upper panel respectively) and FUS aggregates for WT and KO (each lower panel respectively). The bottom left represent the positive control of aβ-aggregates (D) The graph represents the aggregates of FUS protein normalized to WT. Data are presented as mean ± SEM. N = 3 biological replicates. Statistical analysis with two-way ANOVA followed by Tukey's multiple comparison.

### 4.4.2   Investigating nuclear cytoplasmic shuttling and recruitment to stress granules

FUS protein aggregates are a hallmark of FUS-ALS-pathogenesis. Nuclear import defects that are caused by a disrupted NLS are thought to be a key event in FUS- ALS pathology (Dormann et al., 2010; Dormann and Haass 2011; Dormann et al., 2012). These pathological aggregates were described as containing SG protein like TIA-1, recommending that they may had arisen from SGs. It was recommended that SGs might had undergone a slow maturation process resulting in the formation of aggregates (Liu-Yesucevitz et al., 2010). To address this question the spinal motor neurons were stressed with arsenite (500 µM for 1 hour, oxidative stress) to induce the formation of SGs and the properties of these granules were analyzed later the cells were fixed and immunofluorescence staining with TIAR as a SG marker was performed. The co-localization of FUS and SG was then automatically quantified. Surprisingly, our results did not show any FUS-mislocalization in to the SG granules under stress condition (Figure 4.7 A and B). Moreover, no nucleus to cytoplasmic FUS shuttling had been seen.

Of note, quantification revealed that there was no difference in the stress granules numbers themselves between WT and KO. Additionally, SG mean size had not changed between WT and KO when the neurons were stressed (Figure 4.7 C and D).
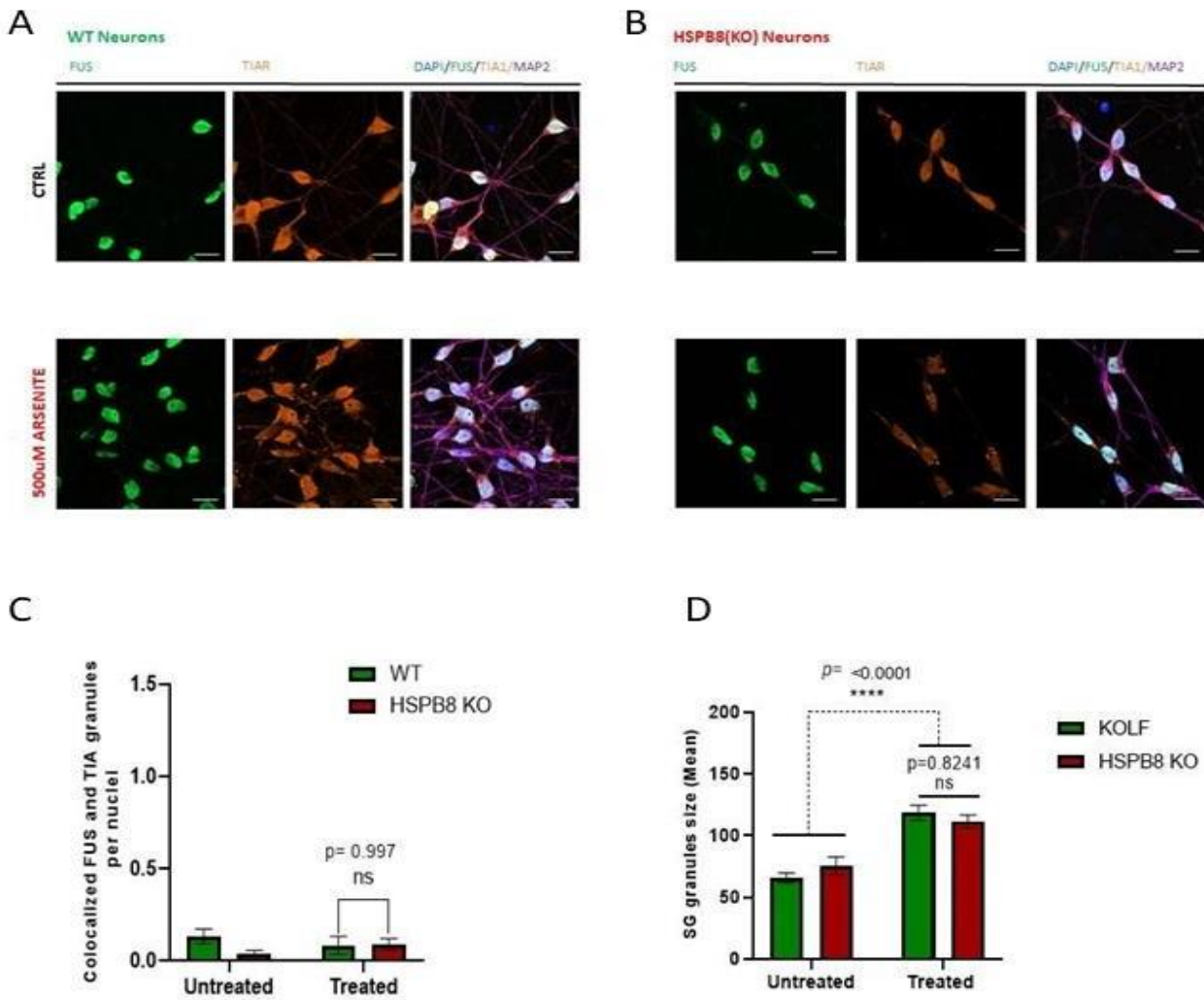
*Figure 4.7:* **FUS and stress granules analysis**

(A) Representative picture shows immunofluorescence staining detecting FUS protein in spinal motor neurons. The graph represents the level of FUS protein normalized to β-actin. Data are presented as mean ± SEM. N = 3 biological replicates. Statistical analysis with unpaired two-tailed student's t-test. (B) Image shows fluorescent Western Blot detecting HSPB8 protein in ALS-cell line derived spinal motor neurons (C) Representative picture of the filter trap assay for FUS aggregates. Total protein aggregates for WT and KO (each upper panel respectively) and FUS aggregates for WT and KO (each lower panel respectively). The bottom left represent the positive control of aβ-aggregates (D) The graph represents the aggregates of FUS protein normalized to WT. Data are presented as mean ± SEM. N = 3 biological replicates. Statistical analysis with two-way ANOVA followed by Tukey's multiple comparison.

## 4.5 Delineating the kinetics/dynamics of stress granules assembly and disassembly

### 4.5.1 The knockout of HSPB8 does not abolish SG formation but instead prolong SG-dissolution

Since HSPB8 is thought as an important player in maintaining SG solubility, as it is described for Hela cells (Ganassi et al., 2016), it was questioned whether knocking out of HSPB8 leads to and impairment in neurons. Additionally, the kinetics of the SG disassembly process was also intriguing for us. To answer this question, we investigated the proper disassembly of SG in WT and HSPB8(KO). For this purpose, firstly the time course experiments for the SG disassembly were checked with the progenitors' cells (data not shown here). Later when the proper SG disassembly time-point has been observed in progenitors same time-course experiments were performed on the neurons (data not shown here). To determine the SG disassembly, WT and HSPB8(KO) neurons were stressed with sodium arsenite for 1 hour, as previously. After that, the sodium arsenite treatment was withdrawn and the cells were let to recover from 2 hours up to 8 hours until we did not observe traces of SGs (Figure 4.8 A). After every 2 hours of the recovery until 8 hours of recovery the cells were fixed, labelled with DAPI to visualize cell nuclei and fluorescence microscopy images were acquired. Next, the number of SG granules per cell was automatically quantified using Cell Profiler 2.2.0. While HSPB8 (KO) neurons showed similar amounts of SG after 1h of arsenite stress, there was a significant increase in the number of stress granules in KO neurons compared to WT post recovery of 2 hour and 4 hour (Shown in Figure 4.8 B). Quantification revealed that SG disassembly took more time in KO condition (Fig. 4.8 B). This result shows that the kinetics of the disassembly process is severely affected in the KO. Furthermore, the survival of the neurons was evaluated directly after the sodium arsenite treatment or after 2 hours of recovery until 8 hours of recovery (Figure 4.8 C). For this purpose, Presto Blue assay was used as descried in the section 3.2.10.4.

Results were evident showing high vulnerability towards stress in KO condition. There was a significant difference in the survival between WT and KO neurons directly after the stress and after the recovery as well. Overall, this data indicated HSPB8 KO had a significant impact on the disassembly of the granules and on the cell survival.
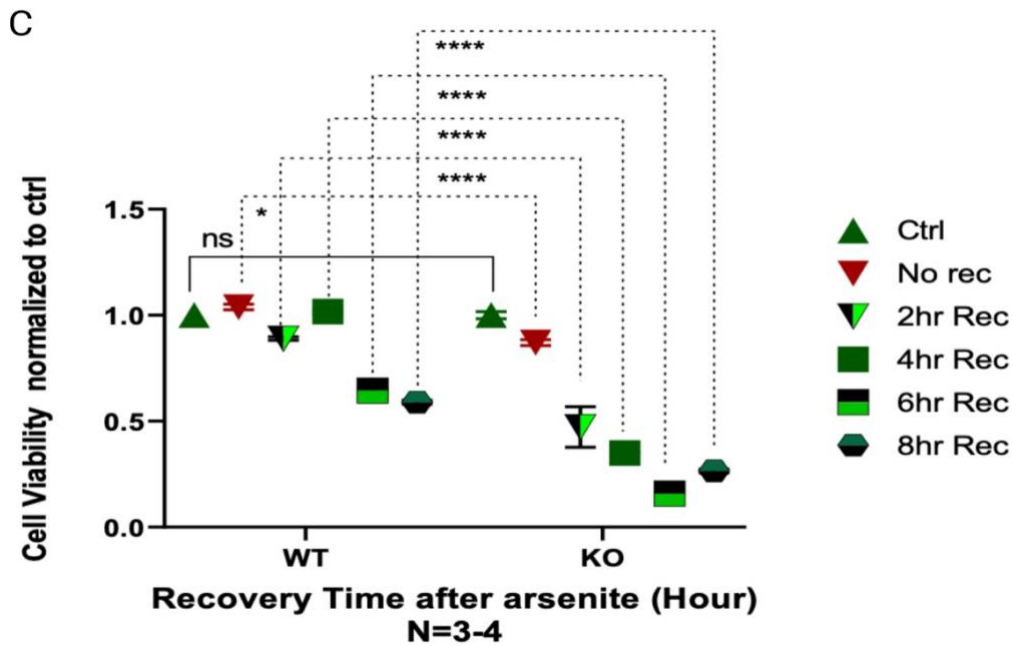
A

Recovery Time after arsenite (Hour)

B
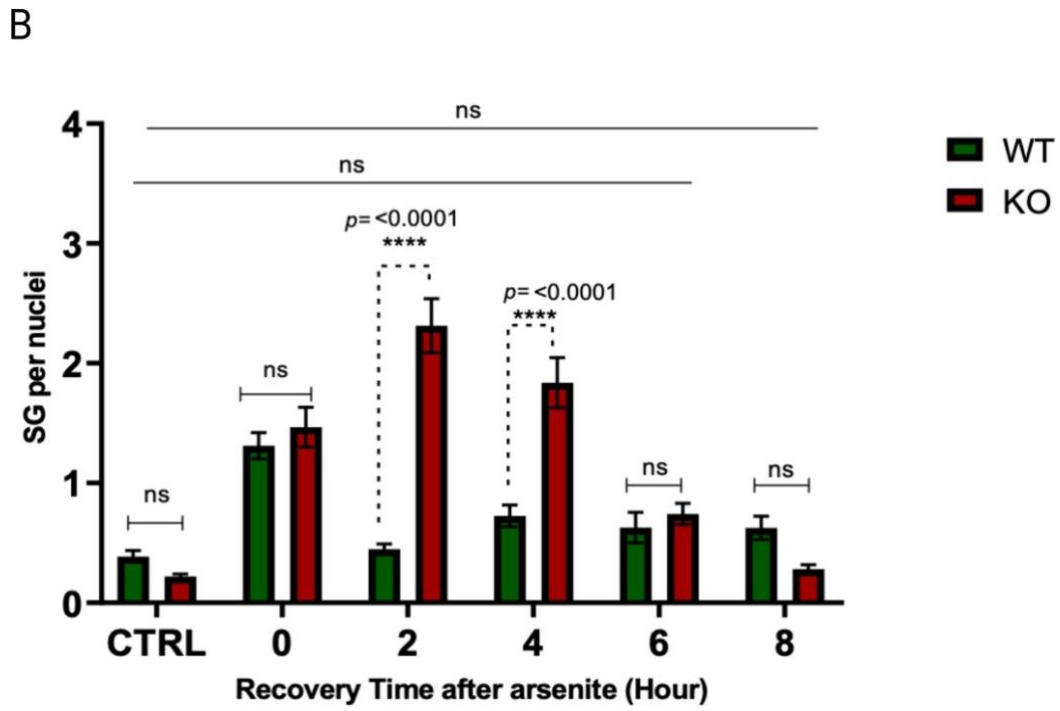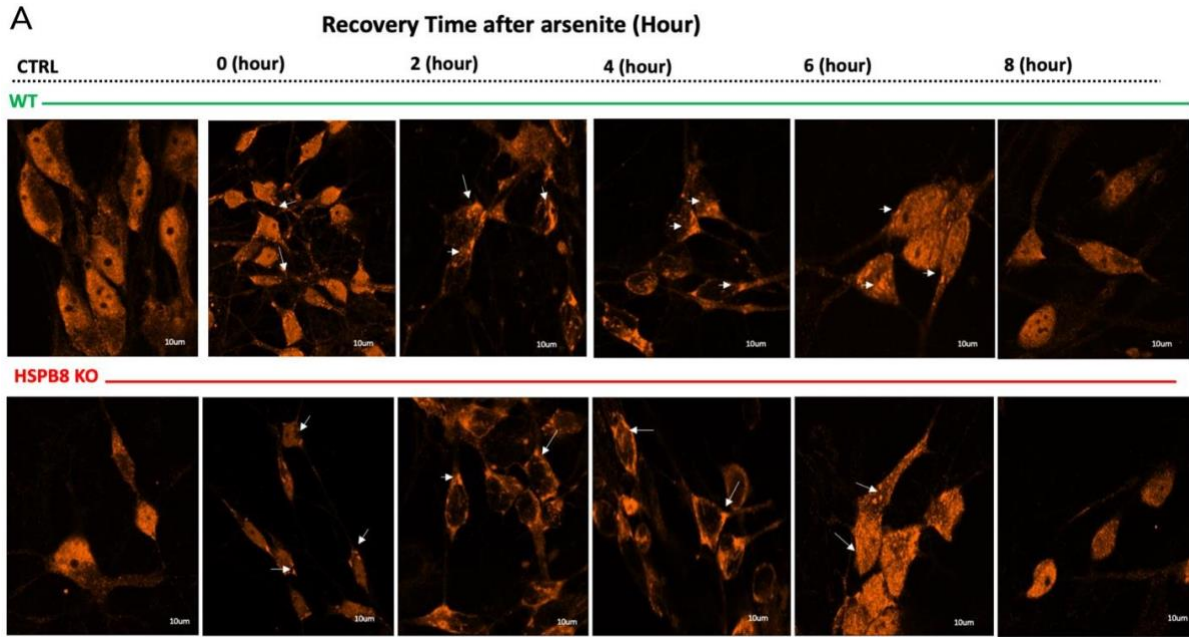
*Figure 4.8:* **Kinetics of stress granules assembly and disassembly**

(A) Representative immunofluorescence pictures depict the expression of TIAR antibody in the WT neurons (upper lane) stressed with aresnite and KO neurons (lower lane) stressed with arsenite. SGs are marked with the white arrows. Scale bar 10 µm. (B) An automated quantification of SG granules was performed using Cell Profiler 2.2.0. Quantification reveals that KO neurons takes prolonged time to disintegrate the stress granules. Data are presented as mean ± SEM. N = 3 biological replicates, for each condition 15-30 images were analyzed. Statistical analysis with two-way ANOVA followed by Tukey's multiple comparison. (C) The graph represents the cell survival analysis for the cells with sodium arsenite with or without recovery. The analysis was performed with Presto Blue assay. The cell viability is shown as a percent of untreated control. N = 4 biological replicates, for each 2-3 technical replicates. All the graphs represent mean ± SEM. Statistical analysis was performed with two-way ANOVA followed by Tukey's multiple comparison.

## 4.6 Investigating the role of chaperone-assisted selective autophagy in proteotoxic maintenance and stress granules disassembly.

### 4.6.1 The dynamics of CASA as an adaptive response during cell insult

The results reported in the previous sections exhibited the assembly and disassembly process of SG beside this, a high level of neuronal death was observed after stress and post recovery in KO, indicating arsenite stress is lethal for spinal motor neuron survival. It is intriguing to know that very small portion of SGs is dependent on autophagic clearance, majority of SG disintegration is based on chaperone-dependent and autophagy-independent way (Tedesco B et al.,2022). Ganassi et al., 2016 have reported the importance of CASA complex (HSPB8-BAG3-HSP70) was involved o play a surveillance role by guarding the proper composition of SG and impede them from being persistent. Chaperone-assisted selective autophagy is a selective autophagy, meaning that it targets specific proteins or protein aggregates for degradation rather than degrading all proteins indiscriminately. HSPB8, BAG3, HSC70, CHIP/STUB and HSP70 are the key components of CASA have been shown to play a role in the clearance of protein aggregates in cells (Carra S et al., 2008; Ganassi et al., 2016 and Tedesco B et al.,2022). To understand the decisive role of this selective autophagy in HSPB8(KO) being the major player in the CASA, the protein levels of all the chaperones were analyzed using Western Blot. To understand the proper role of CASA in stress granules disassembly, we ensured to follow the entitled conditions: Control (no treatment), 1hour arsenite treatment with no recovery, 4-hour recovery after the 1-hour treatment and 8-hour recovery condition after the treatment (look Figure 4.9 A and B). Interestingly, each chaperone showed a different level at the distinct condition. CHIP did not show any significant differences in the KO neurons independent of treatment or recovery, despite a trend of reduced expression in case of KO (Figure 4.9 E). BAG3, a crucial member of CASA which physically interacts with HSPB8 (Fuchs M et al., 2009) and facilitates in rescuing of the aggregated proteins via autophagy (Crippa V et al.,2010 and Rusmini P et al., 2015). Remarkably, in the HSPB8(KO) the BAG3 levels tremendously upregulated independent on the condition and remained consistently high in the KO ( Figure 4.9 A, B and F). HSP70 is an important co-chaperone of the CASA-complex, which is crucial for the degradation of SG components (Ganassi et al., 2016). We decided to evaluate the expression of HSP70 through Western blot. In absence of HSPB8, HSP70 remained significantly low under basal conditions (non-treated). Additionally, expression level of HSP70 remained consistently low in the KO 1-hour treated spinal motor neurons. After a 4-hour

recovery, we observed a trend of increased HSP70 expression in KO, but the levels of HSP70 did not show any significant differences. After a 8-hour recovery, the level of HSP70 remarkably enhanced in the KO-neurons (Figure A, B and C). We had also investigated the role of HSC70 another crucial member. Heat shock cognate 71 kDa protein (Hsc70), also known as HSPA8, is a member of the heat shock protein 70 family (Hsp70). Unlike Hsp70, it is a constitutively expressed chaperone protein and is involved in diverse cellular processes including protein folding and protein degradation. Surprising, unlike the HSP70 reduced expression in KO-neurons, HSC70 had significantly increased expression at the basal levels, after 1-hour arsenite treatment the level remained remarkably high but post treatment, in the recovery phase we observed a trend of high expression in KO but it was non-significant (Figure A, B and D).

A — WT Neurons

B — HSPB8 KO Neurons

C

D

E

F
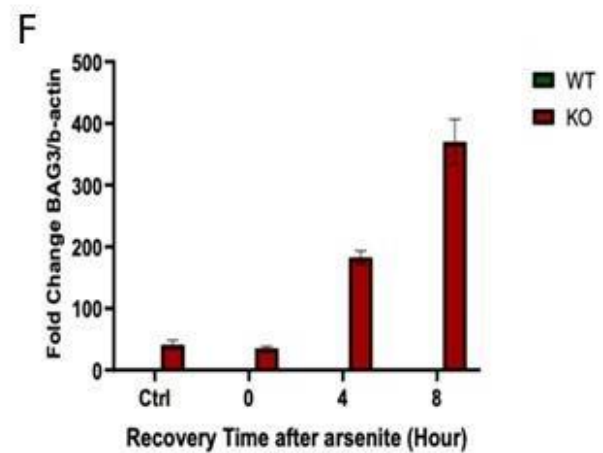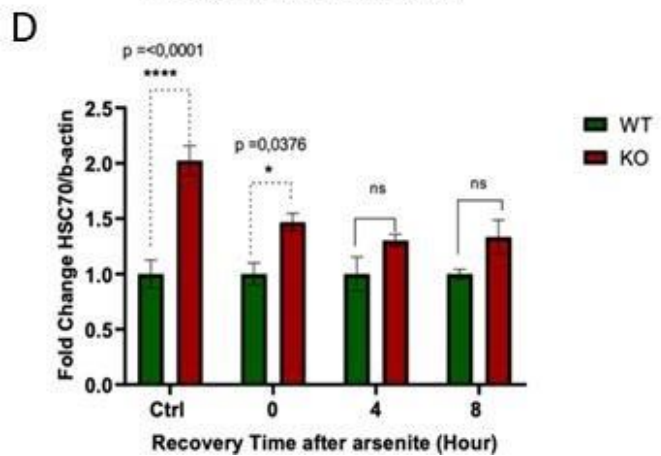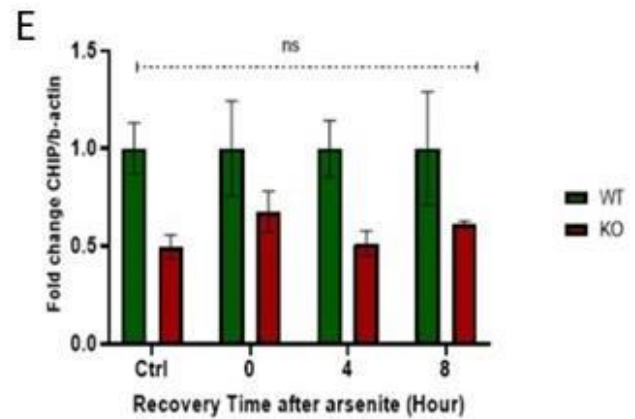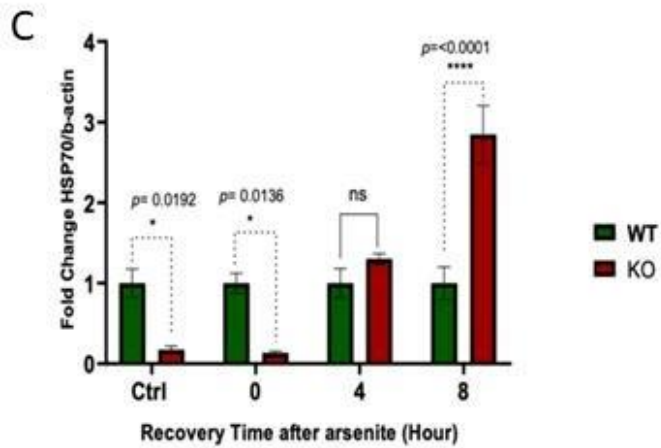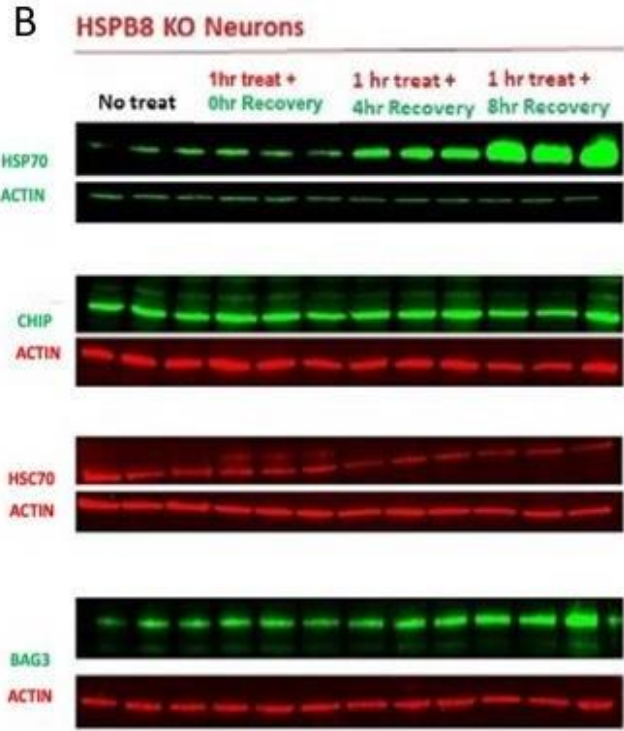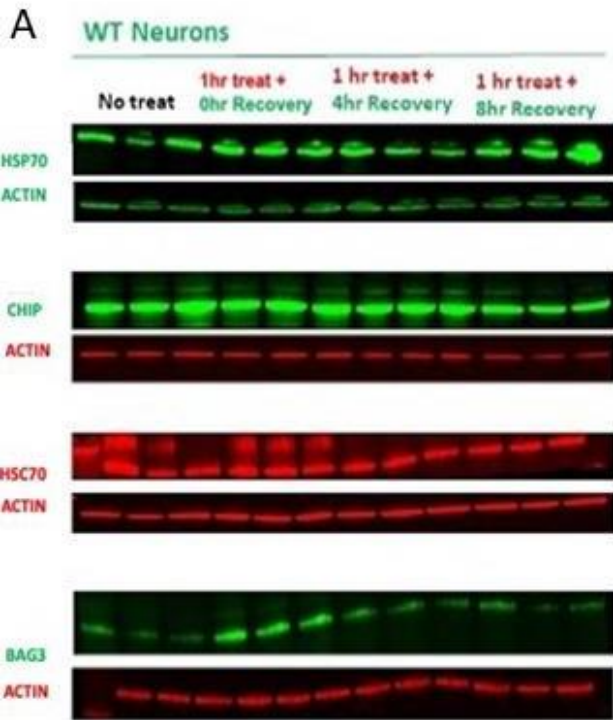
*Figure 4.9*: **Chaperones from the CASA-complex in KOLF neurons Chaperones**

(A) Representative images of fluorescence Western Blot for a panel of chaperones in control conditions (no treatment), 1-hour arsenite treated with no recovery, 4-hour post recovery and 8-hour post recovery in WT neurons. First blot showing HSP70 (top) and β-actin (bottom); second blot shows CHIP (top) and β-actin (bottom); Third shows CHIP (top) and β-actin (bottom) and last blot reveals BAG3 (top) and β-actin (bottom). (B) Pictures of fluorescence Western Blot for a panel of chaperones in control conditions (no treatment), 1-hour arsenite treated with no recover, 4hour post recovery and 8hour post recovery in KO neurons. First blot showing HSP70 (top) and β-actin (bottom); second blot shows CHIP (top) and β-actin (bottom); Third shows CHIP (top) and β-actin (bottom) and last blot reveals BAG3 (top) and β-actin (bottom). (C) The graph represents the level of HSP70 each analyzed protein in every condition normalized to β-actin and to WT. (D) The graph represents the level of HSC70 each analyzed protein in every condition normalized to β-actin and to WT. (E) The graph represents the level of CHIP each analyzed protein in every condition normalized to β-actin and to WT. (F) The graph represents the level of BAG3 each analyzed protein in every condition normalized to β-actin and to WT. All the quantifications were performed based on the fluorescence intensity using Image Studio Lite software. All the graphs are presented as mean ± SEM. N = 3 biological replicates, one-way ANOVA with Tukey's multiple comparison.

For this purpose of study, apart from CASA major members there were several chaperons and co-chaperones which had shown to be involved directly in this selective autophagy and these chaperons also played an important role in the SG assesmbly or disassembly. To explore these roles, we had also investigated these (Figure 4.10 A and B) namely: Hsp90, BAG1, DNAJB6 and Hsp40 (DnajB1). Levels of HSP90 in KO were significantly upregulated in the untreated, treated condition and 4hour post recovery. Surprisingly, post 8-hour recovery levels of HSP90 significantly suppressed in the KO neurons compared to WT (look Figure 4.10 A, B and C). The levels of HSP40 showed significant increase in the KO neurons as compared to the WT in the control. Later, the levels started decreasing, but still non significantly, in the treated neurons. Post 4hour recovery the HSP40 levels moderately but non-remarkable decreased in the HSPB8(KO).The levels significantly dropped after 8-hour redemption from the arsenite treatment (Figure 4.10 A, B and D). Additionally, the level of BAG1 also remained persistently high in the HSPB8(KO) in distinct conditions (Figure 4.10 A, B and E). CASA crosstalk with the UPS based on co-chaperons BAG3 or BAG1, any insult in the cell leads to the activation of the adaptive responses that can switch between a BAG1-dependent proteasomal activity or BAG3-mediated autophagy (Gamerdinger et al., 2011 and Minoia et al., 2014). Indeed, it is fascinating to reveal that in absence if HSPB8 both the pathways remained remarkably overexpressed in comparison to the WT. DNAJB6 member of DNAJ family has been reported to take part in the CASA (Sarparanta et al., 2012, 2020). Thus, we investigated the expression levels of DNAJB6 in our spinal motor neurons. Having said this in our neurons the levels of DNAJB6 were non quantifiable both in WT and KO (Figure 4.10F).
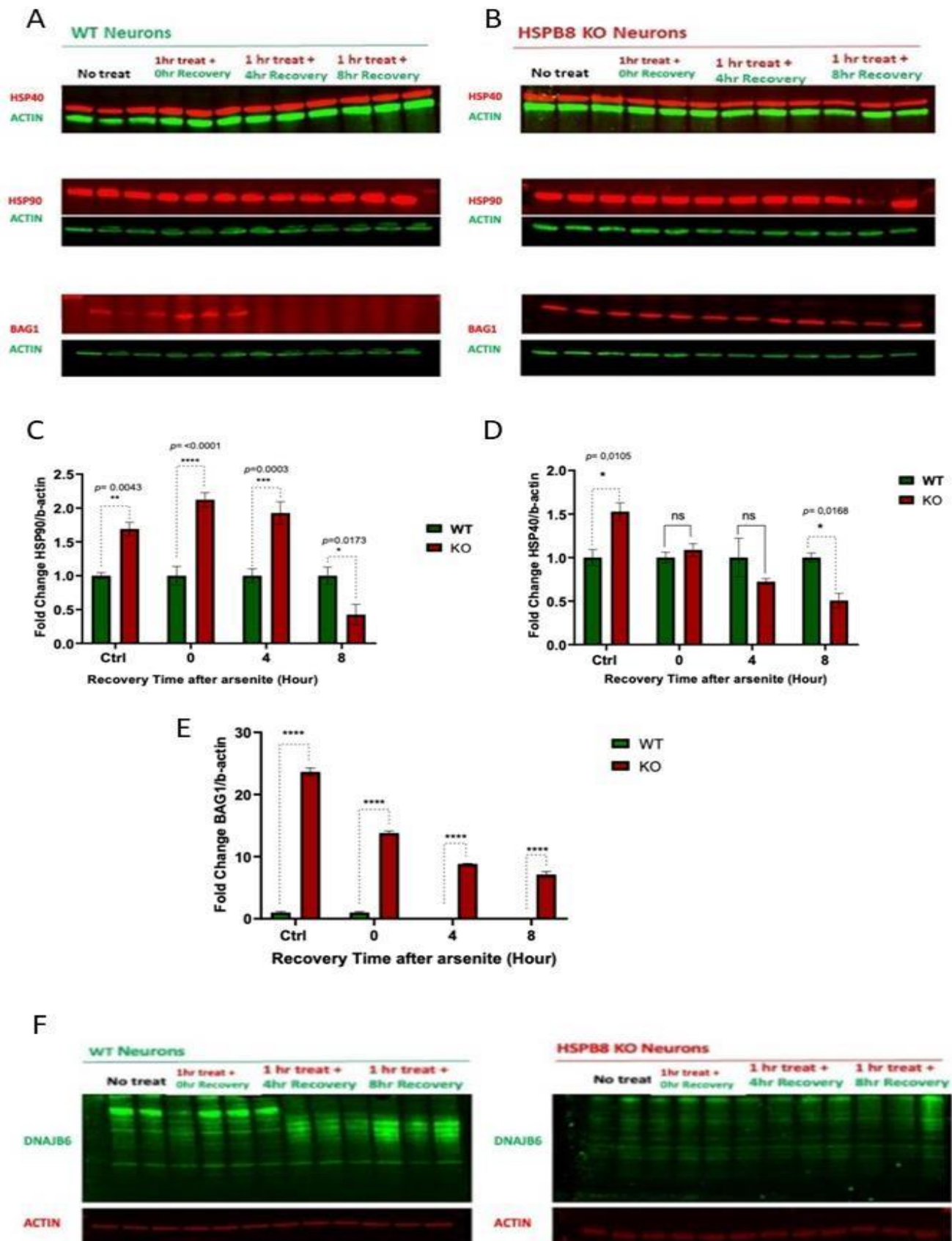
*Figure 4.10*: **Chaperones assist CASA-complex members**

(A) Representative images of fluorescence Western Blot for a panel of chaperones in control conditions (no treat), 1-hour arsenite treated and no recovery, followed by 4hour recovery and 8-hour post recovery in WT neurons. First blot showing HSP40 (red) and β-actin (green); second blot shows HSP90 (red) and β-actin (green) and last blot reveals BAG1 (red) and β-actin (green). (B) Pictures of fluorescence Western Blot for a panel of chaperones in control conditions (no treat), 1-hour arsenite treated with no recovery, followed by 4hour recovery and 8hour recovery in KO neurons. First blot showing HSP40 (red) and β-actin (green); second blot shows HSP90 (red) and β-actin (green) and last blot reveals BAG1 (red) and β-actin (green). (C) The graph represents the level of HSP90 each analyzed protein in every condition normalized to β-actin and to WT. (D) The graph represents the level of HSP40 each analyzed protein in every condition normalized to β-actin and to WT. (E) The graph represents the level of BAG1 each analyzed protein in every condition normalized to β-actin and to WT. (F) Representative images of fluorescence Western Blot for DNAJB6 (green) and β-actin (red) in control conditions (no treat), 1-hour arsenite treated with no recovery followed by 4hour recovery and 8-hour post recovery in WT and KO neurons. All the quantifications were performed based on the fluorescence intensity using Image Studio Lite software. All the graphs are presented as mean ± SEM. N = 3 biological replicates, one-way ANOVA with Tukey's multiple comparison.

## 4.6.2    Switch between CASA and UPS or interaction between CASA and the UPS

To keep the proteome healthy, the proteostasis network pathways work together on multiple levels. HSPAs (including HSP70) serve as a foundation for client proteins and their interacting partners to decide whether to fold or dispose of them like by interacting with HSP90 (heat shock protein 90), HSPAs support the folding of newly synthesized proteins (Wegele et al., 2004). The fate of substrates routed for degradation through ubiquitination, towards autophagy or the UPS, is determined by interacting co-chaperones. Under normal conditions, ubiquitination and proteasome- mediated degradation is the preferred route. However, the narrow core tunnel of the proteasome can be a limitation for processing stable higher-order structures such as oligomers or aggregates, that are unable to be fully unfolded. Additionally, an excess of misfolded substrates can overwhelm the proteasome, leading to the activation of complementary systems to reduce the accumulation of toxic misfolded proteins. A possible adaptive response is to shift from BAG1-dependent proteasomal activity to BAG3-mediated autophagy for protein degradation (Gamerdinger M et al., 2009 and Minoia M et al., 2014).  The quantitative findings presented in the earlier section revealed that in the HSPB8(KO) neurons, there were higher levels of both the chaperones BAG3 and BAG1 independent of the conditions (look Figure 4.9 F and 4.10 E). To comprehend the crucial role of this switch, we examined the BAG3:BAG1 ratio from the above-mentioned western blot in the KO (untreated

conditions) and found that KO neurons had both pathways upregulated compared to WT. However, BAG3 had always higher levels suggesting BAG3 -mediated autophagy being higher compared to BAG1-dependent proteosomal pathway (Figure 4.11).
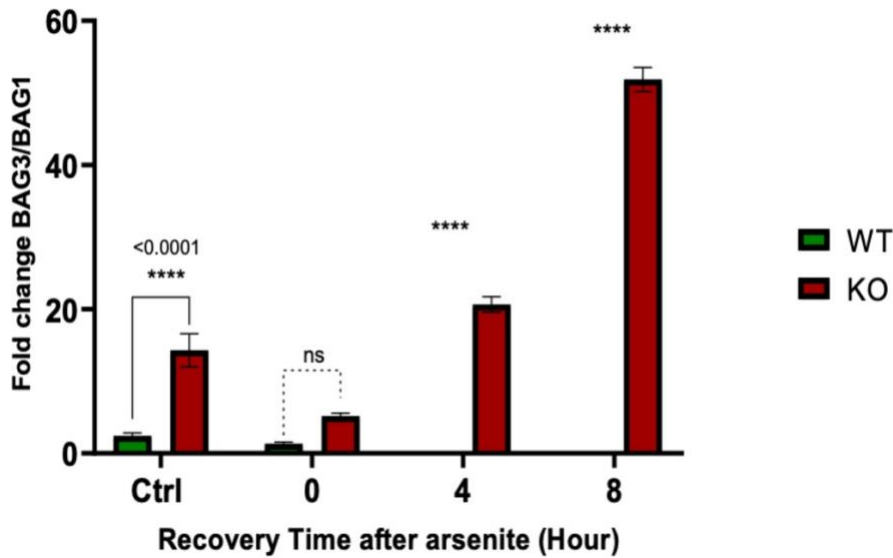


*Figure 4.11:* **BAG3:BAG1 levels in the KO neurons remain significantly high**

The graph represents the level of BAG3/BAG1 each analyzed protein in every condition normalized to β-actin and to WT. All the quantifications were performed based on the fluorescence intensity using Image Studio Lite software. All the graphs are presented as mean ± SEM. N = 3 biological replicates, one-way ANOVA with Tukey's multiple comparison.

### 4.6.3 Absence of HSPB8 other chaperons from CASA are not the integral part of the SG constituent and regulator of stress granules assembly

To investigate the results of previous section (Figure 4.8 A and B) where knocking out of HSPB8 did not abolish SGs nevertheless stress granules took a prolonged period to dissolve in contrast to WT. HSPB8 is known to be recruited to the SG in response to insult (e.g., oxidative stress or proteosome inhibition) later upon stress recovery, HSPB8 recruits HSP70 and BAG3 to remove the misfolded substrate from SGs (Ganassi et al., 2016). This made SG disassembly in the KO neurons more questionable, in the above section we had also acknowledged that the CASA-complex was compromised. Further able to answer why SGs dissolution were prolonged in KO we decided to check the members of CASA whether they were recruited to SG in absence of HSPB8. The major CASA-chaperone was investigated for this purpose namely- BAG3, HSP70, HSC70 and HSP40. Literature suggest that HSP70 recruits to SGs in ALS-SOD1 pathogenesis (Mateju et al., 2017). Additionally, both Hsp70 and Hsp40 proteins can be localized within stress granules in yeast and mammalian cells autophagy (Cherkasov et al., 2013; Mazroui et al., 2007; Walters et al., 2015). For this purpose, the neurons were stressed for 1 hour with sodium arsenite as previously stated. The cells were fixed after 1hour of treatment, stained with DAPI to label the nucleus and after that, fluorescence microscopy images were acquired. Surprisingly, we do not observe any of the chaperone colocalizing with the SGs neither in the WT nor in the KO neurons (Figure 4.12 A and B). Exceptionally, we observed something quiet intriguing in KO-treated neurons only with HSP40 chaperone. There were nuclear or perinuclear puncta which did not colocalize with TIAR-1 stress granule marker (look Figure 4.11B).
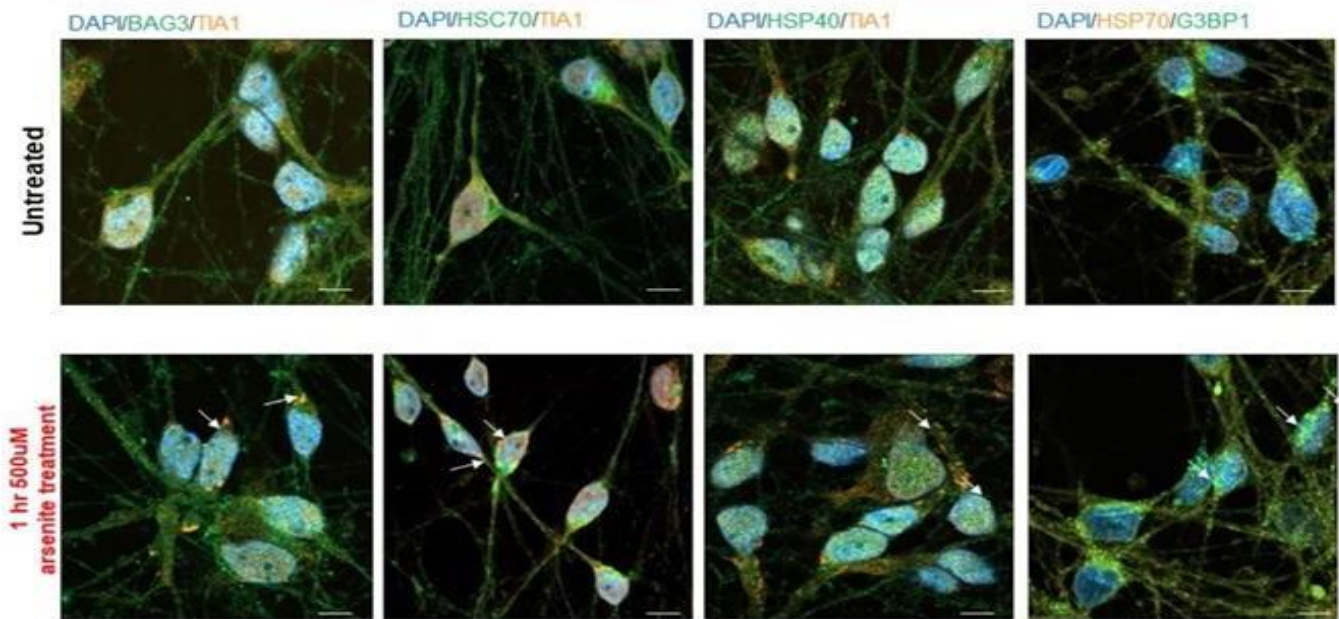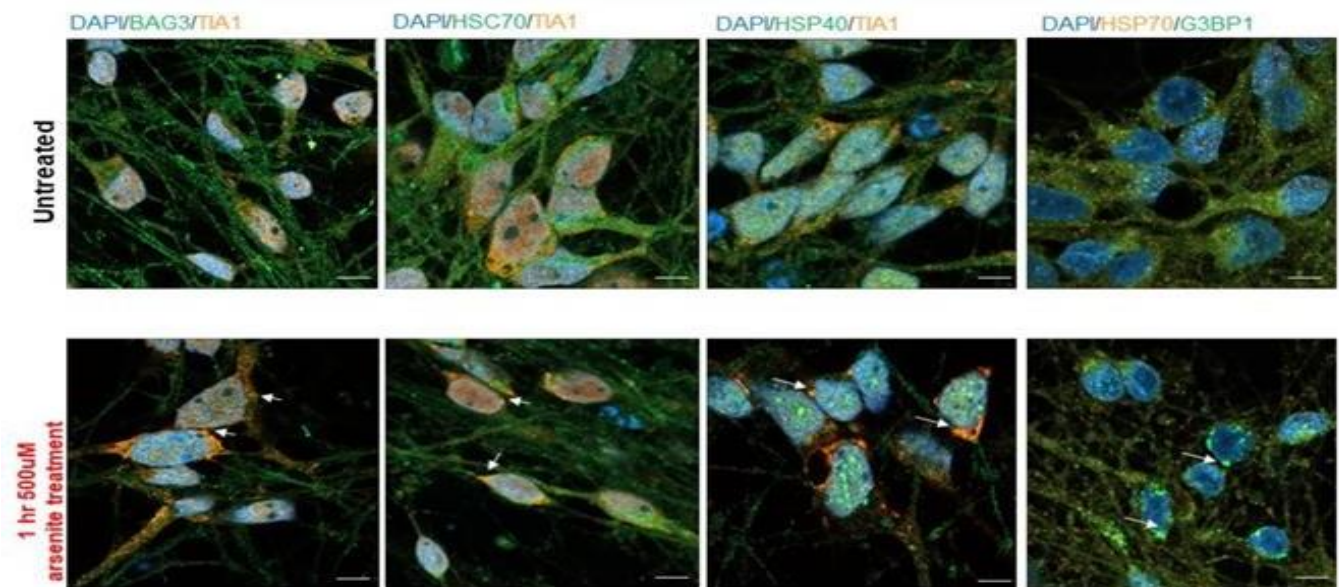
*Figure 4.12:* **Expression of BAG3, HSP70, HSC70 and HSP40 via immunofluorescence**

(A) Representative pictures depict the expression of BAG3, HSC70, HSP40 and HSP70 in the WT neurons, upper lane represents the Control conditions lower lane shows the neurons which are stressed with aresnite showing SGs mark with white arrows. Each lane represents the individual chaperone in Control and treated conditions. (B) Representative image of Immunofluorescence for HSPB8(KO) neurons upper lane represents the untreated conditions lower lane represents the treated conditions for BAG3, HSC70, HSP40 and HSP70 respectively showing SGs mark with white

arrows. Third bottom image for HSP40 (arsenite treated) depicts nuclear puncta positive for HSP40 which does not colocalized with TIAR-1. For all the immunofluorescence images TIAR or G3BP1 has been used as a SG marker. Scale bar 10 µm

## 4.7 Compromised BAG3-HSP70-HSPB8 ternary complex for the autophagy-lysosomal clearance in HSPB8(KO)

### 4.7.1 HSPB8KO neurons explicit lower number of autophagosomes and autolysosomes

Multiple evidence implies during the autophagy flux, the fusion step of autophagosomes and lysosomes requires HSPB8. The autophagosome-lysosome pathway (APLP) is activated by HSPB8, resulting in the clearance of the mutant G93A-SOD1 (V Crippa et al., 2010). Suppression of HSPB8 impeded the fusion of autophagosomes and lysosomes (Li et al., 2017). Elevated levels of HSPB8 correct a deficient autophagic flux and ensure that misfolded proteins are effectively directed to autophagy for clearance (P Rusmini et al., 2017). The CASA complex can identify and bind multiple misfolded proteins, and it transports them along microtubules to the microtubule organization center (MTOC) for inclusion into autophagosomes and eventual degradation by lysosomes (R Cristofani et al., 2021). To study the function of HSPB8 in APLP the spinal motor neurons were incubated with the Tandem Sensor RFP-GFP-LC3B (Figure 4.13A). To analyze the influence of autophagosomes and autolysosomes on WT and KO neurons the neurons were treated with Premo Autophagy Assays with Sensor Tandem Sensor RFP-GFP-LC3B. autophagosomes identified by their positive staining for both GFP and RFP. Once the lysosome fused with an autophagosome, the pH droped and caused the GFP to be quenched, resulting in autolysosomes appearing red followed by live-cell imaging through LSM (Figure 4.13 A and B). Later quantification was done by using ImageJ Fiji as using cell counter feature. As shown in Figure 4.13 C, the number of autophagosomes and autolysosomes in KO neurons were found to be significant lower in comparison to those in WT neurons.
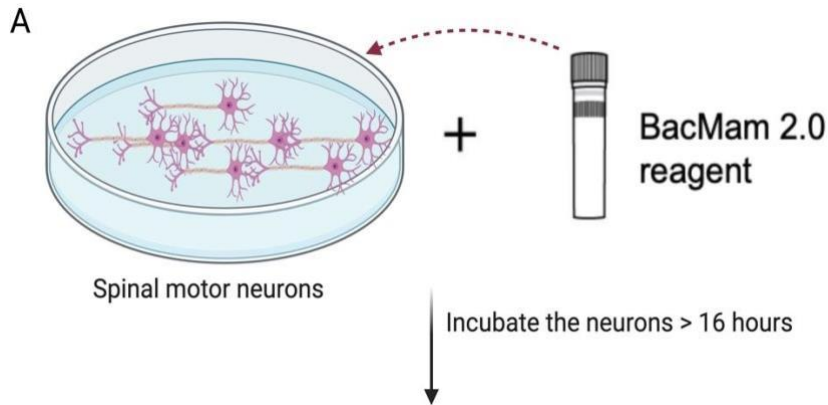
**Working schematic representation of Premo™ Autophagy Tandem Sensor RFP-GFP-LC3B Kit**: By combining an acid-sensitive GFP with an acid-insensitive RFP, the change from autophagosome (neutral pH) to autolysosome (with an acidic pH) can be visualized by imaging the specific loss of the GFP fluorescence, leaving only red fluorescence.
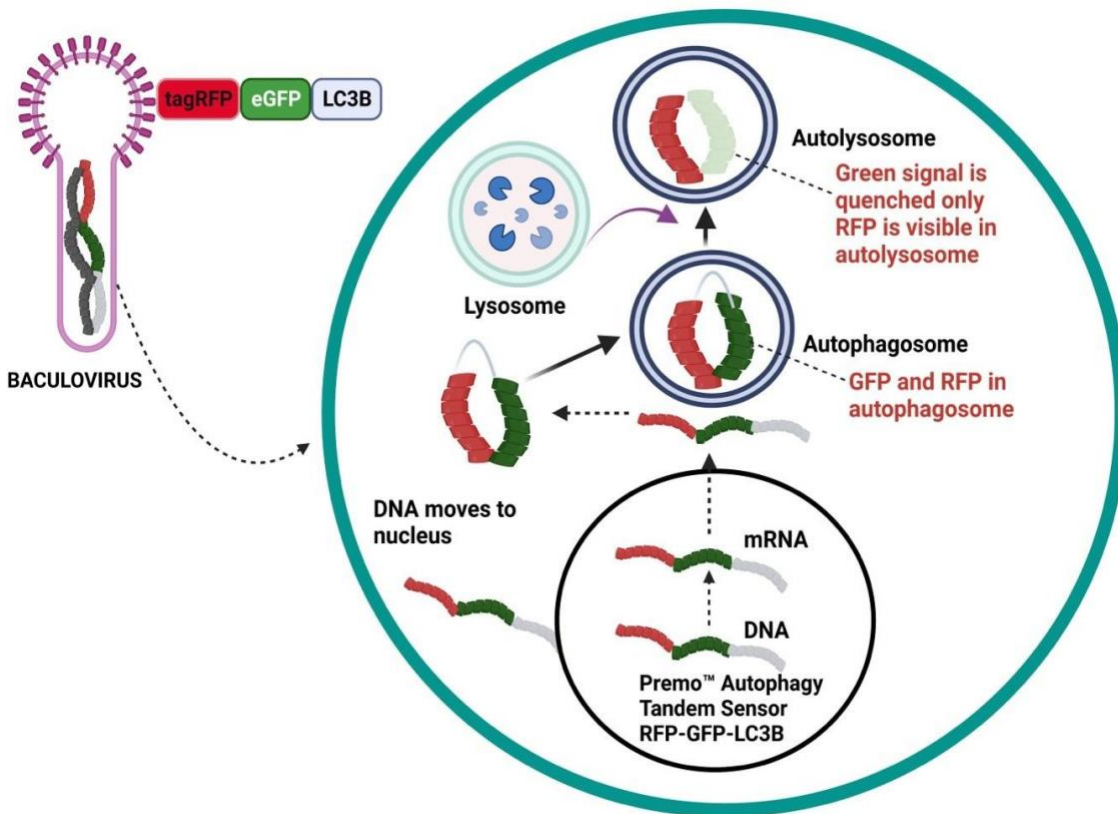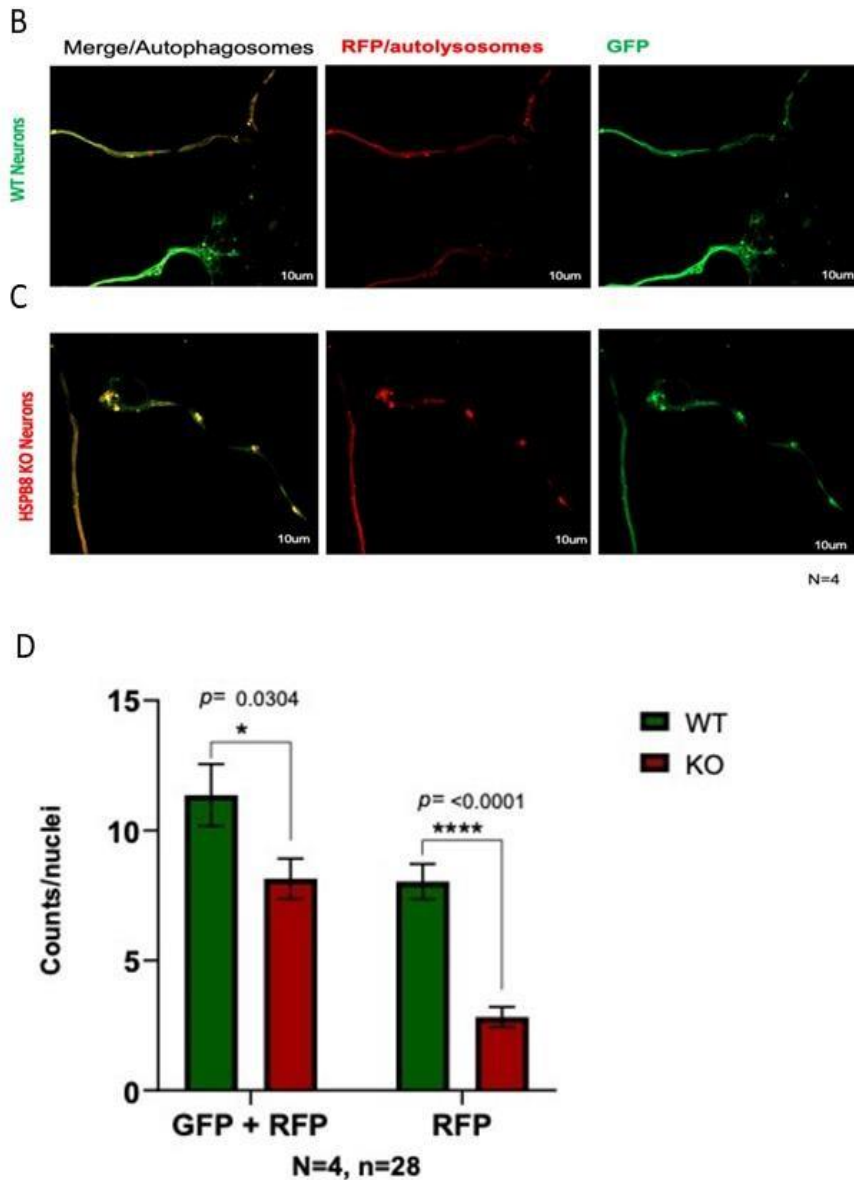
*Figure 4.13:* **Autophagosomes and autolysosomes expression in WT and KO neurons**

(A) Workflow of spinal motor neurons with BacMam2.0 incubation followed by expression/quantification of Tandem Sensor RFP-GFP-LC3B through live cell imaging. Image created by BioRender. (B) Representative pictures depict the expression of autophagosomes (GFP+RFP) and autolysosomes (RFP) in the WT neurons. (C) Representative Images depict the expression of autophagosomes (GFP+RFP) and autolysosomes (RFP) in the KO neurons. Scale bar 10 μm. (D) The graphs represent quantification of A and B with ImageJ Fiji cell counter. Data are presented as mean ± SEM. N = 4 biological replicates, for each condition 6-8 images were analyzed. Statistical analysis with two-way ANOVA followed by Tukey's multiple comparison.

### 4.7.2   Lysosomes area has been reduced in HSPB8(KO)

HSPB8 observed to be involved in the autophagic response triggered by elevated glucose levels, both in in vivo and in vitro settings. Furthermore, it played a pivotal role in mediating the fusion of autophagosomes with lysosomes during the autophagic flux (X. C. Li et al., 2017). Emerging evidence indicated that the HSPB8K141N variant may interfere with the clearance of autophagosomes by impeding their co-localization with lysosomes and subsequent fusion, instead of impacting autophagosomes co-localized with protein aggregates (Kwok et al., 2011). HSPB8, represented a novel mechanism by which autophagy could be regulated and might have had important implications for the treatment of various diseases, including neurodegenerative disorders and cancer, which were associated with defects in lysosomal function and autophagy (Rusmini et al., 2019). Following the results of the previous section 4.7.1. The next step we decided to pursue was to measure the number of lysosomes and area of lysosomes independent of the Tandem Sensor RFP-GFP-LC3B. We investigated the number, size and area of lysosomes via LAMP2 immunofluorescence staining. For this purpose, the neurons were fixed, stained with DAPI to label the nucleus, neuronal marker MAP2 and LAMP2 (look Figure 4.14 A). After that, fluorescence microscopy images were acquired. Next, the area, size and number of Lysosomes per cell was automatically quantified using Cell Profiler 2.2.0. There was a significant decrease in the number and area of lysosomes in KO neurons compared to WT (Shown in Figure 4.14 B). Quantification  also revealed that no changes were observed in the size of the lysosomes in KO neurons compared to the WT (Fig. 4.14 C). These results remain consistent with the above findings that KO neurons had significant low number of autolysosomes. Additionally, the number and area of lysosomes seemed to be affected in the knock-out neurons; however, the size of lysosomes did not change.
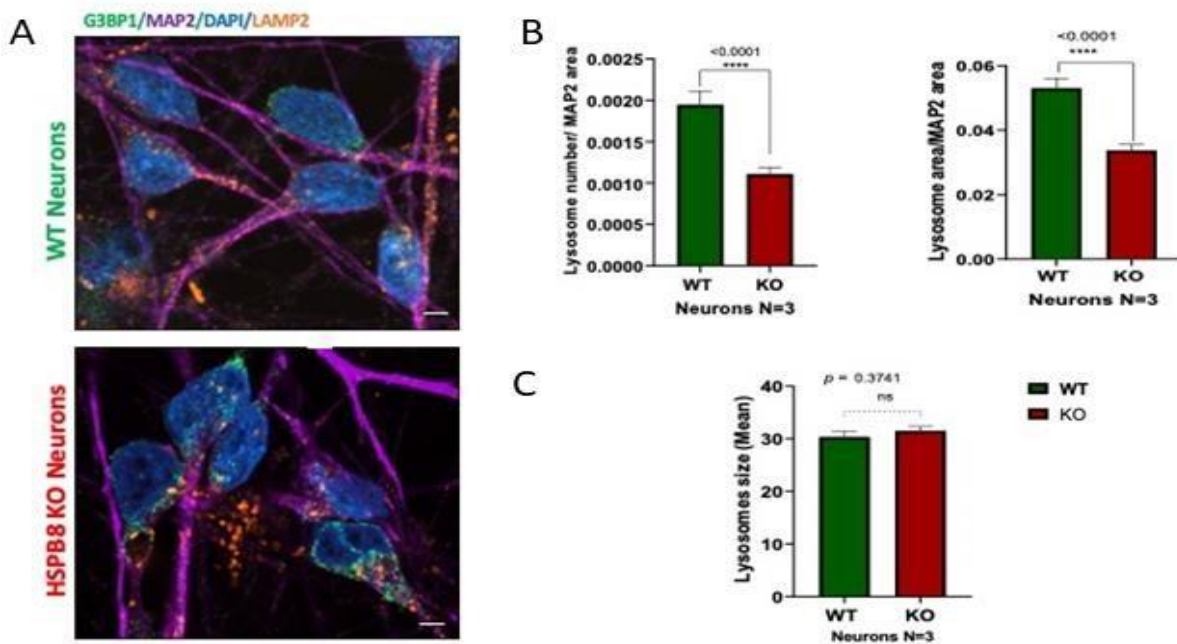
*Figure 4.14:* **Lysosomes expression in WT and KO neurons**

(A) Representative pictures depict the expression of LAMP2 (orange), MAP2 (purple) and DAPI. Upper lanes represent the WT neurons and lower lane shows the KO neurons. Scale bar 10 μm. (B) The graphs represent quantification of A and B with an automated quantification of lysosomes was performed using Cell Profiler 2.2.0. for Lysosomes numbers and lysosomes area. (C) The graphs represent quantification of A and B with an automated quantification of lysosomes size was performed using Cell Profiler 2.2.0. Data are presented as mean ± SEM. N = 4 biological replicates, for each condition 7-8 images were analyzed. Statistical analysis with unpaired two-tailed student's t-test.

### 4.7.3 Delineating the expression of the autophagic receptor SQSTM1/p62

The CASA process involved interaction between the autophagy adapter SQSTM1/p62 (Gamerdinger et al., 2011) and its recognition of substrates with selectivity. Additionally, this adapter had been known to bind to the autophagosomal marker protein LC3, thereby guiding ubiquitinated substrates towards the autophagosomes for degradation via autophagy. The interaction between BAG3 and SQSTM1 triggered the enlistment of HSPB8, BAG3, and HSP70 to specific autophagy-targeted substrates (Crippa et al., 2010a; Gamerdinger et al., 2011). P62 is considered a crucial molecule for protoestasis due to its multifunctional nature. It played a role in the formation of ubiquitinated aggregates and selective autophagy, as well as facilitated communication between cellular clearance pathways and major cytoprotective pathways during oxidative stress. The CASA complex known to facilitate the binding of HSPB8 and BAG3, as well as the HSP70-STUB1 complex. This allows for STUB1-mediated ubiquitination of misfolded substrates, which are then recognized by SQSTM1/p62 and incorporated into the autophagy pathway (Rusmini P et al., 2017). In order to

examine the levels of p62, we employed a protein Isolation technique followed by western blot analysis. We aimed to investigate the contribution of p62 in the disassembly of SGs, and thus treated neurons with arsenite and allowed for a recovery period of up to 8 hours. We assessed the expression levels of p62, as depicted in Figure 4.15 A, and subsequently quantified these levels. As anticipated, we observed that the KO neurons exhibited significantly lower levels of p62 under basal conditions (refer to Figure 4.15B). Furthermore, the levels of p62 remained significantly low after arsenite stress and during recovery from it.
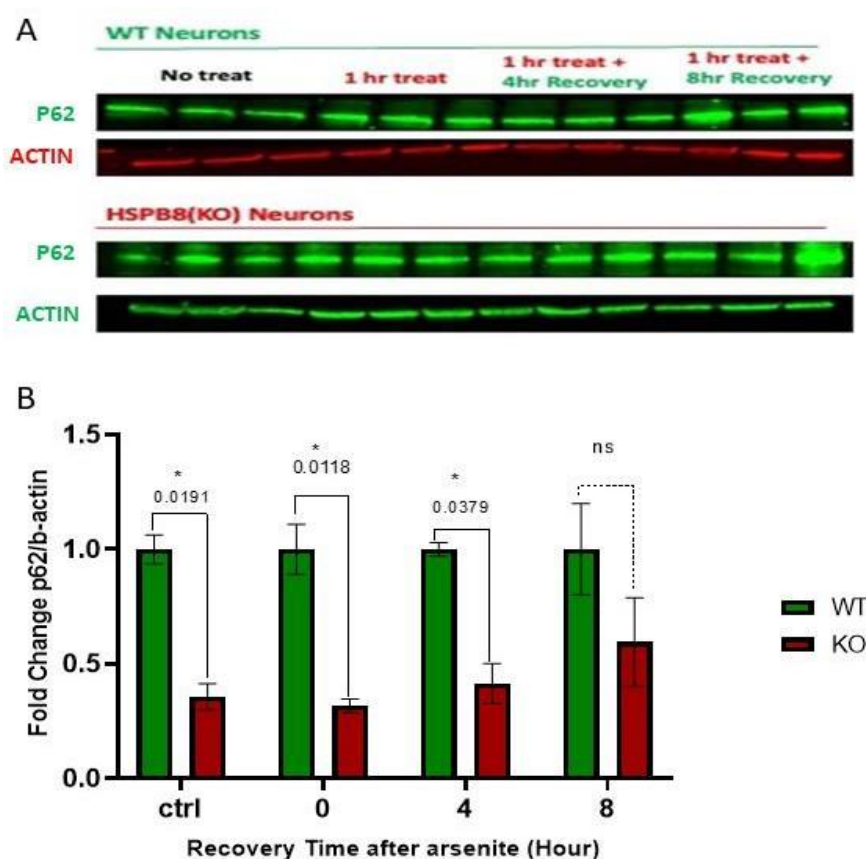


*Figure 4.15*: **P62 levels in WT and KO neurons**

(A) Representative images of fluorescence Western Blot for p62 in control conditions, 1-hour arsenite treated and post recovery in WT (upper row) upper lane represents the p62 and bottom lane represents β-actin and KO (bottom panel) upper lane represents the p62 and bottom lane represents β-actin neurons. (B) The graph represents the level of p62 each analyzed protein in every condition normalized to β-actin and to WT. All the quantifications were performed based on the fluorescence intensity using Image Studio Lite software. All the graphs are presented as mean ± SEM. N = 3 biological replicates, one-way ANOVA with Tukey's multiple comparison.

## 4.8  Exploring the levels of polyubiquitination in HSPB8(KO)

The functions of p62 in selective autophagy had been well established. Specifically, it served as a critical component for the assembly of protein aggregates and functioned as an autophagy receptor by facilitating the connection between ubiquitin-tagged protein aggregates and autophagosomes for subsequent degradation. In cultured cells, p62 formed cytoplasmic inclusion bodies, commonly referred to as p62 bodies, through endogenous or ectopic expression (Bjørkøy et al., 2005). These bodies contained polyubiquitin chains, with K63 polyubiquitin chains preferentially recruited into p62 bodies (Stolz et al., 2014). Following the observed reduction in p62 levels in the preceding section, we proceeded to investigate the levels of K63 polyubiquitination in our spinal motor neurons. Unexpectedly, we did not observe any quantifiable band in the wild-type neurons, while conversely, we detected a band in the KO neurons. There is a prevailing notion that proteins modified by K63 chains serve as substrates for aggrephagy while K48-ubiquitinated proteins undergo degradation via proteasome. Nevertheless, it had been shown that K63, and K48 chains were all capable of eliciting phase separation in vitro through binding to p62, albeit with a lower efficacy than the K48 chain (Sun et al., 2018; Zaffagnini & Martens, 2016). To comprehend the function of K48 polyubiquitination, we opted to examine its levels via western blot (refer to Figure 4.16 B). Through quantification, we determined that there are no distinctions in polyUBK48 levels between WT and KO (as shown in Figure 4.16 C).
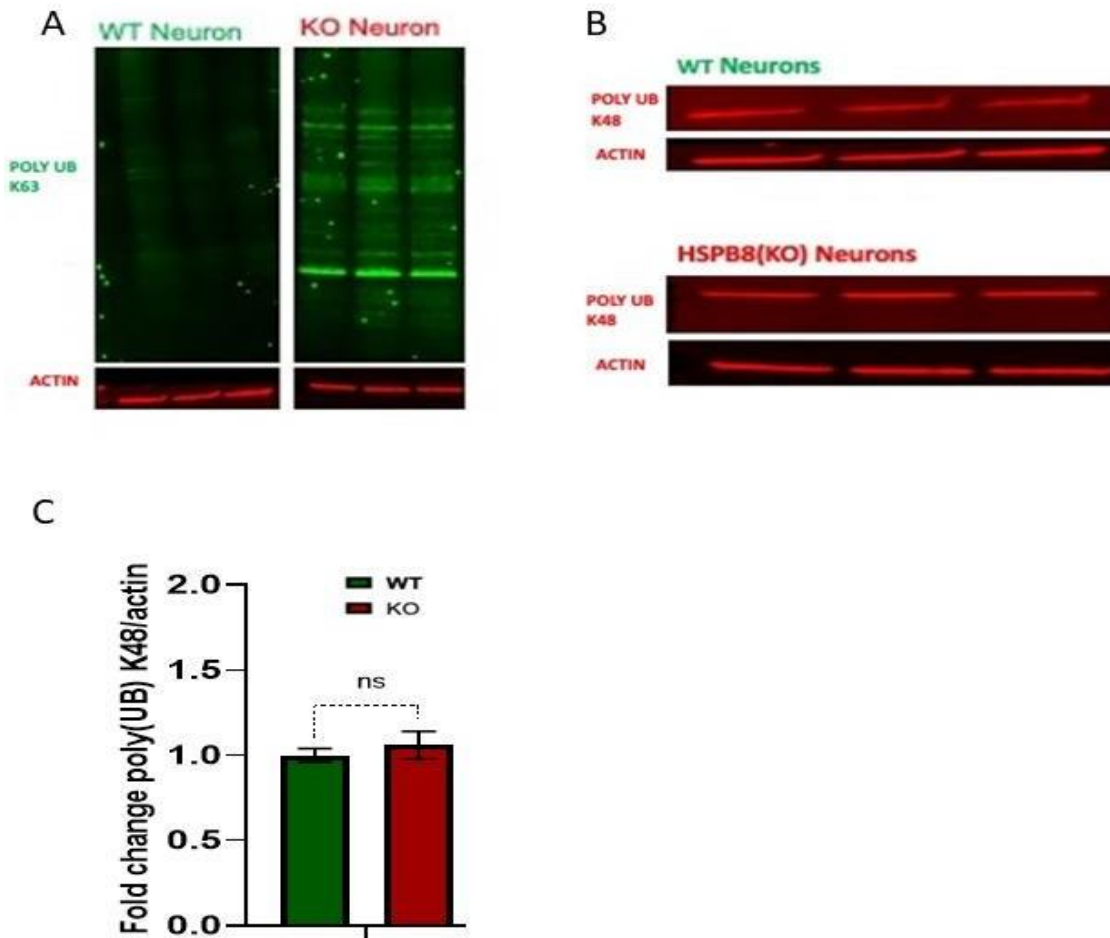
*Figure 4.16:* **Polyubiquitin antibodies levels in WT and KO neurons**

(A) Representative images of fluorescence western Blot for polyK63 in WT (left) upper lane polyK63 and lower lane β-actin and KO (right) neurons upper lane polyK63 and lower lane β-actin. (B) Representative images of fluorescence western Blot for polyK48 in WT (upper lane polyK48 bottom lane β-actin) and KO (upper lane polyK48 and bottom lane β-actin) neurons. (C) The graph represents the level of polyUB K48 protein normalized to β-actin. Data are presented as mean ± SEM. N = 3 biological replicates. Statistical analysis with unpaired two-tailed student's t-test.

# 5 Discussion

The discussion of the thesis revolves around the multifaceted role of HSPB8 in various neurodegenerative diseases. On the one hand, multiple studies have demonstrated that HSPB8 is implicated in the clearance of protein aggregates resulting from genes associated with ALS (Crippa et al., 2010b; Crippa et al., 2016; Carra et al., 2013; Rusmini et al., 2013, 2015). On the other hand, mutations in HSPB8 are causing CMT2L, an autosomal dominant distal axonal motor neuropathy-myofibrillar myopathy syndrome. Furthermore, HSPB8 is highly expressed in the surviving α-MNs of ALS patients' spinal cord. The presented research thus aimed to investigate the role of HSPB8 loss of function on motor neurons, disturbances on neurodegenerative disease pathways such as SG, proteostatis and autophagy and a putative association between HSPB8 chaperone and aggregation prone ALS related proteins, in our case FUS, specifically focusing on the expression pattern and levels of FUS proteins in motor neurons.

## 5.1 HSPB8: A critical regulator of stress granule disassembly and neuronal survival

Stress granules are dynamic cytoplasmic RNA-protein complexes that form in response to various cellular stressors, such as oxidative stress or viral infections (Anderson & Kedersha, 2006; Nover et al., 1989). They have been shown to play a critical role in the cellular stress response and regulation of gene expression. The process of SG formation is complex and involves the recruitment of multiple proteins, including heat shock proteins such as Hsp22 (HspB8), Hsp27 (HspB1), Hsp40, and Hsp70, which are involved in protein homeostasis, including protein folding, degradation, and refolding (Cherkasov et al., 2013; N. L. Kedersha et al., 1999; Walters et al., 2015; Mateju et al., 2017).

To further investigate the role of HSPB8 in SG regulation, we studied the effects of HSPB8 knockout on SG formation and disassembly. Using sodium arsenite treatment, which induces SG formation, we found that HSPB8 knockout did not abolish SG formation in neurons, suggesting that other HSPs may compensate for its loss (Look Figure 4.7 D). Given that HSPB8 is considered a crucial factor in preserving the solubility of stress granules, as it is described for Hela cells (Ganassi et al., 2016). Consistently with this findings, in our spinal motor neurons time course experiments revealed two phenotypes: (1.) HSPB8 knockout cells showed delayed and overshooting SG assembly as well as that SG disassembly takes longer in HSPB8 knockout cells compared to wild-type cells, indicating that HSPB8 plays a critical role in SG dynamics (Fig. 4.8 A,B). Moreover, there was a significant increase in

the number of persistent SGs in KO neurons compared to WT post recovery of 2 hour and 4 hour (Shown in Figure 4.8 B). This was associated with lower survival rate compared to wild-type cells (Fig. 4.8 C).

In conclusion, our findings suggest that HSPB8 plays a crucial role in the regulation of SG dynamics and cell survival. The study also underscores the intricate regulation of SGs and the involvement of multiple chaperones in the process. Understanding the regulation of SGs is important for developing strategies to mitigate the damage caused by stress and improve cellular survival under stressful conditions.

## 5.2 *The importance of chaperone-assisted selective autophagy in stress granule disassembly: A study on the role of HSPB8 in protein homeostasis.*

The study by (Tedesco et al., 2022) sheds light on the importance of chaperone-assisted selective autophagy in stress granule disassembly. The authors found that a very small portion of SGs is dependent on autophagic clearance, and the majority of SG disintegration is based on chaperone-dependent and autophagy-independent pathways. The CASA complex, consisting of HSPB8-BAG3-HSP70-CHIP, surveils the proper composition of SGs and prevents their persistence. CASA targets specific proteins or protein aggregates for degradation (Carra et al., 2008 ; Ganassi et al., 2016). Indeed, the reduction of HSPB8 and BAG3 resulted in a notable rise in the proportion of cells harbouring persistent stress granules, mirroring the observations made in cells depleted of HSP70. The delay in the restoration of translation in cells lacking HSPB8 and BAG3 further supported the persistence of SGs. Interestingly, even in the absence of BAG3 and HSPB8, the expression of HSP70 was induced upon prolonged treatment with MG132, indicating that HSP70's role in SG disassembly is reliant on the presence of BAG3 or HSPB8 and cannot function independently (Ganassi et al., 2016).

Hsp70 chaperone that serves diverse roles in protein quality control processes. Their functions encompass various essential tasks such as facilitating the folding of newly synthesized proteins, assisting in the refolding of proteins damaged by stress, aiding in protein transport and membrane translocation, as well as contributing to protein degradation mechanisms (Kim YE et al., 2013). HSP40 regulates the HSP70 reaction cycle (Hart FU et al., 2009, Maye MP et al., 2010). HSP40 recruits HSP70 to non-native substrate protein, this interaction with HSP70 strongly stimulates (> 1,000 fold) the hydrolysis of HSP70-bound ATP to ADP, resulting in stable substrate binding by HSP70 in the closed

conformation (Hart FU et al., 2009, Maye MP et al., 2010, Kim YE et al., 2013). Proteins which are unable to utilize HSP70 mechanistic paradigms in protein folding or clearance are transferred to HSP90 system also many signalling proteins in eukaryotes are transferred from HSP70 to the ATP-dependent HSP90 chaperone system for completion of folding and conformational regulation. The mechanistic way by which HSP90 recognizes the non-native proteins is alike HSP70 ATP-regulated facilitated by other co-chaperones which bring unfolded proteins (Kim YE et al., 2013).

Ensuring the proper folding and preservation of newly synthesized proteins is vital for maintaining a functional proteome. While significant progress has been made in the mechanisms of the proteostasis network (PN), our comprehension of the collaborative functioning of different chaperone systems within the network, along with their coordination with protein transport and degradation machinery, remains limited (Kim YE et al., 2013). The breakdown of proteostasis is associated with diseases and the detrimental consequences of aging (Balch WE et al., 2008). Molecular chaperones play pivotal roles within the PN by their capacity to identify misfolded proteins, thereby assuming multiple crucial functions. The proteostasis network demonstrates a fundamental characteristic in its organization by tightly interconnecting the functions of molecular chaperones with protein degradation pathways. These degradation pathways serve the crucial role of eliminating non-functional, misfolded, or aggregated proteins that have the potential to disturb proteostasis. Within the PN, the degradation branch encompasses both the ubiquitin-proteasome system and the machinery involved in autophagy. Aggregated proteins that cannot be unfolded for proteasomal degradation may be removed by autophagy and lysosomal degradation. Loss of autophagy causes inclusion body formation and neurodegeneration, even in the absence of additional stress, demonstrating the importance of this pathway for proteostasis (Komatsu M et al., 2006, Kim YE et al., 2013). The pathways of autophagy include CASA and Chaperone-mediated autophagy (Kettern N et al., 2010, Kon M et al., 2010, Arias E et al., 2011).

We decide to investigate the role of CASA as HSPB8 is an important regulator of CASA. This is the first time we have elucidated the novel HSPB8 knockout role in spinal motor neurons and impaired selective autophagy in *invitro* system . This study examined the levels of chaperones and co-chaperones involved in CASA and their response to various conditions. The protein levels of major CASA components were globally dysregulated in knockout motor neurons. Reports have revealed that BAG3 plays a crucial role in the granulostasis meaning it helps in clearing the SG dissolution and

is strongly upregulated in the stress recovery phase, the same time period when SGs dissolve (Ganassi et al., 2016 ; Mateju et al., 2017; Mediani et al., 2020). In line with these reports the absence of HSPB8 resulted in tremendously upregulated BAG3, which was not affected by arsenite induced SG assembly/disassembly (Fig. 4.9 F). It has been reported by Meister-Broekema M et al., 2018 that due to the toxic gain-of-function, BAG3 impairs the functionality of HSP70. Consequently, CASA-complexes containing mutant BAG3 accumulates at the aggresome along with their associated clients and co-factors. This accumulation hinders the degradation of misfolded cargo bound to Hsp70 and results in the sequestration of crucial proteostasis factors such as HSPB8, SQSTM1/p62, and ubiquitin. In our study, we observed a notable increase in BAG3 expression in knockout neurons compared to wild-type neurons. This finding suggests the possibility that under knockout conditions, BAG3's functionality becomes dysregulated, impairing its ability to effectively clear misfolded cargo. Alternatively, it may indicate a compensatory upregulation of BAG3 that, despite its efforts, proves insufficient to fully restore stress granule dynamics.

HSPB8, which lacks enzymatic activity, cannot independently refold its clients. Instead, it relies on collaborative interactions with ATP-driven chaperones like Hsp70 to facilitate client refolding (Meister-Broekema M et al., 2018, Tedesco et al., 2022). To gain a deeper understanding of this phenomenon, we made a novel discovery by demonstrating that the knockout of HSPB8 results in remarkably low levels of HSP70 (HspA1A, HspA1B) under basal conditions. Additionally, we observed that any subsequent neuronal insult does not further increase the expression of HSP70. However, upon recovery from arsenite stress, there is a substantial amplification of HSP70 levels, which becomes significantly upregulated after 8 hours of recovery (Figure 4.9 C). Previous study has reported the colocalization of HSP70 with stress granules (Mateju D et al., 2017). However, in our investigation, focusing on human motor neurons, we did not observe any colocalization between HSP70 and SGs. It is important to note that the absence of colocalization may vary depending on the cell types used, as our study employed human motor neurons while other study utilized HeLa cells. Our findings indicate the absence of colocalization between HSP70 and SGs in both wild-type (WT) and HSPB8 knockout (KO) neurons. It is worth emphasizing that, consistent with previous research, HSP70 plays a vital role in the disassembly of stress granules (Ganassi et al., 2016, Mateju D et al., 2017, Szewczyk et al., 2023). Our findings align with this understanding, as we observed that reduced expression levels of HSP70 in the absence of HSPB8 result in prolonged disintegration of SGs. This

suggests that HSP70's involvement is critical for the efficient disassembly of SGs, and the lower levels observed in the absence of HSPB8 contribute to the extended persistence of SGs.

Another critical component of the CASA complex is HSC70, the constitutively expressed form of HSP70, which also contributes significantly to chaperone-mediated autophagy (Kim YE et al., 2013). Considering this, we aimed to investigate the involvement of HSC70 in our study. Interestingly, unlike HSP70, we observed a significant upregulation of HSC70 in both untreated and treated conditions. Furthermore, after recovery, HSC70 levels remained moderately but non-significantly elevated in HSPB8KO neurons compared to the wild type (refer to Figure 4.9 D). These findings indicate that HSC70 may play a distinct role in the cellular response, particularly in the absence of HSPB8, suggesting its potential involvement in compensatory mechanisms to maintain cellular proteostasis. In order to ubiquitinate client proteins bound to HSP70, an essential regulator known as U-box-dependent ubiquitin ligase CHIP is required. Intriguingly, our study revealed no significant differences in CHIP expression levels among the knockout neurons, irrespective of treatment or recovery conditions (refer to Figure 4.9E for specific data). This lack of variation may be attributed to the low expression of HSP70 in the KO neurons, as the reduced levels hinder the transfer of misfolded proteins to CHIP. Consequently, the absence of misfolded protein transfer to CHIP may explain the absence of noticeable differences in CHIP expression within the KO neurons.

In light of the observed dysregulation of major components within the CASA-complex in knockout neurons, we further investigated the upstream component of this complex, namely the HSP40 chaperone. The role of HSP40 (DNAJB) chaperone is well-established in recognizing unfolded proteins and facilitating their delivery to HSP70 for subsequent downstream processing (Kim YE et al., 2013). Given the critical role of HSP40 in the chaperone network, we conducted an investigation to gain a thorough comprehension of the dysregulation observed within the CASA complex. In addition to assessing the overall expression of HSP40, we focused on examining the expression levels of a specific member of the HSP40 family, DNAJB6, a member of the DNAJ family, has been reported to be involved in the CASA complex according to previous studies (Sarparanta et al., 2012, 2020). Therefore, we explored the expression levels of both HSP40 and DNAJB6 in our spinal motor neurons to gain insights into their potential contributions to the dysregulation observed within the CASA complex. In our study, the levels of HSP40 exhibited a significant increase in KO neurons compared to wild-type neurons under control conditions. However, these levels showed a non-significant

decrease in treated neurons and a moderate but not noteworthy decrease in HSPB8(KO) neurons after a 4-hour recovery period. Notably, after an 8-hour redemption from arsenite treatment, HSP40 levels experienced a significant drop (refer to Figure 4.10 C and D for detailed data). This observation could be attributed to HSP40's involvement in carrying a substantial load of misfolded proteins under KO conditions. Further insult to the cells may overwhelm the system, leading to a reduction in HSP40 levels. On the other hand, the levels of DNAJB6 were indiscernible in both the wild-type and knockout neurons (refer to Figure 4.10 E). These findings suggest that HSP40 plays a dynamic role in response to different conditions, while the presence of DNAJB6 may be negligible in the specific context of our spinal motor neuron study. While previous research conducted by Walters et al. in 2015 reported the colocalization of HSP40 with SGs, our study presents contrasting findings. In our investigation, we did not observe any colocalization between SGs and HSP40. This discrepancy in observations may be attributed to several factors. One possibility is that the use of a GFP tag in Walters' study could have influenced the colocalization patterns. Additionally, the lack of colocalization could also be influenced by differences in the cell types employed between the two studies. It is important to consider these factors when comparing our results to those reported by Walters et al., highlighting the need for further exploration and understanding of the intricate relationship between HSP40 and SGs in different experimental settings. Furthermore, in our study, we made an interesting observation of nuclear or perinuclear puncta of HSP40 in knockout-treated neurons. These puncta were distinct and did not colocalize with the stress granule marker TIAR-1 (refer to Figure 4.12 A, B). In comparison, wild-type neurons did not exhibit similar results. This finding suggests a potential alteration in the subcellular localization or behaviour of HSP40 in the knockout-treated neurons, indicating a possible role for HSP40 in cellular processes independent of stress granule formation. These results emphasize the need for further investigations to unravel the precise mechanisms and functional implications of HSP40 puncta formation in knockout-treated neurons.

In addition to investigating the upstream components of the CASA complex, we also explored another ATP-dependent chaperone system known as the HSP90 chaperone system. This chaperone system comes into play when proteins are unable to utilize the mechanistic paradigms of HSP70 for proper folding or clearance. In such cases, these proteins are transferred to the HSP90 system for the completion of folding and regulation of their conformation. Furthermore, it is worth noting that the ATP-dependent HSP90 chaperone system plays a crucial role in handling various signaling proteins in eukaryotic cells, ensuring their folding and conformational regulation. Therefore,

recognizing the dysregulation of the HSP70 chaperone system in KO neurons, we sought to investigate the involvement of the HSP90 chaperone system in our study. Our findings reveal that the levels of HSP90 were significantly upregulated in KO neurons under untreated and treated conditions after a 4-hour recovery period. However, intriguingly, these levels were significantly suppressed after an 8-hour recovery period compared to the wild-type (WT) neurons (refer to Figure 4.10 C for specific data). These results suggest that the HSP90 chaperone system may be attempting to compensate for protein folding and quality control processes in the absence of HSPB8, as evidenced by its upregulation in the control and treated KO neurons. However, the downstream processing of proteins may be affected due to the absence of HSPB8, a crucial regulator responsible for maintaining protein homeostasis. These findings shed light on the intricate interplay between chaperone systems and highlight the importance of HSPB8 in ensuring proper protein folding and quality control.

In addition to the selective autophagy pathway represented by the CASA complex, the ubiquitin-proteasome system (UPS) plays a crucial role in protein quality control. Previous research conducted by Cristofani et al. in 2017 demonstrated that when dynein-mediated transport of misfolded proteins by BAG3 to autophagy fails, cells activate an alternative pathway involving BAG1. This BAG1-mediated rerouting of misfolded protein substrates directs them towards the proteasome for degradation. This indicates that cells employ a compensatory mechanism to restore protein homeostasis when one of the degradative pathways is overwhelmed or impaired, rather than modifying the degradative pathway itself. When there are too many misfolded substrates, the proteasome may become overloaded, causing other systems to activate and prevent the buildup of harmful misfolded proteins. One way the body may adapt to this is by transitioning from using BAG1-dependent proteasomal activity to BAG3-mediated autophagy as a means of degrading proteins or vice-versa (Gamerdinger M et al., 2009 and Minoia M et al., 2014). The results showed that in the absence of HSPB8, both the proteasomal and autophagy pathways were remarkably overexpressed compared to the wild type (Fig. 4.11).

Collectively, the findings of this study indicate that the CASA complex, consisting of HSPB8, BAG3, HSP70, and CHIP, may not be the sole mechanism involved in the dissolution of stress granules. It is evident that the dysregulation caused by an excessive accumulation of misfolded proteins also affects the upstream components of the CASA complex. Moreover, the study highlights the

compensatory efforts of the HSP90 molecular pathway to maintain protein homeostasis; however, it does not fully compensate for the loss of HSPB8. Additionally, besides the selective autophagy pathway represented by CASA, the proteasomal system also shows increased expression in the absence of HSPB8, further emphasizing the complexity of protein quality control mechanisms. These findings enhance our understanding of the intricate network of cellular processes involved in protein homeostasis and shed light on the potential limitations and compensatory mechanisms in the absence of key components like HSPB8.

## Neuropathological features of HSPB8(KO)
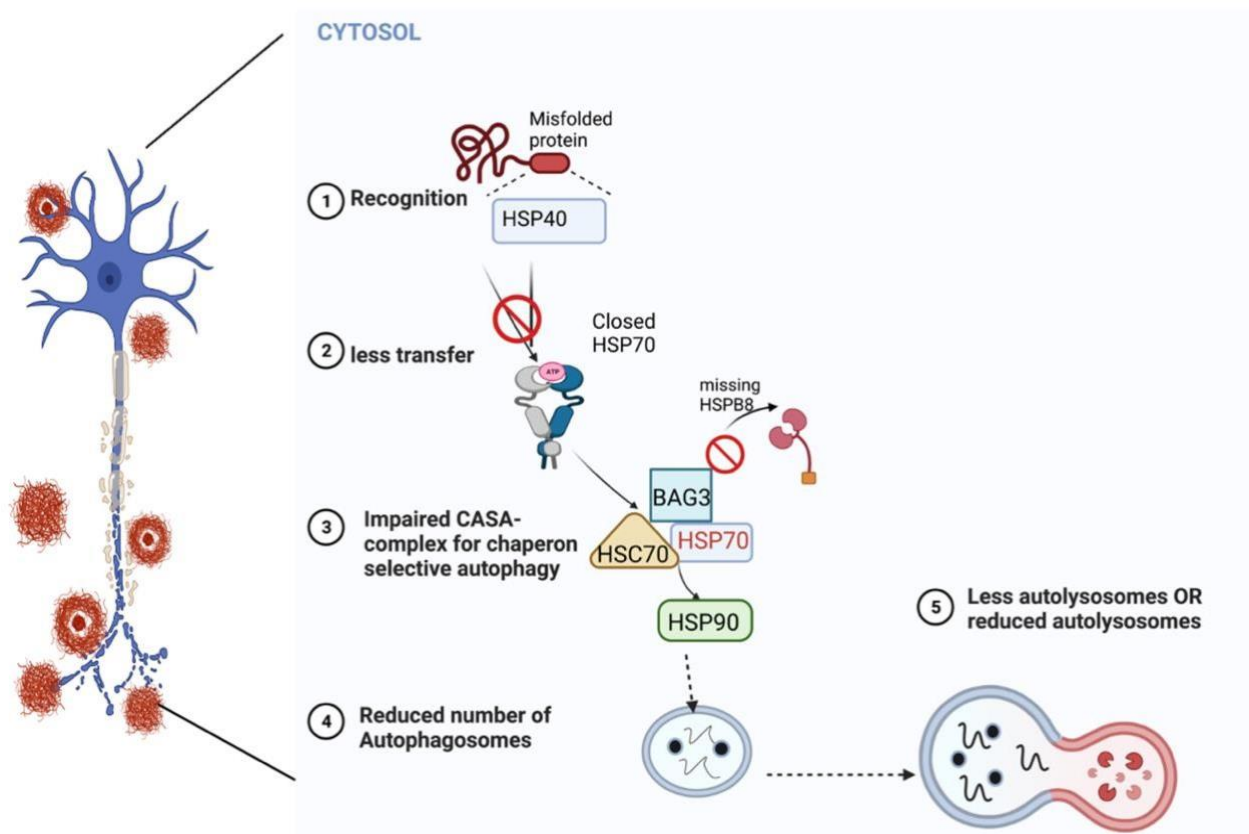
*Figure 5.1:* **Neuropathological features of HSPB8-KO:**

1) Misfolded proteins recognized by HSP40 chaperone 2) In absence of HSPB8, HSP70 protein is not functionally active because of the closed structure (no exchange of ATP), less transfer of non-native proteins to HSP70 3) As HSPB8 is an important regulator of CASA, B8 Knock-out cause impairment in CASA 4) Impaired CASA-complex leads to reduced number of autophagosomes 5) This can cause issue with the downstream processing of autophagosomes fusion with autolysosomes. Figure has been genererated by Biorender.

## 5.3 The crucial role of HSPB8 in the autophagy-lysosome pathway

The autophagy-lysosome pathway is a crucial mechanism for clearing misfolded proteins and damaged organelles from cells. The fusion step between autophagosomes and lysosomes is a critical step in this pathway, and studies suggest that HSPB8 is required for this process (Crippa et al., 2010; XC Li et al., 2017; Rusmini et al., 2017). Crippa et al. (2010) found that HSPB8 activates the autophagy-lysosome pathway resulting in clearance of the mutant G93A-SOD1. The study also suggests that suppression of HSPB8 impairs the fusion of autophagosomes and lysosomes. Similarly, XC Li et al. (2017) also found that HSPB8 is essential for the fusion of autophagosomes and lysosomes.

Another study by P Rusmini et al. (2017) indicates that elevated levels of HSPB8 help to correct a deficient autophagic flux and ensure that misfolded proteins are effectively directed to autophagy for clearance. This finding is particularly important since misfolded proteins are often implicated in several neurodegenerative diseases, and autophagy is a critical mechanism for maintaining the health of neurons.

In order to investigate the impact of HSPB8 knock-out on the autophagy-lysosome pathway, we utilized the Tandem Sensor RFP-GFP-LC3B, which enables live-cell imaging of autophagosomes and autolysosomes. Our results revealed a significant reduction in the number of autophagosomes and autolysosomes in HSPB8 KO neurons compared to WT neurons (Figure 4.13 D). This finding provides compelling evidence supporting the crucial role of HSPB8 in facilitating proper functioning of the autophagy-lysosome pathway.

Expanding on this, we delved deeper into the lysosomes of these neurons by quantifying their number and area using LAMP2 immunofluorescence staining, independent of the tandem sensor. Our analysis demonstrated a noteworthy decrease in both the number and area of lysosomes in HSPB8 KO neurons as compared to wild-type neurons (Fig. 4.14 B). However, no significant differences were observed in the size of the lysosomes between the two groups (Fig. 4.14 C). These findings contribute significantly to our understanding of HSPB8's involvement in lysosomal function, underscoring that its absence leads to a reduction in the number of autophagosomes and autolysosomes. Moreover, the diminished number and area of lysosomes further highlight the

importance of HSPB8 in maintaining lysosomal homeostasis.

The above discussed process, known as CASA, plays a crucial role in maintaining cellular homeostasis by facilitating the clearance of misfolded and ubiquitinated proteins via the autophagy pathway. The key molecule involved in this process is SQSTM1/p62, which acts as an autophagy adapter and binds to both ubiquitinated substrates and autophagosomal marker protein LC3. This interaction between SQSTM1/p62 and its substrates with selectivity is crucial for the specific targeting of misfolded proteins for degradation via autophagy (Gamerdinger et al., 2011; Crippa et al., 2010a; Gamerdinger et al., 2011). The formation of the CASA complex, which includes HSPB8, BAG3, HSP70, and STUB1, allows for the ubiquitination of misfolded substrates by STUB1, which are then recognized by SQSTM1/p62 and incorporated into the autophagy pathway. P62 is considered a multifunctional molecule that plays a critical role in protoestasis and facilitates communication between cellular clearance pathways and cytoprotective pathways during oxidative stress (Crippa et al., 2010a; Rusmini et al., 2017).

In our investigation of the involvement of p62 in the disassembly of stress granules and its role downstream of the CASA complex, we made significant observations. Specifically, we found that HSPB8 KO neurons exhibited notably lower levels of p62 under basal conditions, and even up to 8 hours after recovery from treatment, the levels remained significantly decreased (Figure 4.15B). Our findings provide evidence that lower levels of p62 serve as an indicator of impairment within the CASA complex. This impairment can disrupt the downstream targeting or recruiting of p62 to misfolded proteins, resulting in hindered clearance of these proteins through the autophagy pathway. The proper functioning of p62 is crucial for maintaining cellular homeostasis and ensuring the efficient removal of misfolded proteins. The observed decrease in p62 levels highlights the critical role it plays in coordinating the clearance of misfolded proteins and emphasizes its significance in maintaining cellular health.

The results of this study indicate that the absence of HSPB8 due to knockout leads to decreased levels of p62, on one hand implying a potential deficiency in proper protein ubiquitination in knockout conditions. Consequently, this disruption in protein ubiquitination adversely affects cellular aggregate clearance (CASA), resulting in reduced p62 levels. On the other hand, it also hampers the normal formation of autophagosomes and autolysosome (Figure 4.15B), thereby impairing the

biogenesis of these crucial cellular components. These findings collectively underscore the critical role of p62 in facilitating the clearance of misfolded proteins and emphasize its significance in maintaining proper cellular function. The dysregulation observed in HSPB8 KO neurons highlights the disruption of protein homeostasis and the impaired functionality of the autophagy pathway.

The role of p62 in selective autophagy is well established, and it serves as a critical component for the assembly of protein aggregates and functions as an autophagy receptor. The formation of cytoplasmic inclusion bodies known as p62 bodies, containing polyubiquitin chains, is facilitated by p62 (Stolz A et al., 2014; Bjørkøy G et al., 2015). The presence of K63 polyubiquitin chains in p62 bodies suggests that these chains play a role in aggrephagy, while K48-ubiquitinated proteins undergo proteasomal degradation (Zaffagnini G et al., 2016; Sun D et al., 2018).

In our study, we investigated the levels of K63 and K48 polyubiquitination in spinal motor neurons of both wild-type and HSPB8-knockout conditions. Interestingly, we did not observe a quantifiable band for K63 polyubiquitination in wild-type neurons, while a band was detected in the knockout neurons (refer to Figure 4.16 A for detailed data). These findings suggest that the role of K63 polyubiquitination in the process of aggrephagy, particularly in our experimental system, remains unclear due to the lack of K63 polyubiquitination expression in wild-type neurons. It is important to note that these results may be influenced by technical factors such as the antibody used or the possibility of an alternative polyubiquitination pathway in wild-type neurons. Further investigations are required to elucidate the involvement of K63 polyubiquitination in aggrephagy and to explore other potential mechanisms underlying protein degradation in wild-type neurons and HSPB8 KO neurons.

The levels of K48 polyubiquitination in both wild-type and knockout neurons to assess the efficiency of protein degradation. Surprisingly, we did not observe any significant differences between the two groups (refer to Figure 4.16 B, C). K48 polyubiquitination is considered a classical marker of protein degradation. The absence of significant changes in K48 polyubiquitination levels observed in HSPB8 knockout neurons aligns with the findings of decreased p62 levels. These results collectively strengthen the evidence that polyubiquitination is impaired in the absence of HSPB8, indicating a disruption in protein degradation mechanisms in HSPB8 knockout conditions. This suggests that HSPB8 plays a crucial role in maintaining the proper functioning of polyubiquitination

processes and underscores its importance in protein homeostasis and cellular clearance pathways.

## 5.4 Role of HSPB8 to FUS Aggregation beyond Stress Granules and Mislocalization

Multiple studies have provided substantial evidence linking the expression pattern and level of the HSPB8 chaperone to the clearance of aggregated proteins associated with ALS. These studies, including works by Anagnostou et al. (2010), Crippa et al. (2010a, 2010b, 2016), and Cristofani et al. (2017), consistently support the association between HSPB8 and the removal of ALS-associated protein aggregates. First, we investigated the relation between HSPB8 and FUS. We decided to analyze the expression levels of FUS in the WT and KO neurons, there is no significant difference in FUS protein expression between WT and HSPB8 KO motor neurons, indicating that HSPB8 does not affect FUS protein expression itself (Fig. 4.6 A). Interestingly, when investigating HSPB8 KO neurons, the levels of FUS aggregates were found to be higher in KO motor neurons, indicating that HSPB8 plays a role in the clearance of aggregated FUS proteins (Fig. 4.6 C and D). We next investigated whether HSPB8 expression is thus affected in case of FUS-ALS mutations. However, the expression of HSPB8 was not homogenous when FUS-ALS cell line-derived neurons were investigated (Fig. 4.6 C). Because of the mentioned problems with unspecific binding of all HSPB8 antibodies in IFF stainings, we were unfortunately unable to look at HSPB8 expression within distinct cellular compartments in FUS-ALS neurons.

To overcome this shortcoming we speculated that HSPB8 might affect other key factors of FUS pathogenesis, including FUS nuclear-cytoplasmic distribution and SG dynamics. The present investigation thus aimed to explore the properties of stress granules and their association with FUS-mislocalization under stress conditions, since prior research has demonstrated FUS' colocalization with SGs and its role in SG dynamics (Gal et al., 2011; Marrone et al., 2018; Szewczyk et al., 2023). The results showed no FUS-mislocalization into SG granules in HSPB8(KO), suggesting the involvement of other factors in the formation of FUS aggregates in ALS pathology. This observation may be attributed to the EGFP-tagged FUS protein used in previous studies, as EGFP-FUS was found to colocalize with SGs. Additionally, unpublished data from Marcel Naumann and the Hermann laboratory showed no FUS mislocalization to the cytoplasm or stress granule targeting in mutated non-tagged induced pluripotent stem cell (iPSC)-derived motor neurons from control subjects under oxidative stress conditions. These findings further support the hypothesis that FUS localization to SGs

is influenced by the abundance of FUS in the cytoplasm. The inconsistent reports on the incorporation of wild-type FUS into SGs under stress conditions, with some researchers reporting such incorporation under oxidative or heat stress (Andersson et al., 2008; Marrone et al., 2018), could also be explained by this hypothesis.

These findings are important as they provide insight into the role of HSPB8 in ALS-pathogenesis and the formation of FUS aggregates. The results suggest that HSPB8 may play a role in the clearance of FUS aggregates, but not in the regulation of FUS protein expression and proper nucleus-cytoplasmic shuttling.

# 6  CONCLUSION

In conclusion, this thesis has provided valuable insights into the role of chaperone-assisted selective autophagy in stress granule disassembly and the overall proteostasis network. The study demonstrated that CASA, mediated by the CASA complex consisting of HSPB8-BAG3-HSP70-CHIP, plays a critical role in the clearance of SGs and prevents their persistence. The absence of HSPB8 and BAG3 resulted in the prolonged disintegration of SGs, emphasizing their importance in the efficient removal of misfolded cargo. Furthermore, the study highlighted the collaborative functioning of different chaperone systems within the proteostasis network. Molecular chaperones such as HSP70 and HSP40, along with co-chaperones like HSC70, HSP90, and CHIP, play vital roles in protein quality control, folding, and degradation. The dysregulation observed in chaperone components within HSPB8 knockout neurons strongly indicates impaired mechanisms for maintaining cellular proteostasis. This deficiency in proteostasis maintenance renders cells vulnerable to additional insults, thereby resulting in detrimental effects (look Figure 6.1). Moreover, the findings revealed the dynamic nature of chaperone expression levels under different conditions. HSP70 exhibited a significant reduction in the absence of HSPB8, resulting in prolonged SG disintegration. HSC70 showed significant upregulation, potentially playing a distinct role in cellular response and compensatory mechanisms. Additionally, HSP40 exhibited dynamic expression patterns, with potential involvement in misfolded protein handling and cellular processes independent of SG formation. Furthermore, the study emphasized the interplay between chaperone systems, as proteins that cannot be folded or cleared by HSP70 are transferred to the ATP-dependent HSP90 chaperone system. The dysregulation of the HSP70 chaperone system in the absence of HSPB8 led to the upregulation of HSP90, suggesting its compensatory role in protein folding and quality control. However, the downstream processing of proteins may be affected due to the absence of HSPB8, emphasizing its crucial role in protein homeostasis. The results showed that in the absence of HSPB8, both the proteasomal (BAG1) and autophagy (BAG3) pathways were remarkably upregulated compared to the wild type. Overall, this thesis provides insights into the intricate mechanisms of chaperone-assisted selective autophagy, the coordination of chaperone systems in protein quality control, and the importance of maintaining proteostasis for cellular function.

The thesis explores the disassembly of stress granules and focuses on the role of heat shock proteins, particularly HSPB8, in regulating SG dynamics. Our investigation aimed to understand the impact of HSPB8 knockout on SG regulation and its implications for cellular response to stress. Interestingly, we found that the absence of HSPB8 did not completely abolish SG formation, but prolonged it. Furthermore, HSPB8 knockout did significantly affect SG disassembly. Thus prolonged assembly and disassembly time led to to prolonged SG persistence and an extended recovery period after stress exposure. This impaired SG dynamics was associated with increased vulnerability to stress and resulted in lower cell survival rates, indicating the critical role of HSPB8 in cellular stress response. These findings shed light on the complex and intricate regulation of SGs, demonstrating the involvement of multiple chaperones and highlighting the significance of HSPB8 in the process of selective autophagy. The impairment in the CASA complex, of which HSPB8 is a key component, suggests that HSPB8 plays a crucial role in coordinating the timely disassembly of SGs.

The present study also shed light on that this impairment hinders the targeting and recruitment of p62 to misfolded proteins, leading to compromised clearance through the autophagy pathway. The proper functioning of p62 is crucial for maintaining cellular homeostasis and efficient removal of misfolded proteins. The decrease in p62 levels emphasizes its critical role in coordinating protein clearance and underscores its significance in preserving cellular health. Moreover, autophagy-lysosome pathway is a critical mechanism for maintaining the health of neurons, and the fusion step between autophagosomes and lysosomes is essential for this process. HSPB8 is necessary for the proper functioning of this pathway as it is required for the fusion of autophagosomes and lysosomes. The absence of HSPB8 leads to a decrease in the number and area of lysosomes. This investigation adds to the body of knowledge surrounding lysosomal function and its relationship with HSPB8. The diminished number of autophagosomes and autolysosomes downstream of p62 further highlights the extensive impact of HSPB8 deficiency on the autophagy pathway. The dysregulation observed in HSPB8 knockout neurons reveals disruption in protein homeostasis and impaired autophagy functionality (Figure 6.1).

Additionally, the levels of K48 polyubiquitination, a classical marker of protein degradation, did not show significant differences between wild-type and knockout neurons. This aligns with the findings of decreased p62 levels and strengthens the evidence of impaired polyubiquitination in the absence of HSPB8.

Interestingly, the present study contributes to the growing body of knowledge surrounding the role of HSPB8 in the pathogenesis of ALS. The findings suggest that HSPB8 may be involved in the clearance of FUS aggregates (Figure 6.1), but not in the regulation of FUS protein expression. The study also highlights the potential involvement of other factors in the formation of FUS aggregates in ALS pathology, beyond SG formation and FUS-mislocalization. The results provide valuable insight into the mechanisms underlying the development of ALS and may inform future research aimed at developing treatments for this devastating disease.

In conclusion, my thesis presents novel insights into regulatory mechanism of HSPB8 in human motor neurons, culminating in a series of dysregulatory events impacting CASA and various components critical for maintaining the integrity of protein degradation systems, including the autophagy-lysosomal pathway. This perturbation ultimately results in the inability topolyubiquitinate proteins, leading to the aggregation of misfolded proteins and, ultimately, a reduction in cellular viability. These findings hold great importance for the field of neurodegenerativedisease treatment, as they provide valuable insights into the molecular mechanisms underlying autophagy. By elucidating the intricate interplay between HSPB8 and the autophagy-lysosomal pathway, our research expands our knowledge of the molecular basis of autophagy and its implications in neurodegeneration. This knowledge opens new avenues for future investigations aimed at identifying potential targets for therapeutic intervention.
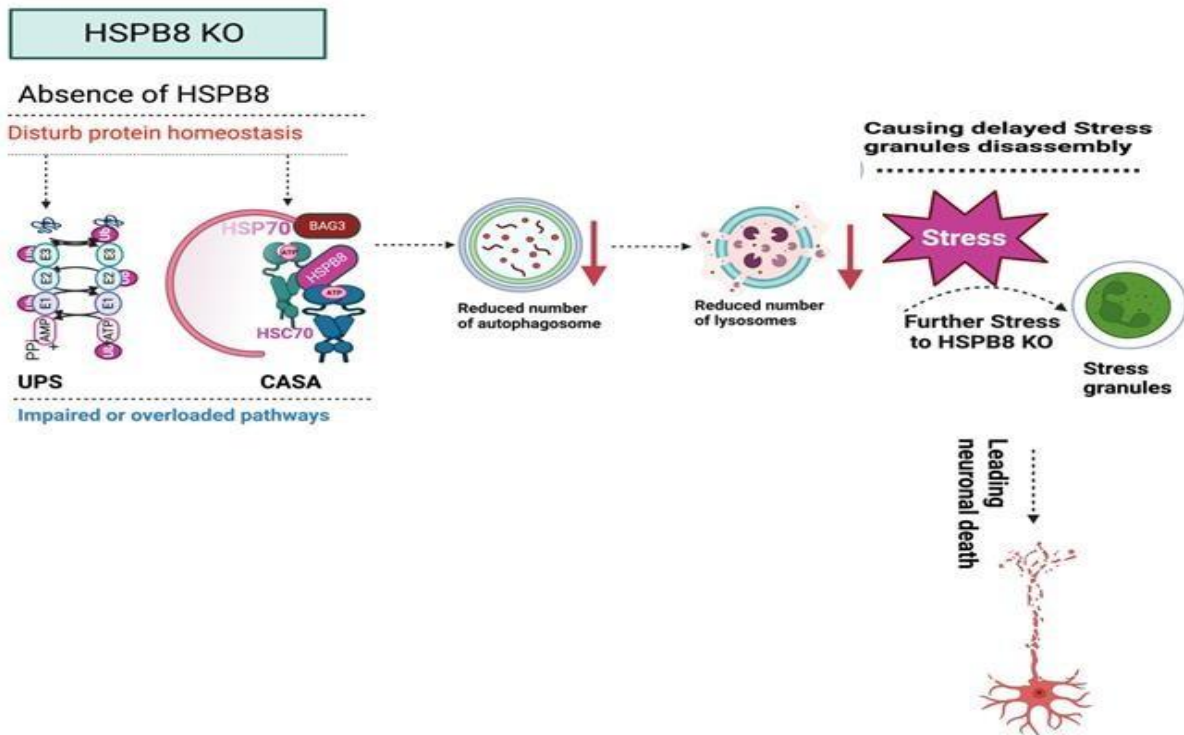
*Figure 6.1:* **Cycle showing misregulation caused by HSPB8-KO:**

Absence of HSPB8 leads distruption of protein homeostasis pathway either UPS and CASA pathways are impaired or they are overloaded. Following these pathways impairement cause the autophagosomes reduction. Reduction in autophagosomes leads to autolysosomes decreased. Additionally, any stress can delay the SGs dissolution causing further harm and neurons survival becomes more vulnerable. Figure has been genererated by Biorender.

# 7  LIMITATIONS

Several limitations are associated with this thesis. Firstly, a limitation arises from the non-specific binding issue observed with all HSPB8 antibodies used in immunofluorescence stainings. This limitation hindered our ability to accurately assess the expression of HSPB8 within specific cellular compartments in all investigated cells, and especially in the FUS-ALS neurons. This also disabled us from investigating the potential recruitment of HSPB8 into stress granules specifically in the case of FUS-ALS mutations. Lastly, the Western blot analysis conducted on multiple FUS-ALS derived-neurons revealed high variability in the expression of HSPB8, even in wild-type samples. Whether this is due to low expression per se and fluctuations around the detection level, or whether it means that HSPB8 expression is very sensitive and already varies due to small experimental variations remains elusive.

Another limitation of this study pertains to the kinetics of stress granule disassembly. An argument can be made that the observed overshooting of SG disassembly in knockout neurons, compared to wild-type neurons, after a 2-hour and 4-hour recovery from stress may be attributed to an assembly problem. This limitation arises from the absence of investigation into different time points of SG assembly, such as 30 minutes or 40 minutes of arsenite treatment. It is important to acknowledge the influence of heat stress and the significance of heat shock proteins in regulating cellular responses to heat. However, due to various constraints related to our technical and experimental setups, we were unable to fully explore this aspect. Furthermore, our experiments using HSPB8 antibodies were hindered by technical errors. These limitations restricted our ability to investigate the role of chaperones and stress granules under heat stress conditions as comprehensively as desired. Another limitation revolves around the exploration of polyubiquitination. Specifically, we encountered a challenge related to the expression of K63 antibody in wild-type neurons, which resulted in a lack of sufficient data to comprehensively elucidate the role of polyubiquitination in this specific cell line. As a result, our ability to investigate and provide detailed insights into the involvement of polyubiquitination in the context of our study was constrained.

## 8   OUTLOOK

The present study contributes to the growing understanding of the role of HSPB8 and the specific molecular mechanisms underlying the impairment of CASA and the autophagy-lysosomal pathway in the absence of HSPB8. A subsequent study that blocks autophagosomes or autolysosomes could provide answers regarding autophagy clearance in KO and proteostatic capacity. Understanding the precise interactions and signalling pathways involved will provide valuable insights into potential therapeutic targets for neurodegenerative diseases. Additionally, exploring the potential role of other heat shock proteins and chaperones in SG regulation and autophagy could shed light on the complex network of protein quality control mechanisms. Investigating the interplay between HSPB8 and other key players in the selective autophagy process may uncover new avenues for therapeutic interventions. In terms of therapeutic applications, future studies could explore strategies to enhance or restore the function of the CASA complex and the autophagy-lysosomal pathway. This could involve developing small molecules or gene therapies that modulate the expression or activity of key components involved in these processes.

The thesis highlights the need for further studies to investigate the potential cross-talk between the autophagy-lysosomal pathway and other cellular clearance pathways, such as the proteasome system. It would be of scientific interest to comprehensively elucidate the precise relationship with ubiquitination. The exploration of HSP70 or BAG3 antagonists presents an intriguing avenue for investigating the potential complete cessation of stress granule disassembly and its subsequent impact on cellular viability. Conducting Fluorescence Recovery After Photobleaching (FRAP) experiments would be of scientific interest to assess the liquid-like characteristics of HSPB8 knockout SGs. These all could provide a more comprehensive understanding of protein homeostasis and its dysregulation in neurodegenerative diseases.

Additionally, studying the relationship between HSPB8 and the clearance of FUS aggregates in ALS pathology holds promise for future investigations. Further exploring the involvement of HSPB8 in the regulation of FUS protein aggregation and mislocalization will contribute to our understanding of the molecular basis of ALS. Investigating the potential role of other factors in FUS aggregation and elucidating the complex interactions between SG formation, autophagy dysfunction, and

neurodegeneration will be crucial for developing targeted interventions for ALS and related disorders. Investigating small molecule modulators or gene therapies that can restore or enhance the functionality of HSPB8 and other chaperones may offer potential avenues for the treatment of neurodegenerative diseases.

In conclusion, this thesis has provided valuable insights into the intricate mechanisms underlying chaperone-assisted selective autophagy and its role in maintaining proteostasis. By investigating the impact of HSPB8 deficiency on SG disassembly, autophagy-lysosome pathway, protein ubiquitination, and its potential involvement in ALS pathology, this research expands our understanding of the molecular basis of autophagy and its implications in neurodegeneration. These findings pave the way for future investigations aiming to identify therapeutic targets and develop interventions for the treatment of neurodegenerative diseases characterized by proteostasis dysregulation.

# 9  REFERENCES

Al-Tahan, S., Weiss, L., Yu, H., Tang, S., Saporta, M., Vihola, A., Mozaffar, T., Udd, B., & Kimonis, V. (2019). New family with HSPB8-associated autosomal dominant rimmed vacuolar myopathy. *Neurology: Genetics*, *5*(4). https://doi.org/10.1212/NXG.0000000000000349

Anagnostou, G., Akbar, M. T., Paul, P., Angelinetta, C., Steiner, T. J., & de Belleroche, J. (2010). Vesicle associated membrane protein B (VAPB) is decreased in ALS spinal cord. *Neurobiology of Aging*, *31*(6), 969–985. https://doi.org/10.1016/j.neurobiolaging.2008.07.005

Anderson, P., & Kedersha, N. (2006). RNA granules. In *Journal of Cell Biology* (Vol. 172, Issue 6, pp. 803–808). https://doi.org/10.1083/jcb.200512082

Anderson, P., & Kedersha, N. (2009). RNA granules: Post-transcriptional and epigenetic modulators of gene expression. In *Nature Reviews Molecular Cell Biology* (Vol. 10, Issue 6, pp. 430–436). https://doi.org/10.1038/nrm2694

Aquilina, J. A., Shrestha, S., Morris, A. M., & Ecroyd, H. (2013). Structural and functional aspects of hetero-oligomers formed by the small heat shock proteins αB-crystallin and HSP27. *Journal of Biological Chemistry*, *288*(19), 13602–13609. https://doi.org/10.1074/jbc.M112.443812

Arimoto, K., Fukuda, H., Imajoh-Ohmi, S., Saito, H., & Takekawa, M. (2008). Formation of stress granules inhibits apoptosis by suppressing stress-responsive MAPK pathways. *Nature Cell Biology*, *10*(11), 1324–1332. https://doi.org/10.1038/ncb1791

Arndt, V., Dick, N., Tawo, R., Dreiseidler, M., Wenzel, D., Hesse, M., Fürst, D. O., Saftig, P., Saint, R., Fleischmann, B. K., Hoch, M., & Höhfeld, J. (2010). Chaperone-Assisted Selective Autophagy Is Essential for Muscle Maintenance. *Current Biology*, *20*(2), 143–148. https://doi.org/10.1016/j.cub.2009.11.022

Arias E, Cuervo AM. Chaperone-mediated autophagy in protein quality control. *Curr Opin Cell Biol*. 2011;23(2):184-189. Doi:10.1016/j.ceb.2010.10.009

Arrigo, A. P. (2013). Human small heat shock proteins: Protein interactomes of homo- and hetero-oligomeric complexes: An update. In *FEBS Letters* (Vol. 587, Issue 13, pp. 1959–1969). https://doi.org/10.1016/j.febslet.2013.05.011

Arrigo, A. P. (2017). Mammalian HspB1 (Hsp27) is a molecular sensor linked to the physiology and environment of the cell. In *Cell Stress and Chaperones* (Vol. 22, Issue 4, pp. 517–529). Cell Stress and Chaperones. https://doi.org/10.1007/s12192-017-0765-1

Aulas, A., Fay, M. M., Lyons, S. M., Achorn, C. A., Kedersha, N., Anderson, P., & Ivanov, P. (2017). Stress-specific differences in assembly and composition of stress granules and related foci. *Journal of Cell Science*, *130*(5), 927–937. https://doi.org/10.1242/jcs.199240

Balch WE, Morimoto RI, Dillin A, Kelly JW. Adapting proteostasis for disease intervention. *Science*. 2008;319(5865):916-919. Doi:10.1126/science.1141448

Bagnéris, C., Bateman, O. A., Naylor, C. E., Cronin, N., Boelens, W. C., Keep, N. H., & Slingsby, C. (2009). Crystal Structures of α-Crystallin Domain Dimers of αB-Crystallin and Hsp20. *Journal of Molecular Biology*, *392*(5), 1242–1252. https://doi.org/10.1016/j.jmb.2009.07.069

Bakthisaran, R., Tangirala, R., & Rao, C. M. (2015). Small heat shock proteins: Role in cellular functions and pathology. In *Biochimica et Biophysica Acta — Proteins and Proteomics* (Vol. 1854, Issue 4, pp. 291–319). Elsevier. https://doi.org/10.1016/j.bbapap.2014.12.019

Baldwin, A. J., Lioe, H., Hilton, G. R., Baker, L. A., Rubinstein, J. L., Kay, L. E., & Benesch, J. L. P. (2011). The polydispersity of αb-crystallin is rationalized by an interconverting polyhedral architecture. *Structure*, *19*(12), 1855–1863. https://doi.org/10.1016/j.str.2011.09.015

Bartelt-Kirbach, B., & Golenhofen, N. (2014). Reaction of small heat-shock proteins to different kinds of cellular stress in cultured rat hippocampal neurons. *Cell Stress and Chaperones*, *19*(1), 145–153. https://doi.org/10.1007/s12192-013-0452-9

Bartelt-Kirbach, B., Slowik, A., Beyer, C., & Golenhofen, N. (2017). Upregulation and phosphorylation of HspB1/Hsp25 and HspB5/αB-crystallin after transient middle cerebral artery occlusion in rats. *Cell Stress and Chaperones*, *22*(4), 653–663. https://doi.org/10.1007/s12192-017-0794-9

Basha, E., O'Neill, H., & Vierling, E. (2012). Small heat shock proteins and α-crystallins: Dynamic proteins with flexible functions. In *Trends in Biochemical Sciences* (Vol. 37, Issue 3, pp. 106–117). https://doi.org/10.1016/j.tibs.2011.11.005

Benesch, J. L. P., Aquilina, J. A., Baldwin, A. J., Rekas, A., Stengel, F., Lindner, R. A., Basha, E., Devlin, G. L., Horwitz, J., Vierling, E., Carver, J. A., & Robinson, C. V. (2010). The quaternary organization and dynamics of the molecular chaperone HSP26 are thermally regulated. *Chemistry and Biology*, *17*(9), 1008–1017. https://doi.org/10.1016/j.chembiol.2010.06.016

Benndorf, R., Sun, X., Gilmont, R. R., Biederman, K. J., Molloy, M. P., Goodmurphy, C. W., Cheng, H., Andrews, P. C., & Welsh, M. J. (2001). HSP22, a New Member of the Small Heat Shock Protein Superfamily, Interacts with Mimic of Phosphorylated HSP27 (3DHSP27). *Journal of Biological Chemistry*, *276*(29), 26753–26761. https://doi.org/10.1074/jbc.M103001200

Bennett, E. J., Bence, N. F., Jayakumar, R., & Kopito, R. R. (2005). Global impairment of the ubiquitin-proteasome system by nuclear or cytoplasmic protein aggregates precedes inclusion body formation. *Molecular Cell*, *17*(3), 351–365. https://doi.org/10.1016/j.molcel.2004.12.021

Boros, S., Kamps, B., Wunderink, L., De Bruijn, W., De Jong, W. W., & Boelens, W. C. (2004). Transglutaminase catalyzes differential crosslinking of small heat shock proteins and amyloid-β. *FEBS Letters*, *576*(1–2), 57–62. https://doi.org/10.1016/j.febslet.2004.08.062

Bouhy, D., Juneja, M., Katona, I., Holmgren, A., Asselbergh, B., De Winter, V., Hochepied, T., Goossens, S., Haigh, J. J., Libert, C., Ceuterick-de Groote, C., Irobi, J., Weis, J., & Timmerman, V. (2018). A knock-in/knock-out mouse model of HSPB8-associated distal hereditary motor neuropathy and myopathy reveals toxic gain-of-function of mutant Hspb8. *Acta Neuropathologica*, *135*(1), 131–148. https://doi.org/10.1007/s00401-017-1756-0

Bova, M. P., Mchaourab, H. S., Han, Y., & K-K Fung, B. (2000). *Subunit Exchange of Small Heat Shock Proteins ANALYSIS OF OLIGOMER FORMATION OF A-CRYSTALLIN AND Hsp27 BY FLUORESCENCE RESONANCE ENERGY TRANSFER AND SITE-DIRECTED TRUNCATIONS\**. http://www.jbc.org

Boyer, J. G., Murray, L. M., Scott, K., De Repentigny, Y., Renaud, J. M., & Kothary, R. (2013). Early onset muscle weakness and disruption of muscle proteins in mouse models of spinal muscular atrophy. *Skeletal Muscle*, *3*(1). https://doi.org/10.1186/2044-5040-3-24

Bjørkøy, G., Lamark, T., Brech, A., Outzen, H., Perander, M., Øvervatn, A., Stenmark, H., & Johansen, T. (2005). P62/SQSTM1 forms protein aggregates degraded by autophagy and has a protective effect on huntingtin-induced cell death. *Journal of Cell Biology*, *171*(4), 603–614. https://doi.org/10.1083/jcb.200507002

Brangwynne, C. P., Tompa, P., & Pappu, R. V. (2015). Polymer physics of intracellular phase transitions. *Nature Physics*, *11*(11), 899–904. https://doi.org/10.1038/nphys3532

Bruinsma, I. B., Bruggink, K. A., Kinast, K., Versleijen, A. A. M., Segers-Nolten, I. M. J., Subramaniam, V., Bea Kuiperij, H., Boelens, W., de Waal, R. M. W., & Verbeek, M. M. (2011). Inhibition of α-synuclein aggregation by small heat shock proteins. *Proteins: Structure, Function and Bioinformatics*, *79*(10), 2956–2967. https://doi.org/10.1002/prot.23152

Buchan, J. R., Kolaitis, R. M., Taylor, J. P., & Parker, R. (2013). Xeukaryotic stress granules are cleared by autophagy and Cdc48/VCP function. *Cell*, *153*(7), 1461. https://doi.org/10.1016/j.cell.2013.05.037

Buchan, J. R., & Parker, R. (2009). Eukaryotic Stress Granules: The Ins and Outs of Translation. In *Molecular Cell* (Vol. 36, Issue 6, pp. 932–941). https://doi.org/10.1016/j.molcel.2009.11.020

Bukach, O. V., Glukhova, A. E., Seit-Nebi, A. S., & Gusev, N. B. (2009). Heterooligomeric complexes formed by human small heat shock proteins HspB1 (Hsp27) and HspB6 (Hsp20). *Biochimica et Biophysica Acta — Proteins and Proteomics*, *1794*(3), 486–495. https://doi.org/10.1016/j.bbapap.2008.11.010

Bukach, O. V., Seit-Nebi, A. S., Marston, S. B., & Gusev, N. B. (2004). Some properties of human small heat shock protein Hsp20 (HspB6). *European Journal of Biochemistry*, *271*(2), 291–302. https://doi.org/10.1046/j.1432-1033.2003.03928.x

Carra, S. (2009). The stress-inducible HspB8-Bag3 complex induces the eIF2α kinase pathway: Implications for protein quality control and viral factory degradation? *Autophagy*, *5*(3), 428–429. https://doi.org/10.4161/auto.5.3.7894

Carra, S., Rusmini, P., Crippa, V., Giorgetti, E., Boncoraglio, A., Cristofani, R., Naujock, M., Meister, M., Minoia, M., Kampinga, H. H., & Poletti, A. (2013). Different anti-aggregation and pro-degradative functions of the members of the mammalian sHSP family in neurological disorders. In *Philosophical Transactions of the Royal Society B: Biological Sciences* (Vol. 368, Issue 1617, pp. 1–13). Royal Society of London. https://doi.org/10.1098/rstb.2011.0409

Carra, S., Seguin, S. J., Lambert, H., & Landry, J. (2008). HspB8 chaperone activity toward poly(Q)-containing proteins depends on its association with Bag3, a stimulator of macroautophagy. *Journal of Biological Chemistry*, *283*(3), 1437–1444. https://doi.org/10.1074/jbc.M706304200

Carra, S., Sivilotti, M., Zobel, A. T. C., Lambert, H., & Landry, J. (2005). HspB8, a small heat shock protein mutated in human neuromuscular disorders, has in vivo chaperone activity in cultured cells. *Human Molecular Genetics*, *14*(12), 1659–1669. https://doi.org/10.1093/hmg/ddi174

Carver, J. A., Grosas, A. B., Ecroyd, H., & Quinlan, R. A. (2017). The functional roles of the unstructured N- and C-terminal regions in αB-crystallin and other mammalian small heat-shock proteins. *Cell Stress and Chaperones*, *22*(4), 627–638. https://doi.org/10.1007/s12192-017-0789-6

Chang, Z. (2015). Understanding What Small Heat Shock Proteins Do for Bacterial Cells. https://doi.org/10.1007/978-3-319-16077-1_22

Charpentier, A. H., Bednarek, A. K., Daniel, R. L., Hawkins, K. A., Laflin, K. J., Gaddis, S., Macleod, M. C., & Aldaz, C. M. (n.d.). *Effects of Estrogen on Global Gene Expression: Identification of Novel Targets of Estrogen Action 1.* http://aacrjournals.org/cancerres/article-pdf/60/21/5977/3249884/ch210005977p.pdf

Cherkasov, V., Hofmann, S., Druffel-Augustin, S., Mogk, A., Tyedmers, J., Stoecklin, G., & Bukau, B. (2013). Coordination of translational control and protein homeostasis during severe heat stress. *Current Biology*, *23*(24), 2452–2462. https://doi.org/10.1016/j.cub.2013.09.058

Chernov, K. G., Barbet, A., Hamon, L., Ovchinnikov, L. P., Curmi, P. A., & Pastré, D. (2009). Role of microtubules in stress granule assembly: Microtubule dynamical instability favors the formation of micrometric stress granules in cells. *Journal of Biological Chemistry*, *284*(52), 36569–36580. https://doi.org/10.1074/jbc.M109.042879

Chierichetti, M., Cerretani, M., Ciammaichella, A., Crippa, V., Rusmini, P., Ferrari, V., Tedesco, B., Casarotto, E., Cozzi, M., Mina, F., Pramaggiore, P., Galbiati, M., Piccolella, M., Bresciani, A., Cristofani, R., & Poletti, A. (2022). Identification of HSPB8 modulators counteracting misfolded protein accumulation in neurodegenerative diseases. *Life Sciences*, 121323. https://doi.org/10.1016/j.lfs.2022.121323

Cichanover, A. (2005). Intracellular protein degradation: From a vague idea thru the lysosome and the ubiquitin-proteasome system and onto human diseases and drug targeting. Cell Death and Differentiation, 12(9), 1178–1190. https://doi.org/10.1038/sj.cdd.4401692

Ciechanover, A., & Kwon, Y. T. (2015). Degradation of misfolded proteins in neurodegenerative diseases: therapeutic targets and strategies. In *Experimental and Molecular Medicine* (Vol. 47, Issue 3). Springer Nature. https://doi.org/10.1038/EMM.2014.117

Clouser, A. F., & Klevit, R. E. (2017). pH-dependent structural modulation is conserved in the human small heat shock protein HSBP1. *Cell Stress and Chaperones*, *22*(4), 569–575. https://doi.org/10.1007/s12192-017-0783-z

Cortes, C. J., Ling, S. C., Guo, L. T., Hung, G., Tsunemi, T., Ly, L., Tokunaga, S., Lopez, E., Sopher, B. L., Bennett, C. F., Shelton, G. D., Cleveland, D. W., & La Spada, A. R. (2014). Muscle expression of mutant androgen receptor accounts for systemic and motor neuron disease phenotypes in spinal and bulbar muscular atrophy. *Neuron*, *82*(2), 295–307. https://doi.org/10.1016/j.neuron.2014.03.001

Crippa, V., Carra, S., Rusmini, P., Sau, D., Bolzoni, E., Bendotti, C., De Biasi, S., & Poletti, A. (2010). A role of small heat shock protein B8 (HspB8) in the autophagic removal of misfolded proteins responsible for neurodegenerative diseases. In *Autophagy* (Vol. 6, Issue 7, pp. 958–960). Taylor and Francis Inc. https://doi.org/10.4161/auto.6.7.13042

Crippa, V., Cicardi, M. E., Ramesh, N., Seguin, S. J., Ganassi, M., Bigi, I., Diacci, C., Zelotti, E., Baratashvili, M., Gregory, J. M., Dobson, C. M., Cereda, C., Pandey, U. B., Poletti, A., & Carra, S. (2016). The chaperone HSPB8 reduces the accumulation of truncated TDP-43 species in cells and protects against TDP-43-mediated toxicity. *Human Molecular Genetics*, *25*(18), 3908–3924. https://doi.org/10.1093/hmg/ddw232

Crippa, V., Sau, D., Rusmini, P., Boncoraglio, A., Onesto, E., Bolzoni, E., Galbiati, M., Fontana, E., Marino, M., Carra, S., Bendotti, C., de Biasi, S., & Poletti, A. (2010). The small heat shock protein B8 (HspB8) promotes autophagic removal of misfolded proteins involved in amyotrophic lateral sclerosis (ALS). *Human Molecular Genetics*, *19*(17), 3440–3456. https://doi.org/10.1093/hmg/ddq257

Cristofani, R., Crippa, V., Rusmini, P., Cicardi, M. E., Meroni, M., Licata, N. V., Sala, G., Giorgetti, E., Grunseich, C., Galbiati, M., Piccolella, M., Messi, E., Ferrarese, C., Carra, S., & Poletti, A. (2017). Inhibition of retrograde transport modulates misfolded protein accumulation and clearance in motoneuron diseases. *Autophagy*, *13*(8), 1280–1303. https://doi.org/10.1080/15548627.2017.1308985

Cristofani, R., Crippa, V., Vezzoli, G., Rusmini, P., Galbiati, M., Cicardi, M. E., Meroni, M., Ferrari, V., Tedesco, B., Piccolella, M., Messi, E., Carra, S., & Poletti, A. (n.d.). *The small heat shock protein B8 (HSPB8) efficiently removes aggregating species of dipeptides produced in C9ORF72-related neurodegenerative diseases*. https://doi.org/10.1007/s12192-017-0806-9

Cristofani, R., Piccolella, M., Crippa, V., Tedesco, B., Marelli, M. M., Poletti, A., & Moretti, R. M. (2021). The role of HSPB8, a component of the chaperone-assisted selective autophagy machinery, in cancer. In *Cells* (Vol. 10, Issue 2, pp. 1–23). MDPI. https://doi.org/10.3390/cells10020335

Datskevich, P. N., Mymrikov, E. V., & Gusev, N. B. (2012). Utilization of fluorescent chimeras for investigation of heterooligomeric complexes formed by human small heat shock proteins. *Biochimie*, *94*(8), 1794–1804. https://doi.org/10.1016/j.biochi.2012.04.012

De Jong, W. W., Caspers, G.-J., & Leunissen, J. A. M. (1998). Genealogy of the h-crystallin-small heat-shock protein superfamily. In *International Journal of Biological Macromolecules* (Vol. 22).

Depre, C., Hase, M., Gaussin, V., Zajac, A., Wang, L., Hittinger, L., Ghaleh, B., Yu, X., Kudej, R. K., Wagner, T., Sadoshima, J., & Vatner, S. F. (2002). H11 kinase is a novel mediator of myocardial hypertrophy in vivo. *Circulation Research*, *91*(11), 1007–1014. https://doi.org/10.1161/01.RES.0000044380.54893.4B

Díaz-Villanueva, J. F., Díaz-Molina, R., & García-González, V. (2015). Protein folding and mechanisms of proteostasis. In *International Journal of Molecular Sciences* (Vol. 16, Issue 8, pp. 17193–17230). MDPI AG. https://doi.org/10.3390/ijms160817193

Dobson 1999. (n.d.).

Dormann D, Haass C. TDP-43 and FUS: a nuclear affair. *Trends Neurosci*. 2011 ;34(7) :339-348. Doi : 10.1016/j.tins.2011.05.002

Dormann, D., Madl, T., Valori, C. F., Bentmann, E., Tahirovic, S., Abou-Ajram, C., Kremmer, E., Ansorge, O., MacKenzie, I. R. A., Neumann, M., & Haass, C. (2012). Arginine methylation next to the

PY-NLS modulates Transportin binding and nuclear import of FUS. EMBO Journal, 31(22), 4258–4275. https://doi.org/10.1038/emboj.2012.261

Dormann, D., Rodde, R., Edbauer, D., Bentmann, E., Fischer, I., Hruscha, A., Than, M. E., MacKenzie, I. R. A., Capell, A., Schmid, B., Neumann, M., & Haass, C. (2010). ALS-associated fused in sarcoma (FUS) mutations disrupt transportin-mediated nuclear import. EMBO Journal, 29(16), 2841–2857. https://doi.org/10.1038/emboj.2010.143

Duan, Y., Du, A., Gu, J., Duan, G., Wang, C., Gui, X., Ma, Z., Qian, B., Deng, X., Zhang, K., Sun, L., Tian, K., Zhang, Y., Jiang, H., Liu, C., & Fang, Y. (n.d.). *PARylation regulates stress granule dynamics, phase separation, and neurotoxicity of disease-related RNA-binding proteins.* https://doi.org/10.1038/s41422-019-0141-z

Eaton, P., Fuller, W., & Shattock, M. J. (2002). S-Thiolation of HSP27 regulates its multimericaggregate size independently of phosphorylation. *Journal of Biological Chemistry*, *277*(24), 21189– 21196. https://doi.org/10.1074/jbc.M200591200

Eisinger-Mathason, T. S. K., Andrade, J., Groehler, A. L., Clark, D. E., Muratore-Schroeder, T. L., Pasic, L., Smith, J. A., Shabanowitz, J., Hunt, D. F., Macara, I. G., & Lannigan, D. A. (2008). Codependent functions of RSK2 and the apoptosis-promoting factor TIA-1 in stress granule assembly and cell survival. *Molecular Cell*, *31*(5), 722–736. https://doi.org/10.1016/j.molcel.2008.06.025

Erickson, S. L., & Lykke-Andersen, J. (2011). Cytoplasmic mRNP granules at a glance. In *Journal of Cell Science* (Vol. 124, Issue 3, pp. 293–297). https://doi.org/10.1242/jcs.072140

Fischbeck, K. H. (1997). Kennedy disease. *Journal of Inherited Metabolic Disease*, *20*(2), 152–158. https://doi.org/10.1023/A:1005344403603

Fontaine, J. M., Sun, X., Benndorf, R., & Welsh, M. J. (2005). Interactions of HSP22 (HSPB8) with HSP20, αb-crystallin, and HSPB3. *Biochemical and Biophysical Research Communications*, *337*(3), 1006–1011. https://doi.org/10.1016/j.bbrc.2005.09.148

Franck, E., Madsen, O., Van Rheede, T., Ricard, G., Huynen, M. A., & De Jong, W. W. (2004). Evolutionary diversity of vertebrate small heat shock proteins. *Journal of Molecular Evolution*, *59*(6), 792–805. https://doi.org/10.1007/s00239-004-0013-z

Freilich, R., Betegon, M., Tse, E., Mok, S. A., Julien, O., Agard, D. A., Southworth, D. R., Takeuchi, K., & Gestwicki, J. E. (2018). Competing protein-protein interactions regulate binding of Hsp27 to its client protein tau. *Nature Communications*, *9*(1). https://doi.org/10.1038/s41467-018-07012-4

Fuchs, M., Luthold, C., Guilbert, S. M., Varlet, A. A., Lambert, H., Jetté, A., Elowe, S., Landry, J., & Lavoie, J. N. (2015). A Role for the Chaperone Complex BAG3-HSPB8 in Actin Dynamics, Spindle Orientation and Proper Chromosome Segregation during Mitosis. *PloS Genetics*, *11*(10). https://doi.org/10.1371/journal.pgen.1005582

Fuchs, M., Poirier, D. J., Seguin, S. J., Lambert, H., Carra, S., Charrette, S. J., & Landry, J. (2010). Identification of the key structural motifs involved in HspB8/HspB6-Bag3 interaction. *Biochemical Journal*, *425*(1), 245–255. https://doi.org/10.1042/BJ20090907

Gal, J., Zhang, J., Kwinter, D. M., Zhai, J., Jia, H., Jia, J., & Zhu, H. (2011). Nuclear localization sequence of FUS and induction of stress granules by ALS mutants. Neurobiology of Aging, 32(12), 2323.e27-2323.e40. https://doi.org/10.1016/j.neurobiolaging.2010.06.010

Gamerdinger, M., Kaya, A. M., Wolfrum, U., Clement, A. M., & Behl, C. (2011). BAG3 mediates chaperone-based aggresome-targeting and selective autophagy of misfolded proteins. EMBO Reports, 12(2), 149–156. https://doi.org/10.1038/embor.2010.203

Ganassi, M., Mateju, D., Bigi, I., Mediani, L., Poser, I., Lee, H. O., Seguin, S. J., Morelli, F. F., Vinet, J., Leo, G., Pansarasa, O., Cereda, C., Poletti, A., Alberti, S., & Carra, S. (2016). A Surveillance Function of the HSPB8-BAG3-HSP70 Chaperone Complex Ensures Stress Granule Integrity and Dynamism. Molecular Cell, 63(5), 796–810. https://doi.org/10.1016/j.molcel.2016.07.021

Gamerdinger, M., Kaya, A. M., Wolfrum, U., Clement, A. M., & Behl, C. (2011). BAG3 mediates chaperone-based aggresome-targeting and selective autophagy of misfolded proteins. *EMBO Reports*, *12*(2), 149–156. https://doi.org/10.1038/embor.2010.203

Ghaoui, R., Palmio, J., Brewer, J., Lek, M., Needham, M., Evilä, A., Hackman, P., Jonson, P. H., Penttilä, S., Vihola, A., Huovinen, S., Lindfors, M., Davis, R. L., Waddell, L., Kaur, S., Yiannikas, C., North, K., Clarke, N., Macarthur, D. G., … Udd, B. (2016). Mutations in HSPB8 causing a new phenotype of distal myopathy and motor neuropathy. *Neurology*, *86*(4), 391–398. https://doi.org/10.1212/WNL.0000000000002324

Gilks et al., 2004. (n.d.).

Guilbert, S. M., Lambert, H., Rodrigue, M. A., Fuchs, M., Landry, J., & Lavoie, J. N. (2018). Hspb8 and bag3 cooperate to promote spatial sequestration of ubiquitinated proteins and coordinate the cellular adaptive response to proteasome insufficiency. *FASEB Journal*, *32*(7), 3518–3535. https://doi.org/10.1096/fj.201700558RR

Gomes, E., & Shorter, J. (2019). The molecular language of membraneless organelles. Journal of Biological Chemistry, 294(18), 7115–7127. https://doi.org/10.1074/jbc.TM118.001192

Hartl FU, Hayer-Hartl M. Converging concepts of protein folding in vitro and in vivo. *Nat Struct Mol Biol*. 2009;16(6):574-581. Doi:10.1038/nsmb.1591

Haslbeck, M., Franzmann, T., Weinfurtner, D., & Buchner, J. (2005). Some like it hot: The structure and function of small heat-shock proteins. *Nature Structural and Molecular Biology*, *12*(10), 842–846. https://doi.org/10.1038/nsmb993

Haslbeck, M., & Vierling, E. (2015). A first line of stress defense: Small heat shock proteins and their function in protein homeostasis. *Journal of Molecular Biology*, *427*(7), 1537–1548. https://doi.org/10.1016/j.jmb.2015.02.002

Haslbeck, M., Weinkauf, S., & Buchner, J. (2019). Small heat shock proteins: Simplicity meets complexity. In *Journal of Biological Chemistry* (Vol. 294, Issue 6, pp. 2121–2132). American Society for Biochemistry and Molecular Biology Inc. https://doi.org/10.1074/jbc.REV118.002809

Hayes, D., Napoli, V., Mazurkie, A., Stafford, W. F., & Graceffa, P. (2009). Phosphorylation dependence of Hsp27 multimeric size and molecular chaperone function. *Journal of Biological Chemistry*, *284*(28), 18801–18807. https://doi.org/10.1074/jbc.M109.011353

Heirbaut, M., Lermyte, F., Martin, E. M., Beelen, S., Sobott, F., Strelkov, S. V., & Weeks, S. D. (2017). Specific sequences in the N-terminal domain of human small heat-shock protein HSPB6 dictate preferential hetero-oligomerization with the orthologue HSPB1. *Journal of Biological Chemistry*, *292*(24), 9944–9957. https://doi.org/10.1074/jbc.M116.773515

Hilario, E., Martin, F. J. M., Bertolini, M. C., & Fan, L. (2011). Crystal structures of xanthomonas small heat shock protein provide a structural basis for an active molecular chaperone oligomer. *Journal of Molecular Biology*, *408*(1), 74–86. https://doi.org/10.1016/j.jmb.2011.02.004

Hofmann, S., Cherkasova, V., Bankhead, P., Bukau, B., & Stoecklin, G. (2012). Translation suppression promotes stress granule formation and cell survival in response to cold shock. *Molecular Biology of the Cell*, *23*(19), 3786–3800. https://doi.org/10.1091/mbc.E12-04-0296

Hofmann, S., Kedersha, N., Anderson, P., & Ivanov, P. (2021). Molecular mechanisms of stress granule assembly and disassembly. In *Biochimica et Biophysica Acta — Molecular Cell Research* (Vol. 1868, Issue 1). Elsevier B.V. https://doi.org/10.1016/j.bbamcr.2020.118876

Horwitz, J. (2009). Alpha crystallin: The quest for a homogeneous quaternary structure. In *Experimental Eye Research* (Vol. 88, Issue 2, pp. 190–194). https://doi.org/10.1016/j.exer.2008.07.007

Huang, C., Chen, Y., Dai, H., Zhang, H., Xie, M., Zhang, H., Chen, F., Kang, X., Bai, X., & Chen, Z. (2020). UBAP2L arginine methylation by PRMT1 modulates stress granule assembly. Cell Death and Differentiation, 27(1), 227–241. https://doi.org/10.1038/s41418-019-0350-5

Irobi, J., Dierick, I., Jordanova, A., Claeys, K. G., De Jonghe, P., & Timmerman, V. (2006). Unraveling the genetics of distal hereditary motor neuronopathies. In *NeuroMolecular Medicine* (Vol. 8, Issues 1–2, pp. 131–146). Humana Press Inc. https://doi.org/10.1385/NMM:8:1-2:131

Irobi, J., Holmgren, A., Winter, V. De, Asselbergh, B., Gettemans, J., Adriaensen, D., Groote, C. C. de, Coster, R. Van, Jonghe, P. De, & Timmerman, V. (2012). Mutant HSPB8 causes protein aggregates and a reduced mitochondrial membrane potential in dermal fibroblasts from distal hereditary motor

neuropathy patients. *Neuromuscular Disorders*, *22*(8), 699–711. https://doi.org/10.1016/j.nmd.2012.04.005

Irobi, J., Van Impe, K., Seeman, P., Jordanova, A., Dierick, I., Verpoorten, N., Michalik, A., De Vriendt, E., Jacobs, A., Van Gerwen, V., Vennekens, K., Mazanec, R., Tournev, I., Hilton-Jones, D., Talbot, K., Kremensky, I., Van Den Bosch, L., Robberecht, W., Vandekerckhove, J., … Timmerman, V. (2004). Hot-spot residue in small heat-shock protein 22 causes distal motor neuropathy. *Nature Genetics*, *36*(6), 597–601. https://doi.org/10.1038/ng1328

Ito, H., Kamei, K., Iwamoto, I., Inaguma, Y., Nohara, D., & Kato, K. (2001). Phosphorylation-induced Change of the Oligomerization State of αB-crystallin. *Journal of Biological Chemistry*, *276*(7), 5346–5352. https://doi.org/10.1074/jbc.M009004200

Ito, H., Okamoto, K., Nakayama, H., Isobe, T., & Kato, K. (1997). *Phosphorylation of B-Crystallin in Response to Various Types of Stress\**. http://www.jbc.org

Jain, S., Wheeler, J. R., Walters, R. W., Agrawal, A., Barsic, A., & Parker, R. (2016). ATPase-Modulated Stress Granules Contain a Diverse Proteome and Substructure. Cell, 164(3), 487–498. https://doi.org/10.1016/j.cell.2015.12.038

Jaya, N., Garcia, V., & Vierling, E. (n.d.). *Substrate binding site flexibility of the small heat shock protein molecular chaperones*. www.pnas.org/cgi/content/full/

Jehle, S., Vollmar, B. S., Bardiaux, B., Dove, K. K., Rajagopal, P., Gonen, T., Oschkinat, H., & Klevit, R. E. (n.d.). *N-terminal domain of αB-crystallin provides a conformational switch for multimerization and structural heterogeneity*. https://doi.org/10.1073/pnas.1014656108/-/DCSupplemental

Johnston, J. A., Illing, M. E., & Kopito, R. R. (2002). Cytoplasmic dynein/dynactin mediates the assembly of aggresomes. *Cell Motility and the Cytoskeleton*, *53*(1), 26–38. https://doi.org/10.1002/cm.10057

Kampinga, H. H., Hageman, J., Vos, M. J., Kubota, H., Tanguay, R. M., Bruford, E. A., Cheetham, M. E., Chen, B., & Hightower, L. E. (2009). Guidelines for the nomenclature of the human heat shock proteins. In *Cell Stress and Chaperones* (Vol. 14, Issue 1, pp. 105–111). https://doi.org/10.1007/s12192-008-0068-7

Kappé, G., Franck, E., Verschuure, P., Boelens, W. C., Leunissen, J. A. M., & De Jong, W. W. (2003). The human genome encodes 10-crystallin-related small heat shock proteins: HspB1-10. In *Cell Stress & Chaperones* (Vol. 8, Issue 1). Cell Stress Society International. www.gene.ucl.ac.uk/nomenclature

Kasakov, A. S., Bukach, O. V., Seit-Nebi, A. S., Marston, S. B., & Gusev, N. B. (2007). Effect of mutations in the β5-β7 loop on the structure and properties of human small heat shock protein HSP22 (HspB8, H11). *FEBS Journal*, *274*(21), 5628–5642. https://doi.org/10.1111/j.1742-4658.2007.06086.x

Kazakov, A. S., Markov, D. I., Gusev, N. B., & Levitsky, D. I. (2009). Thermally induced structural changes of intrinsically disordered small heat shock protein Hsp22. *Biophysical Chemistry*, *145*(2–3), 79–85. https://doi.org/10.1016/j.bpc.2009.09.003

Kedersha, N., Chen, S., Gilks, N., Li, W., Miller, I. J., Stahl, J., & Anderson, P. (2002). Evidence That Ternary Complex (eIF2-GTP-tRNA I Met )-Deficient Preinitiation Complexes Are Core Constituents of Mammalian Stress Granules. *Molecular Biology of the Cell*, *13*, 195–210. https://doi.org/10.1091/mbc.01

Kedersha, N., Ivanov, P., & Anderson, P. (2013). Stress granules and cell signaling: More than just a passing phase? In *Trends in Biochemical Sciences* (Vol. 38, Issue 10, pp. 494–506). https://doi.org/10.1016/j.tibs.2013.07.004

Kedersha, N. L., Gupta, M., Li, W., Miller, I., & Anderson, P. (1999). RNA-binding Proteins TIA-1 and TIAR Link the Phosphorylation of eIF-2 to the Assembly of Mammalian Stress Granules. In *The Journal of Cell Biology* (Vol. 147, Issue 7). http://www.jcb.org

Kettern N, Dreiseidler M, Tawo R, Höhfeld J. Chaperone-assisted degradation: multiple paths to destruction. *Biol Chem*. 2010;391(5):481-489. Doi:10.1515/BC.2010.058

Kim et al., 1998. (n.d.).

Kim YE, Hipp MS, Bracher A, Hayer-Hartl M, Hartl FU. Molecular chaperone functions in protein folding and proteostasis. *Annu Rev Biochem*. 2013;82:323-355. Doi:10.1146/annurev-biochem-060208-092442

Kim, M. V., Kasakov, A. S., Seit-Nebi, A. S., Marston, S. B., & Gusev, N. B. (2006). Structure and properties of K141E mutant of small heat shock protein HSP22 (HspB8, H11) that is expressed in human neuromuscular disorders. *Archives of Biochemistry and Biophysics*, *454*(1), 32–41. https://doi.org/10.1016/j.abb.2006.07.014

Kim, M. V., Seit-Nebi, A. S., Marston, S. B., & Gusev, N. B. (2004). Some properties of human small heat shock protein Hsp22 (H11 or HspB8). *Biochemical and Biophysical Research Communications*, *315*(4), 796–801. https://doi.org/10.1016/j.bbrc.2004.01.130

Kirbach, B. B., & Golenhofen, N. (2011). Differential expression and induction of small heat shock proteins in rat brain and cultured hippocampal neurons. *Journal of Neuroscience Research*, *89*(2), 162–175. https://doi.org/10.1002/jnr.22536

Komatsu M, Waguri S, Chiba T, et al. Loss of autophagy in the central nervous system causes neurodegeneration in mice. *Nature*. 2006;441(7095):880-884. Doi:10.1038/nature04723

Kon M, Cuervo AM. Chaperone-mediated autophagy in health and disease. *FEBS Lett*. 2010;584(7):1399-1404. Doi:10.1016/j.febslet.2009.12.025

Kulig, M., & Ecroyd, H. (2012). The small heat-shock protein αB-crystallin uses different mechanisms of chaperone action to prevent the amorphous versus fibrillar aggregation of α-lactalbumin. *Biochemical Journal*, *448*(3), 343–352. https://doi.org/10.1042/BJ20121187

Kumar CHOWDARY, T., Raman, B., Ramakrishna, T., & Mohan RAO, C. (2004). Mammalian Hsp22 is a heat-inducible small heat-shock protein with chaperone-like activity. In *Biochem. J* (Vol. 381). http://portlandpress.com/biochemj/article-pdf/381/2/379/714282/bj3810379.pdf

Kwok, A. S., Phadwal, K., Turner, B. J., Oliver, P. L., Raw, A., Simon, A. K., Talbot, K., & Agashe, V. R. (2011). HspB8 mutation causing hereditary distal motor neuropathy impairs lysosomal delivery of autophagosomes. *Journal of Neurochemistry*, *119*(6), 1155–1161. https://doi.org/10.1111/j.1471-4159.2011.07521.x

Laganowsky, A., Benesch, J. L. P., Landau, M., Ding, L., Sawaya, M. R., Cascio, D., Huang, Q., Robinson, C. V., Horwitz, J., & Eisenberg, D. (2010). Crystal structures of truncated 121 lpha and alphaB crystallins reveal structural mechanisms of polydispersity important for eye lens function. *Protein Science : A Publication of the Protein Society*, *19*(5), 1031–1043. https://doi.org/10.1002/pro.380

Lambert, H., Charrette, S. J., Bernier, A. F., Guimond, A., & Landry, J. (1999). *HSP27 Multimerization Mediated by Phosphorylation-sensitive Intermolecular Interactions at the Amino Terminus*. http://www.jbc.org

Lavut, A., & Raveh, D. (2012). Sequestration of highly expressed mrnas in cytoplasmic granules, p-bodies, and stress granules enhances cell viability. *PloS Genetics*, *8*(2). https://doi.org/10.1371/journal.pgen.1002527

Lee, G. J., & Vierling, E. (2000). *A Small Heat Shock Protein Cooperates with Heat Shock Protein 70 Systems to Reactivate a Heat-Denatured Protein 1*. https://academic.oup.com/plphys/article/122/1/189/6091920

Lelj-Garolla, B., & Mauk, A. G. (2006). Self-association and chaperone activity of Hsp27 are thermally activated. *Journal of Biological Chemistry*, *281*(12), 8169–8174. https://doi.org/10.1074/jbc.M512553200

Leroux, M. R., Melki, R., Gordon, B., Rard Batelier, G., Peter, E., & Candido, M. (1997). *Structure-Function Studies on Small Heat Shock Protein Oligomeric Assembly and Interaction with Unfolded Polypeptides*. http://www.jbc.org

LETTERS TO NATURE. (1991).

Leung, A. K. L., Todorova, T., Ando, Y., & Chang, P. (2012). Poly(ADP-ribose) regulates post-transcriptional gene regulation in the cytoplasm. RNA Biology, 9(5), 542–548. https://doi.org/10.4161/rna.19899

Leung, A. K. L., Vyas, S., Rood, J. E., Bhutkar, A., Sharp, P. A., & Chang, P. (2011). Poly(ADP-Ribose) Regulates Stress Responses and MicroRNA Activity in the Cytoplasm. Molecular Cell, 42(4), 489–499. https://doi.org/10.1016/j.molcel.2011.04.015

Li, X. C., Hu, Q. K., Chen, L., Liu, S. Y., Su, S., Tao, H., Zhang, L. N., Sun, T., & He, L. J. (2017). HSPB8 promotes the fusion of autophagosome and lysosome during autophagy in diabetic neurons. International Journal of Medical Sciences, 14(13), 1335–1341. https://doi.org/10.7150/ijms.20653

Liu-Yesucevitz, L., Bilgutay, A., Zhang, Y. J., Vanderwyde, T., Citro, A., Mehta, T., Zaarur, N., McKee, A., Bowser, R., Sherman, M., Petrucelli, L., & Wolozin, B. (2010). Tar DNA binding protein-43 (TDP-43) associates with stress granules: Analysis of cultured cells and pathological brain tissue. PloS ONE, 5(10). https://doi.org/10.1371/journal.pone.0013250

Li, F., Xiao, H., Hu, Z., Zhou, F., & Yang, B. (2018). Exploring the multifaceted roles of heat shock protein B8 (HSPB8) in diseases. In *European Journal of Cell Biology* (Vol. 97, Issue 3, pp. 216–229). Elsevier GmbH. https://doi.org/10.1016/j.ejcb.2018.03.003

Li, X. C., Hu, Q. K., Chen, L., Liu, S. Y., Su, S., Tao, H., Zhang, L. N., Sun, T., & He, L. J. (2017). HSPB8 promotes the fusion of autophagosome and lysosome during autophagy in diabetic neurons. *International Journal of Medical Sciences*, *14*(13), 1335–1341. https://doi.org/10.7150/ijms.20653

Lieberman, A. P., Yu, Z., Murray, S., Peralta, R., Low, A., Guo, S., Yu, X. X., Cortes, C. J., Bennett, C. F., Monia, B. P., La Spada, A. R., & Hung, G. (2014). Peripheral Androgen Receptor Gene Suppression Rescues Disease in Mouse Models of Spinal and Bulbar Muscular Atrophy. *Cell Reports*, *7*(3), 774–784. https://doi.org/10.1016/j.celrep.2014.02.008

Lin, Y., Protter, D. S. W., Rosen, M. K., & Parker, R. (2015). Formation and Maturation of Phase-Separated Liquid Droplets by RNA-Binding Proteins. *Molecular Cell*, *60*(2), 208–219. https://doi.org/10.1016/j.molcel.2015.08.018

Lindner, R. A., Carver, J. A., Ehrnsperger, M., Buchner, J., Esposito, G., Behlke, J., Lutsch, G., Kotlyarov, A., & Gaestel, M. (2000). Mouse Hsp25, a small heat shock protein. The role of its C-terminal extension in oligomerization and chaperone action. *European Journal of Biochemistry*, *267*(7), 1923–1932. https://doi.org/10.1046/j.1432-1327.2000.01188.x

Loschi, M., Leishman, C. C., Berardone, N., & Boccacio, G. L. (2009). Dynein and kinesin regulate stress-granule and P-body dynamics. *Journal of Cell Science*, *122*(21), 3973–3982. https://doi.org/10.1242/jcs.051383

Mahboubi, H., Kodiha, M., & Stochaj, U. (2013). Automated detection and quantification of granular cell compartments. *Microscopy and Microanalysis*, *19*(3), 617–628. https://doi.org/10.1017/S1431927613000159

Mahboubi, H., & Stochaj, U. (2017). Cytoplasmic stress granules: Dynamic modulators of cell signaling and disease. In *Biochimica et Biophysica Acta — Molecular Basis of Disease* (Vol. 1863, Issue 4, pp. 884–895). Elsevier B.V. https://doi.org/10.1016/j.bbadis.2016.12.022

Malena, A., Pennuto, M., Tezze, C., Querin, G., D'Ascenzo, C., Silani, V., Cenacchi, G., Scaramozza, A., Romito, S., Morandi, L., Pegoraro, E., Russell, A. P., Sorarù, G., & Vergani, L. (2013). Androgen-dependent impairment of myogenesis in spinal and bulbar muscular atrophy. *Acta Neuropathologica*, *126*(1), 109–121. https://doi.org/10.1007/s00401-013-1122-9

Marmor-Kollet, H., Siany, A., Kedersha, N., Knafo, N., Rivkin, N., Danino, Y. M., Moens, T. G., Olender, T., Sheban, D., Cohen, N., Dadosh, T., Addadi, Y., Ravid, R., Eitan, C., Toth Cohen, B., Hofmann, S., Riggs, C. L., Advani, V. M., Higginbottom, A., … Hornstein, E. (2020). Spatiotemporal Proteomic Analysis of Stress Granule Disassembly Using APEX Reveals Regulation by SUMOylation and Links to ALS Pathogenesis. *Molecular Cell*, *80*(5), 876-891.e6. https://doi.org/10.1016/j.molcel.2020.10.032

Mattoo, R. U. H., & Goloubinoff, P. (2014). Molecular chaperones are nanomachines that catalytically unfold misfolded and alternatively folded proteins. In *Cellular and Molecular Life Sciences* (Vol. 71, Issue 17, pp. 3311–3325). Birkhauser Verlag AG. https://doi.org/10.1007/s00018-014-1627-y

Mayer MP. Gymnastics of molecular chaperones. *Mol Cell*. 2010;39(3):321-331. Doi:10.1016/j.molcel.2010.07.012

Mazroui, R., Marco, S. Di, Kaufman, R. J., & Gallouzi, I.-E. (2007). Inhibition of the Ubiquitin-Proteasome System Induces Stress Granule Formation □ D. *Molecular Biology of the Cell*, *18*, 2603–2618. https://doi.org/10.1091/mbc.E06

Meister-Broekema M, Freilich R, Jagadeesan C, Rauch JN, Bengoechea R, Motley WW, Kuiper EFE, Minoia M, Furtado GV, van Waarde MAWH, Bird SJ, Rebelo A, Zuchner S, Pytel P, Scherer SS, Morelli FF, Carra S, Weihl CC, Bergink S, Gestwicki JE, Kampinga HH. Myopathy associated BAG3 mutations lead to protein aggregation by stalling Hsp70 networks. Nat Commun. 2018 Dec 17;9(1):5342. Doi: 10.1038/s41467-018-07718-5. PMID: 30559338; PMCID: PMC6297355.

McDonald, E. T., Bortolus, M., Koteiche, H. A., & McHaourab, H. S. (2012). Sequence, structure, and dynamic determinants of Hsp27 (HspB1) equilibrium dissociation are encoded by the N-terminal domain. *Biochemistry*, *51*(6), 1257–1268. https://doi.org/10.1021/bi2017624

Mchaourab, H. S., Godar, J. A., & Stewart, P. L. (2009). Structure and mechanism of protein stability sensors: Chaperone activity of small heat shock proteins. In *Biochemistry* (Vol. 48, Issue 18, pp. 3828–3837). https://doi.org/10.1021/bi900212j

Marrone, L., Poser, I., Casci, I., Japtok, J., Reinhardt, P., Janosch, A., Andree, C., Lee, H. O., Moebius, C., Koerner, E., Reinhardt, L., Cicardi, M. E., Hackmann, K., Klink, B., Poletti, A., Alberti, S., Bickle, M., Hermann, A., Pandey, U. B., … Sterneckert, J. L. (2018). Isogenic FUS-eGFP iPSC Reporter Lines

Enable Quantification of FUS Stress Granule Pathology that Is Rescued by Drugs Inducing Autophagy. *Stem Cell Reports*, *10*(2), 375–389. https://doi.org/10.1016/j.stemcr.2017.12.018

Mateju, D., Franzmann, T. M., Patel, A., Kopach, A., Boczek, E. E., Maharana, S., Lee, H. O., Carra, S., Hyman, A. A., & Alberti, S. (2017). An aberrant phase transition of stress granules triggered by misfolded protein and prevented by chaperone function. *The EMBO Journal*, *36*(12), 1669–1687. https://doi.org/10.15252/embj.201695957

Mediani, L., Galli, V., Carrà, A. D., Bigi, I., Vinet, J., Ganassi, M., Antoniani, F., Tiago, T., Cimino, M., Mateju, D., Cereda, C., Pansarasa, O., Alberti, S., Mandrioli, J., & Carra, S. (2020). BAG3 and BAG6 differentially affect the dynamics of stress granules by targeting distinct subsets of defective polypeptides released from ribosomes. *Cell Stress and Chaperones*, *25*(6), 1045–1058. https://doi.org/10.1007/s12192-020-01141-w

Minoia, M., Boncoraglio, A., Vinet, J., Morelli, F. F., Brunsting, J. F., Poletti, A., Krom, S., Reits, E., Kampinga, H. H., & Carra, S. (2014). BAG3 induces the sequestration of proteasomal clients into cytoplasmic puncta Implications for a proteasome-to-autophagy switch. *Autophagy*, *10*(9), 1603–1621. https://doi.org/10.4161/auto.29409

Mogk, A., Bukau, B., & Kampinga, H. H. (2018). Cellular Handling of Protein Aggregates by Disaggregation Machines. In *Molecular Cell* (Vol. 69, Issue 2, pp. 214–226). Cell Press. https://doi.org/10.1016/j.molcel.2018.01.004

Mymrikov, E. V., Daake, M., Richter, B., Haslbeck, M., & Buchner, J. (2017). The chaperone activity and substrate spectrum of human small heat shock proteins. *Journal of Biological Chemistry*, *292*(2), 672–684. https://doi.org/10.1074/jbc.M116.760413

Mymrikov, E. V, Seit-Nebi, A. S., & Gusev, N. B. (2011). LARGE POTENTIALS OF SMALL HEAT SHOCK PROTEINS. *Physiol Rev*, *91*, 1123–1159. https://doi.org/10.1152/physrev.00023.2010.-Modern

Nagaraj, R. H., Oya-Ito, T., Padayatti, P. S., Kumar, R., Mehta, S., West, K., Levison, B., Sun, J., Crabb, J. W., & Padival, A. K. (2003). Enhancement of chaperone function of α-crystallin by methylglyoxal modification. *Biochemistry*, *42*(36), 10746–10755. https://doi.org/10.1021/bi034541n

Nakhro, K., Park, J. M., Kim, Y. J., Yoon, B. R., Yoo, J. H., Koo, H., Choi, B. O., & Chung, K. W. (2013). A novel Lys141Thr mutation in small heat shock protein 22 (HSPB8) gene in Charcot-Marie-Tooth disease type 2L. *Neuromuscular Disorders*, *23*(8), 656–663. https://doi.org/10.1016/j.nmd.2013.05.009

 Neil F. Bence 2001. (n.d.).

Niewidok, B., Igaev, M., da Graca, A. P., Strassner, A., Lenzen, C., Richter, C. P., Piehler, J., Kurre, R., & Brandt, R. (2018). Single-molecule imaging reveals dynamic biphasic partition of RNA-binding

proteins in stress granules. *Journal of Cell Biology*, *217*(4), 1303–1318. https://doi.org/10.1083/jcb.201709007

Nover, L., Scharf, K.-D., & Neumann, D. (1989). Cytoplasmic Heat Shock Granules Are Formed from Precursor Particles and Are Associated with a Specific Set of mRNAs. In *MOLECULAR AND CELLULAR BIOLOGY* (Vol. 9, Issue 3). https://journals.asm.org/journal/mcb

Ohn, T., Kedersha, N., Hickman, T., Tisdale, S., & Anderson, P. (2008). A functional RNAi screen links O-GlcNAc modification of ribosomal proteins to stress granule and processing body assembly. *Nature Cell Biology*, *10*(10), 1224–1231. https://doi.org/10.1038/ncb1783

Panas, M. D., Ivanov, P., & Anderson, P. (2016). Mechanistic insights into mammalian stress granule dynamics. In *Journal of Cell Biology* (Vol. 215, Issue 3, pp. 313–323). Rockefeller University Press. https://doi.org/10.1083/jcb.201609081

Patel, A., Lee, H. O., Jawerth, L., Maharana, S., Jahnel, M., Hein, M. Y., Stoynov, S., Mahamid, J., Saha, S., Franzmann, T. M., Pozniakovski, A., Poser, I., Maghelli, N., Royer, L. A., Weigert, M., Myers, E. W., Grill, S., Drechsel, D., Hyman, A. A., & Alberti, S. (2015). A Liquid-to-Solid Phase Transition of the ALS Protein FUS Accelerated by Disease Mutation. *Cell*, *162*(5), 1066–1077. https://doi.org/10.1016/j.cell.2015.07.047

Patel, S., Vierling, E., & Tama, F. (2014). Replica exchange molecular dynamics simulations provide insight into substrate recognition by small heat shock proteins. *Biophysical Journal*, *106*(12), 2644–2655. https://doi.org/10.1016/j.bpj.2014.04.048

Paul Anderson,Nancy Kedersha 2002. (n.d.).

Pereira, B., Billaud, M., & Almeida, R. (2017). RNA-Binding Proteins in Cancer: Old Players and New Actors. In *Trends in Cancer* (Vol. 3, Issue 7, pp. 506–528). Cell Press. https://doi.org/10.1016/j.trecan.2017.05.003

Peschek, J., Braun, N., Franzmann, T. M., Georgalis, Y., Haslbeck, M., Weinkauf, S., Buchner, J., & Huber, R. (n.d.). The eye lens chaperone-crystallin forms defined globular assemblies. www.pnas.org/cgi/content/full/

Poletti, A. (2004). The polyglutamine tract of androgen receptor: From functions to dysfunctions in motor neurons. Frontiers in Neuroendocrinology, 25(1), 1–26. https://doi.org/10.1016/j.yfrne.2004.03.001

Protter, D. S. W., Rao, B. S., Van Treeck, B., Lin, Y., Mizoue, L., Rosen, M. K., & Parker, R. (2018). Intrinsically Disordered Regions Can Contribute Promiscuous Interactions to RNP Granule Assembly. *Cell Reports*, *22*(6), 1401–1412. https://doi.org/10.1016/j.celrep.2018.01.036

Reineke, L. C., & Neilson, J. R. (2019). Differences between acute and chronic stress granules, and how these differences may impact function in human disease. In *Biochemical Pharmacology* (Vol. 162, pp. 123–131). Elsevier Inc. https://doi.org/10.1016/j.bcp.2018.10.009

Reinhardt, P., Glatza, M., Hemmer, K., Tsytsyura, Y., Thiel, C. S., Höing, S., Moritz, S., Parga, J. A., Wagner, L., Bruder, J. M., Wu, G., Schmid, B., Röpke, A., Klingauf, J., Schwamborn, J. C., Gasser, T., Schöler, H. R., & Sterneckert, J. (2013). Derivation and Expansion Using Only Small Molecules of Human Neural Progenitors for Neurodegenerative Disease Modeling. *PloS ONE*, *8*(3). https://doi.org/10.1371/journal.pone.0059252

Rikova, K., Guo, A., Zeng, Q., Possemato, A., Yu, J., Haack, H., Nardone, J., Lee, K., Reeves, C., Li, Y., Hu, Y., Tan, Z., Stokes, M., Sullivan, L., Mitchell, J., Wetzel, R., MacNeill, J., Ren, J. M., Yuan, J., … Comb, M. J. (2007). Global Survey of Phosphotyrosine Signaling Identifies Oncogenic Kinases in Lung Cancer. *Cell*, *131*(6), 1190–1203. https://doi.org/10.1016/j.cell.2007.11.025

Robberecht, W., & Philips, T. (2013). The changing scene of amyotrophic lateral sclerosis. In *Nature Reviews Neuroscience* (Vol. 14, Issue 4, pp. 248–264). https://doi.org/10.1038/nrn3430

Ross Buchan, J. (2014). MRNP granules Assembly, function, and connections with disease. In *RNA Biology* (Vol. 11, Issue 8, pp. 1019–1030). Landes Bioscience. https://doi.org/10.4161/15476286.2014.972208

Rusmini, P., Cortese, K., Crippa, V., Cristofani, R., Cicardi, M. E., Ferrari, V., Vezzoli, G., Tedesco, B., Meroni, M., Messi, E., Piccolella, M., Galbiati, M., Garrè, M., Morelli, E., Vaccari, T., & Poletti, A. (2019). Trehalose induces autophagy via lysosomal-mediated TFEB activation in models of motoneuron degeneration. *Autophagy*, *15*(4), 631–651. https://doi.org/10.1080/15548627.2018.1535292

Rusmini, P., Crippa, V., Cristofani, R., Rinaldi, C., Cicardi, M. E., Galbiati, M., Carra, S., Malik, B., Greensmith, L., & Poletti, A. (2016). The Role of the Protein Quality Control System in SBMA. In *Journal of Molecular Neuroscience* (Vol. 58, Issue 3, pp. 348–364). Springer New York LLC. https://doi.org/10.1007/s12031-015-0675-6

Rusmini, P., Crippa, V., Giorgetti, E., Boncoraglio, A., Cristofani, R., Carra, S., & Poletti, A. (2013). Clearance of the mutant androgen receptor in motoneuronal models of spinal and bulbar muscular atrophy. *Neurobiology of Aging*, *34*(11), 2585–2603. https://doi.org/10.1016/j.neurobiolaging.2013.05.026

Rusmini, P., Cristofani, R., Galbiati, M., Cicardi, M. E., Meroni, M., Ferrari, V., Vezzoli, G., Tedesco, B., Messi, E., Piccolella, M., Carra, S., Crippa, V., & Poletti, A. (2017). The role of the heat shock protein B8 (HSPB8) in motoneuron diseases. In *Frontiers in Molecular Neuroscience* (Vol. 10). Frontiers Media S.A. https://doi.org/10.3389/fnmol.2017.00176

Rusmini, P., Polanco, M. J., Cristofani, R., Cicardi, M. E., Meroni, M., Galbiati, M., Piccolella, M., Messi, E., Giorgetti, E., Lieberman, A. P., Milioto, C., Rocchi, A., Aggarwal, T., Pennuto, M., Crippa, V., & Poletti, A. (2015). Aberrant Autophagic Response in the Muscle of A Knock-in Mouse Model of Spinal and Bulbar Muscular Atrophy. *Scientific Reports*, *5*. https://doi.org/10.1038/srep15174

Saji, H., Iizuka, R., Yoshida, T., Abe, T., Kidokoro, S. I., Ishii, N., & Yohda, M. (2008). Role of the IXI/V motif in oligomer assembly and function of StHsp14.0, a small heat shock protein from the acidothermophilic archaeon, Sulfolobus tokodaii strain 7. *Proteins: Structure, Function and Genetics*, *71*(2), 771–782. https://doi.org/10.1002/prot.21762

Sanbe, A., Daicho, T., Mizutani, R., Endo, T., Miyauchi, N., Yamauchi, J., Tanonaka, K., Glabe, C., & Tanoue, A. (2009). Protective effect of geranylgeranylacetone via enhancement of HSPB8 induction in desmin-related cardiomyopathy. *PloS ONE*, *4*(4). https://doi.org/10.1371/journal.pone.0005351

Sanbe, A., Yamauchi, J., Miyamoto, Y., Fujiwara, Y., Murabe, M., & Tanoue, A. (2007). Interruption of CryAB-amyloid oligomer formation by HSP22. *Journal of Biological Chemistry*, *282*(1), 555–563. https://doi.org/10.1074/jbc.M605481200

Santhanagopalan, I., Degiacomi, M. T., Shepherd, D. A., Hochberg, G. K. A., Benesch, J. L. P., & Vierling, E. (2018). It takes a dimer to tango: Oligomeric small heat shock proteins dissociate to capture substrate. *Journal of Biological Chemistry*, *293*(51), 19511–19521. https://doi.org/10.1074/jbc.RA118.005421

Seguin, S. J., Morelli, F. F., Vinet, J., Amore, D., De Biasi, S., Poletti, A., Rubinsztein, D. C., & Carra, S. (2014). Inhibition of autophagy, lysosome and VCP function impairs stress granule assembly. *Cell Death and Differentiation*, *21*(12), 1838–1851. https://doi.org/10.1038/cdd.2014.103

Seong and Matzinger, 2004. (n.d.).

Sharma, K. K., Kaur, H., & Kester, K. (1997). *Functional Elements in Molecular Chaperone α-Crystallin: Identification of Binding Sites in αB-Crystallin C-terminus are also involved in the chaperone-like* (Vol. 239).

Shatov, V. M., Strelkov, S. V., & Gusev, N. B. (2020). The heterooligomerization of human small heat shock proteins is controlled by conserved motif located in the n-terminal domain. *International Journal of Molecular Sciences*, *21*(12), 1–18. https://doi.org/10.3390/ijms21124248

Shemetov, A. A., & Gusev, N. B. (2011). Biochemical characterization of small heat shock protein HspB8 (Hsp22)-Bag3 interaction. *Archives of Biochemistry and Biophysics*, *513*(1), 1–9. https://doi.org/10.1016/j.abb.2011.06.014

Smith, C. C., Yu, Y. X., Kulka, M., & Aurelian, L. (2000). A novel human gene similar to the protein kinase (PK) coding domain of the large subunit of herpes simplex virus type 2 ribonucleotide

reductase (ICP10) codes for a serine-threonine PK and is expressed in melanoma cells. *Journal of Biological Chemistry*, *275*(33), 25690–25699. https://doi.org/10.1074/jbc.M002140200

Sarparanta, J., Jonson, P. H., Golzio, C., Sandell, S., Luque, H., Screen, M., McDonald, K., Stajich, J. M., Mahjneh, I., Vihola, A., Raheem, O., Penttilä, S., Lehtinen, S., Huovinen, S., Palmio, J., Tasca, G., Ricci, E., Hackman, P., Hauser, M., … Udd, B. (2012). Mutations affecting the cytoplasmic functions of the co-chaperone DNAJB6 cause limb-girdle muscular dystrophy. Nature Genetics, 44(4), 450–455. https://doi.org/10.1038/ng.1103

Sarparanta, J., Jonson, P. H., Kawan, S., & Udd, B. (2020). Neuromuscular diseases due to chaperone mutations: A review and some new results. International Journal of Molecular Sciences, 21(4). https://doi.org/10.3390/ijms21041409

Shashidharamurthy, R., Koteiche, H. A., Dong, J., & Mchaourab, H. S. (2005). Mechanism of chaperone function in small heat shock proteins: Dissociation of the HSP27 oligomer is required for recognition and binding of destabilized T4 lysozyme. Journal of Biological Chemistry, 280(7), 5281–5289. https://doi.org/10.1074/jbc.M407236200

Stolz, A., Ernst, A., & Dikic, I. (2014). Cargo recognition and trafficking in selective autophagy. Nature Cell Biology, 16(6), 495–501. https://doi.org/10.1038/ncb2979

Sun, D., Wu, R., Zheng, J., Li, P., & Yu, L. (2018). Polyubiquitin chain-induced p62 phase separation drives autophagic cargo segregation. Cell Research, 28(4), 405–415. https://doi.org/10.1038/s41422-018-0017-7

Szewczyk, B., Günther, R., Japtok, J., Frech, M. J., Naumann, M., Lee, H. O., & Hermann, A. (2023). FUS ALS neurons activate major stress pathways and reduce translation as an early protective mechanism against neurodegeneration. Cell Reports, 42(2). https://doi.org/10.1016/j.celrep.2023.112025

Sorarù, G., D'Ascenzo, C., Polo, A., Palmieri, A., Baggio, L., Vergani, L., Gellera, C., Moretto, G., Pegoraro, E., & Angelini, C. (2008). Spinal and bulbar muscular atrophy: Skeletal muscle pathology in male patients and heterozygous females. *Journal of the Neurological Sciences*, *264*(1–2), 100–105. https://doi.org/10.1016/j.jns.2007.08.012

Soto, C. (2003). Unfolding the role of protein misfolding in neurodegenerative diseases. *Nature Reviews Neuroscience*, *4*(1), 49–60. https://doi.org/10.1038/nrn1007

Spector, D. L. (2006). SnapShot: Cellular Bodies. In *Cell* (Vol. 127, Issue 5, pp. 1071.e1-1071.e2). Elsevier B.V. https://doi.org/10.1016/j.cell.2006.11.026

Stamler, R., Kappé, G., Boelens, W., & Slingsby, C. (2005). Wrapping the α-crystallin domain fold in a chaperone assembly. *Journal of Molecular Biology*, *353*(1), 68–79. https://doi.org/10.1016/j.jmb.2005.08.025

Stengel, F., Baldwin, A. J., Painter, A. J., Jaya, N., Basha, E., Kay, L. E., Vierling, E., Robinson, C. V., & Benesch, J. L. P. (2010). Quaternary dynamics and plasticity underlie small heat shock protein chaperone function. *Proceedings of the National Academy of Sciences of the United States of America*, *107*(5), 2007–2012. https://doi.org/10.1073/pnas.0910126107

Stromer, T., Fischer, E., Richter, K., Haslbeck, M., & Buchner, J. (2004). Analysis of the regulation of the molecular chaperone Hsp26 by temperature-induced dissociation: The N-terminal domain is important for oligomer assembly and the binding of unfolding proteins. *Journal of Biological Chemistry*, *279*(12), 11222–11228. https://doi.org/10.1074/jbc.M310149200

Sudnitsyna, M. V, Mymrikov, E. V, Seit-Nebi, A. S., & Gusev, N. B. (2012). The Role of Intrinsically Disordered Regions in the Structure and Func-tioning of Small Heat Shock Proteins. In *Current Protein and Peptide Science* (Vol. 13).

Sun, X., Fontaine, J. M., Rest, J. S., Shelden, E. A., Welsh, M. J., & Benndorf, R. (2004). Interaction of Human HSP22 (HSPB8) with Other Small Heat Shock Proteins. *Journal of Biological Chemistry*, *279*(4), 2394–2402. https://doi.org/10.1074/jbc.M311324200

Takalo, M., Salminen, A., Soininen, H., Hiltunen, M., & Haapasalo, A. (2013). Protein aggregation and degradation mechanisms in neurodegenerative diseases. In *Am J Neurodegener Dis* (Vol. 2, Issue 1). www.AJND.us/

Tang, B. S., Zhao, G. hua, Luo, W., Xia, K., Cai, F., Pan, Q., Zhang, R. xu, Zhang, F. feng, Liu, X. min, Chen, B., Zhang, C., Shen, L., Jiang, H., Long, Z. gao, & Dai, H. ping. (2005). Small heat-shock protein 22 mutated in autosomal dominant Charcot-Marie-Tooth disease type 2L. *Human Genetics*, *116*(3), 222–224. https://doi.org/10.1007/s00439-004-1218-3

Tsai, N. P., Ho, P. C., & Wei, L. N. (2008). Regulation of stress granule dynamics by Grb7 and FAK signalling pathway. EMBO Journal, 27(5), 715–726. https://doi.org/10.1038/emboj.2008.19

Taylor, J. P., Brown, R. H., & Cleveland, D. W. (2016). Decoding ALS: From genes to mechanism. In *Nature* (Vol. 539, Issue 7628, pp. 197–206). Nature Publishing Group. https://doi.org/10.1038/nature20413

Tedesco, B., Ferrari, V., Cozzi, M., Chierichetti, M., Casarotto, E., Pramaggiore, P., Mina, F., Piccolella, M., Cristofani, R., Crippa, V., Rusmini, P., Galbiati, M., & Poletti, A. (2022). The role of autophagy-lysosomal pathway in motor neuron diseases. In *Biochemical Society Transactions* (Vol. 50, Issue 5, pp. 1489–1503). Portland Press Ltd. https://doi.org/10.1042/BST20220778

Thedieck, K., Holzwarth, B., Prentzell, M. T., Boehlke, C., Kläsener, K., Ruf, S., Sonntag, A. G., Maerz, L., Grellscheid, S. N., Kremmer, E., Nitschke, R., Kuehn, E. W., Jonker, J. W., Groen, A. K., Reth, M., Hall, M. N., & Baumeister, R. (2013). Xinhibition of mTORC1 by astrin and stress granules prevents apoptosis in cancer cells. *Cell*, *154*(4). https://doi.org/10.1016/j.cell.2013.07.031

Tourrière, H., Chebli, K., Zekri, L., Courselaud, B., Blanchard, J. M., Bertrand, E., & Tazi, J. (2003). The RasGAP-associated endoribonuclease G3BP assembles stress granules. *Journal of Cell Biology*, *160*(6), 823–831. https://doi.org/10.1083/jcb.200212128

Treweek, T. M., Meehan, S., Ecroyd, H., & Carver, J. A. (2015). Small heat-shock proteins: Important players in regulating cellular proteostasis. *Cellular and Molecular Life Sciences*, *72*(3), 429–451. https://doi.org/10.1007/s00018-014-1754-5

Ulbricht, A., Eppler, F. J., Tapia, V. E., Van Der Ven, P. F. M., Hampe, N., Hersch, N., Vakeel, P., Stadel, D., Haas, A., Saftig, P., Behrends, C., Fürst, D. O., Volkmer, R., Hoffmann, B., Kolanus, W., & Höhfeld, J. (2013). Cellular mechanotransduction relies on tension-induced and chaperone-assisted autophagy. Current Biology, 23(5), 430–435. https://doi.org/10.1016/j.cub.2013.01.064

Ulbricht, A., Gehlert, S., Leciejewski, B., Schiffer, T., Bloch, W., & Höhfeld, J. (2015). Induction and adaptation of chaperone-assisted selective autophagy CASA in response to resistance exercise in human skeletal muscle. Autophagy, 11(3), 538–546. https://doi.org/10.1080/15548627.2015.1017186

Van Den Ijssel, P. R. L. A., Overkamp, P., Bloemendal, H., & De Jong, W. W. (1998). Phosphorylation of aB-Crystallin and HSP27 Is Induced by Similar Stressors in HeLa Cells The involvement of HSP27-phosphorylation in the. In *BIOCHEMICAL AND BIOPHYSICAL RESEARCH COMMUNICATIONS* (Vol. 247).

Verschuure, P., Tatard, C., Boelens, W. C., Grongnet, J. F., & David, J. C. (2003). Expression of small heat shock proteins HspB2, HspB8, Hsp20 and cvHsp in different tissues of the perinatal developing pig. European Journal of Cell Biology, 82(10), 523–530. https://doi.org/10.1078/0171-9335-00337

Van Montfort, R. L. M., Basha, E., Friedrich, K. L., Slingsby, C., & Vierling, E. (2001). Crystal structure and assembly of a eukaryotic small heat shock protein. *Nature Structural Biology*, *8*(12), 1025–1030. https://doi.org/10.1038/nsb722

Varlet, A. A., Fuchs, M., Luthold, C., Lambert, H., Landry, J., & Lavoie, J. N. (2017). Fine-tuning of actin dynamics by the HSPB8-BAG3 chaperone complex facilitates cytokinesis and contributes to its impact on cell division. *Cell Stress and Chaperones*, *22*(4), 553–567. https://doi.org/10.1007/s12192-017-0780-2

Walters, R. W., Muhlrad, D., Garcia, J., & Parker, R. (2015). Differential effects of Ydj1 and Sis1 on Hsp70-mediated clearance of stress granules in Saccharomyces cerevisiae. *RNA*, *21*(9), 1660–1671. https://doi.org/10.1261/rna.053116.115

Webster, J. M., Darling, A. L., Uversky, V. N., & Blair, L. J. (2019). Small heat shock proteins, big impact on protein aggregation in neurodegenerative disease. *Frontiers in Pharmacology*, *10*. https://doi.org/10.3389/fphar.2019.01047

Wegele, H., Müller, L., & Buchner, J. (2004). Hsp70 and Hsp90—a relay team for protein folding. Reviews of Physiology, Biochemistry and Pharmacology, 151(January), 1–44. https://doi.org/10.1007/s10254-003-0021-1

Wheeler, J. R., Matheny, T., Jain, S., Abrisch, R., & Parker, R. (2016). Distinct stages in stress granule assembly and disassembly. Elife, 5(Se). https://doi.org/10.7554/eLife.18413

Wilson et al 1899. (n.d.).

Wilhelmus MM, Otte-Höller I, Wesseling P, de Waal RM, Boelens WC, Verbeek MM. Specific association of small heat shock proteins with the pathological hallmarks of Alzheimer's disease brains. *Neuropathol Appl Neurobiol*. 2006;32(2):119-130. Doi:10.1111/j.1365-2990.2006.00689.

Yang, Y., Coleman, M., Zhang, L., Zheng, X., & Yue, Z. (2013). Autophagy in axonal and dendritic degeneration. In *Trends in Neurosciences* (Vol. 36, Issue 7, pp. 418–428). https://doi.org/10.1016/j.tins.2013.04.001

Yew, E. H. J., Cheung, N. S., Choy, M. S., Qi, R. Z., Lee, A. Y. W., Peng, Z. F., Melendez, A. J., Manikandan, J., Koay, E. S. C., Chiu, L. L., Ng, W. L., Whiteman, M., Kandiah, J., & Halliwell, B. (2005). Proteasome inhibition by lactacystin in primary neuronal cells induces both potentially neuroprotective and pro-apoptotic transcriptional responses: A microarray analysis. *Journal of Neurochemistry*, *94*(4), 943–956. https://doi.org/10.1111/j.1471-4159.2005.03220.x

Yu, Y. X., Heller, A., Liehr, T., Smith, C. C., & Aurelian, L. (2001). Expression analysis and chromosome location of a novel gene (Hll) associated with the growth of human melanoma cells. In *INTERNATIONAL JOURNAL OF ONCOLOGY* (Vol. 18). http://www.ncbi.nlm.nih.gov/UniGene

Zantemas, A., Verlaan-De Vries, M., Maasdam, D., Bol, S., & Van Der Eb, A. (1992). *THE JOURNAL OF BIOLOGICAL CHEMISTRY Heat Shock Protein 27 and aB-Crystallin Can Form a Complex, Which Dissociates by Heat Shock\** (Vol. 267, Issue 18).

Zhu, Z., & Reiser, G. (2018). The small heat shock proteins, especially HspB4 and HspB5 are promising protectants in neurodegenerative diseases. In *Neurochemistry International* (Vol. 115, pp. 69–79). Elsevier Ltd. https://doi.org/10.1016/j.neuint.2018.02.006

Zaffagnini, G., & Martens, S. (2016). Mechanisms of Selective Autophagy. Journal of Molecular Biology, 428(9), 1714–1724. https://doi.org/10.1016/j.jmb.2016.02.004

Zou, T., Rao, J. N., Liu, L., Xiao, L., Cui, Y.-H., Jiang, Z., Ouyang, M., Donahue, J. M., & Wang, J.-Y. (2012). Polyamines inhibit the assembly of stress granules in normal intestinal epithelial cells regulating apoptosis. *J Physiol Cell Physiol*, *303*, 102–111. https://doi.org/10.1152/ajpcell.00009.2012.-Polyamines

Zou, T., Yang, X., Pan, D., Huang, J., Sahin, M., & Zhou, J. (2011). SMN deficiency reduces cellular ability to form stress granules, sensitizing cells to stress. *Cellular and Molecular Neurobiology*, *31*(4), 541–550. https://doi.org/10.1007/s10571-011-9647-8

## 10 List of Figures

## 11  List of Tables

## 12 Acknowledgements

have been the backbone of my support system, I cannot thank you enough: Deepika, Najeed, Ammar, Niharika, Haroon, Yatendra, Dilip, Hagera, Priyanka, Tanya, Mousmi, Amrit, Salmaan, Hammad, Neha and Mena. Your unwavering support, encouragement, and motivation have been instrumental in helping me to stay focused and determined throughout this journey. Your presence in my life has been a source of strength and inspiration, and I could not have achieved this without you.

I am grateful to have such a remarkable group of individuals in my life who have supported and encouraged me every step of the way. Thank you all for your contributions to my success, and for being a part of my life.

## 13 Eidesstattliche Erklärung

I, Kanza Saleem, solemnly declare that I have duly presented the following work titled: "Loss-Of HSPB8 leads to prolonged stress granules disassembly via impaired CASA-complex ultimately causing FUS-aggregation." I affirm that I have solely relied on the resources mentioned and have not employed any additional aids. Whenever I have borrowed wording or conveyed ideas from other sources, I have diligently acknowledged the origin by providing appropriate citations.

Furthermore, I hereby assert that I have meticulously adhered to the fundamental principles of good scientific practice, as outlined in the "Rules for Ensuring Good Scientific Practice and for Avoiding Scientific Misconduct" at the University of Rostock, while preparing my scientific endeavor.

Rostock, 18.09.2023

Kanza Saleem

**Kanza Saleem**

**Date of birth:** 29/04/1991 | **Nationality:** Indian | **Gender:** Female |

**Phone number:** (+49) 1788167569 (Mobile) | **Email address:**

saniakanza@gmail.com |

**Address:** Bergstraße 7a, 18057, Rostock, Germany (Home)

● **WORK EXPERIENCE**

01/06/2019 – CURRENT Rostock, Germany
**GRADUATE STUDENT: JUNE 2019-MAY 2023** DZNE AND UNIVERSITY OF ROSTOCK

Project 1: Loss-Of HSPB8 leads to prolonged stress granules disassembly via impaired CASA-complex

·Studied the role of HSPB8 in selective autophagy, autophagosomes and autolysosomes
·Researched and examined the stress in HSPB8-knock-out spinal motor neurons
·Examined the importance of chaperone-assisted selective autophagy in stress granule disassembly

Project 2: Role of HSPB8 to FUS Aggregation beyond Stress Granules and Mislocalization

·Studied the impact of HSPB8 knockout in FUS and stress granules
·Examined how knocking out of HSPB8 can cause FUS-aggregation

01/08/2015 – 01/05/2018 New Delhi, India
**PROJECT ASSISTANT: AUGUST 2015-MAY 2018** NATIONAL BRAIN RESEARCH INSTITUTE

Project 1: Role of miR-320a-VDAC1 axis in HIV-1 neuropathogenesis

·Established a well-characterized model system of human primary astrocytes and neurons, furthermore probed into the molecular mechanism for enhanced ATP release in HIV-1 Tat affected astrocytes
·Evaluated that VDAC1 siRNA or miR-320a mimic rescued the neurons from astroglia-mediated neurotoxicity in HIV-1 neuropathogenesis

Project 2: Role of EphrinA3 in HIV-1 Neuropathogenesis

·Establish that EphrinA3 is expressed on astrocytes and ephA4 is expressed on neurons through Immunofluorescence
·Measured extracellular glutamate levels post ephrinA3 and Tat B transfections

01/12/2014 – 01/04/2015 New Delhi, India
**DISSERTATION : DECEMBER 2014-APRIL 2015** JAMIA HAMDARD UNIVERSITY

Project: Isolation, purification and characterization of Ovalbumin from hen egg and to develop and isolate antibodies against it

·Isolation of ovalbumin (Protein) from hen's egg white followed by purification of ovalbumin by gel permeation chromatography
·Checking the protein on the gel by Native PAGE and SDS PAGE
·Immunization of rats with ovalbumin as a potential antigen later Isolation and quantification of IgG from rat antiserum

01/06/2013 – 30/07/2013 Noida, India
**INTERN : JUNE 2013-JULY 2013** ALELLE LIFE SCIENCES

• Training in General Techniques of Biotechnology
• Isolation of DNA, RNA and Protein from *Plumbago* plant
• Running PCR, qPCR and western blot

30/07/2013 – 30/06/2015 New Delhi, India
**MASTERS IN BIOCHEMISTRY** Jamia Hamdard University

**Address** 782+55X, Mehrauli - Badarpur Rd, near Batra Hospital, Block D, Hamdard Nagar, 110062, New Delhi, India

**Website** http://jamiahamdard.edu/

01/07/2010 – 01/05/2013 Bareilly , India
**BACHELOR IN BIOTECHNOLOGY** Khandelwal College of Management Science and Technology

**Address** 14th K.M, Pilibhit Rd, 243124, Bareilly , India | **Website** https://www.kcmt.in/

**Role of EphrinA3 in HIV-1 Neuropathogenesis** – 2021
Singhal CMS, Jaiswal P, Mehta A, **Saleem K,** Seth P. (2021)

**Novel insights into role of miR-320a-VDAC1 axis in astrocyte-mediated neuronal damage in neuroAIDS**
– 2017
Fatima M, **Saleem K**, Prajapati B, Kumari R, Singal CMS, Seth P. (2017)

## HONOURS AND AWARDS

01/08/2013
**Gold medal – MJP Rohilkhand University, Bareilly, India** Awarded Gold Medal from MJP Rohilkhand University, Bareilly, India (B.Sc Biotechnology, 2013) for securing 1st rank at the University level.

01/08/2013
**Gold Medal – Khandelwal College of Science Technology, Bareilly, India** Awarded Gold Medal from Khandelwal College of Science Technology, Bareilly, India (B.Sc. Biotechnology, 2013) for securing 1st rank at the College level.

**Dr. Khandelwal Merit Scholarship – Khandelwal College of Science Technology, Bareilly, India** Awarded Dr Khandelwal Merit Scholarship, for securing 1st rank at the College level, B.Sc. Biotechnology, 2013.

2014
**Hakeem Abdul Majeed Merit Scholarship, – Jamia Hamdard University** Awarded Hakeem Abdul Majeed Merit Scholarship, M.Sc Biochemistry, 2014

# TECHNICAL SKILLS

## Molecular

**Cell Culture**- Handling and maintenance of spinal motor neurons, handling and maintenance of human primary neural stem cell culture, handling and maintaining iPSCs, handling and maintaining co-cultures of astrocytes and neurons, maintenance of neural progenitor cells, neurons and astrocytes, handling of cancerous cell lines SH- SY5Y and SVG
**Cell Viability assays**- MTT, TUNEL, Pesto Blue, In Situ Hybridization, siRNA/shRNA-mediated knockdown, overexpression using plasmid constructs
**Filter Trap Assay**
**PCR**- PCR, Gradient PCR, Reverse Transcriptase PCR, Real-time PCR, Touchdown PCR, Touchup PCR
**Gene manipulation**- siRNA
**Isolation & Quantification**- RNA isolation from mammalian cells/tissues and quantification, Isolation of human miRNA and profiling, Isolation of DNA, protein, RNA and gel purification, molecular cloning Immunostaining and fluorescent microscopy
**Bacterial Cell Culture**- handling and maintenance of bacterial cell culture cloning
**Chromatography**- Gel filtration chromatography, Ouchterlony double diffusion and Radial immunodiffusion
mice handling for retro-orbital blood collection
**Gel electrophoresis**- Agarose gel electrophoresis, NATIVE-PAGE, SDS-PAGE and western blotting
**Microscopy**- Live cell microscopy, Bright-field and Fluorescence
Southern blotting, FACs (Fluorescence-activated cell sorting), Glutamate Assay, Immunohistochemistry(IHC), Immunocytochemistry(ICC)

## Bioinformatics

**Genetics and Next-Generation Sequencing for Bioinformatics**- Licence from Udemy, August, 2023
Statistical Analysis- Pearson's correlation, Chi-squared test, Analysis of
Variance, Mann–Whitney U and Wilcoxson test
Plots- Heatmap, Correlogram, box plot and other plots generation through R Databases knowledge-
ENCODE, ENSEMBLE, Bio-GPS, GTex, Genecard, Brain Atlas, CORTECON, PFam, SupFam, ExPASY, KEGG, STRING, IPA, UCSC browser
Familiar Languages- R
Primer designing- in-silico PCR, BLAST, ClustalW, primer3

*BE LIKE STEM CELLS, DIFFERENTIATE YOURSELF FROM OTHERS*